Distribution Agreement

In presenting this thesis or dissertation as a partial fulfillment of the requirements for an advanced degree from Emory University, I hereby grant to Emory University and its agents the non-exclusive license to archive, make accessible, and display my thesis or dissertation in whole or in part in all forms of media, now or hereafter known, including display on the world wide web. I understand that I may select some access restrictions as part of the online submission of this thesis or dissertation. I retain all ownership rights to the copyright of the thesis or dissertation. I also retain the right to use in future works (such as articles or books) all or part of this thesis or dissertation.

Signature:

_____ _____

Amanda L. York Date

Spatial organization of acetylcholine receptors at the neuromuscular junction

By

Amanda L. York
Doctor of Philosophy

Graduate Division of Biological and Biomedical Sciences
Biochemistry, Cell, and Developmental Biology

_____
James Q. Zheng, Ph.D.
Advisor

_____
Victor Faundez, M.D., Ph.D.
Committee Member

_____
Andrew P. Kowalczyk, Ph.D.
Committee Member

_____
Shoichiro Ono, Ph.D.
Committee Member

_____
Winfield S. Sale, Ph.D.
Committee Member

Accepted:

_____
Lisa A. Tedesco, Ph.D.
Dean of the James T. Laney School of Graduate Studies

_____
Date

Spatial organization of acetylcholine receptors at the neuromuscular junction

By

Amanda L. York
B.S., Georgia Institute of Technology, 2011

Advisor: James Q. Zheng, Ph.D.

An abstract of
A dissertation submitted to the Faculty of the
James T. Laney School of Graduate Studies of Emory University
in partial fulfillment of the requirements for the degree of
Doctor of Philosophy
in Graduate Division of Biological and Biomedical Sciences
Biochemistry, Cell, and Developmental Biology
2017

Abstract

Spatial organization of acetylcholine receptors at the neuromuscular junction

By Amanda L. York

The coordinated movement of humans' everyday lives is dependent in part upon the neuromuscular junction (NMJ). The NMJ is a large synapse that connects motor neurons to skeletal muscles for precise and controlled movement. Defects in the development or function of this synapse commonly underlie many neuromuscular diseases, such as amyotrophic lateral sclerosis (ALS) and myasthenia gravis. Of all of the molecular components at the NMJ, the neurotransmitter receptor, acetylcholine receptor (AChR), plays one of the largest roles in the initiation of muscle contraction. AChRs are highly concentrated at the NMJ on the surface of the muscle fiber where they are responsible for receiving and responding to neurotransmitter released from the motor neuron terminal. This dissertation focuses on the organization of AChRs and the developmental processes that lead to such an organization. I have identified a novel organization of acetylcholine receptors at the postsynaptic membrane of the adult NMJ. The postsynaptic membrane of the NMJ contains numerous infoldings in which many key postsynaptic proteins, including AChRs, are segregated to either the top of the folds or the bottom of the infolded membrane. Using super-resolution microscopy, I found that AChRs located at the top of membrane folds are specifically concentrated in the area directly opposite that of presynaptic neurotransmitter release sites, and not distributed across the entire top of the membrane fold as previously thought. I also examined the developmental processes responsible for the spatial organization of AChRs and found that the actin cytoskeleton, including the actin binding proteins cortactin and profilin, plays a significant role in the clustering of AChRs. A highly dynamic actin cytoskeleton was found to be necessary for the clustering of AChRs during synaptogenesis. Thus, the data presented in this dissertation reveal a novel organization of AChRs, whereby the actin cytoskeleton plays a significant role in orchestrating this organization during development.

Spatial organization of acetylcholine receptors at the neuromuscular junction

By

Amanda L. York
B.S., Georgia Institute of Technology, 2011

Advisor: James Q. Zheng, Ph.D.

A dissertation submitted to the Faculty of the
James T. Laney School of Graduate Studies of Emory University
in partial fulfillment of the requirements for the degree of
Doctor of Philosophy
in Graduate Division of Biological and Biomedical Sciences
Biochemistry, Cell, and Developmental Biology
2017

Acknowledgements

The work presented in this dissertation represents the culmination of over 6 years of work and would not have been possible without the support and advice from many people. First and foremost, I would like to thank my advisor James Zheng for his guidance and support. He has helped me develop my critical thinking and science communication skills, which I will cherish and carry with me through all my future endeavors. I would also like to thank my committee members, Victor Faundez, Andy Kowalczyk, Sho Ono, Win Sale, and Grace Pavlath for helping to keep me on track and for the advice and engaging discussions over the years.

I would also like to thank the members of the Zheng Lab, specifically Julia Omotade, Ken Myers, Stephanie Pollitt, Will Lei, and Yanfang Rui for their advice, experimental help, and ultimately friendship throughout my time in graduate school.

I also owe a large debt of gratitude to the lifelong friends (and now family) that I have made during my time here at Emory. Julia, Kevin, and Chelsey, I am so grateful to have you all by my side through this process. It was your support, words of encouragement, friendship, and those much-needed moments of distraction that helped keep me sane during the inevitable rough patches in graduate school. We made it, guys!

Ultimately, none of this work would have been possible without the unconditional love and support of my family. If I have learned only one thing from my time in graduate school it is the importance of family, and how truly blessed I am to call the Yorks/Perrys, Craigs, and Omotades my family. Mom and Dad, thank you for everything you sacrificed in order to provide us with every opportunity growing up. You taught me to be fearless and that no dream is too big with hard work and dedication. I am only here because of y'all. Ashley and Evan, I am forever grateful to have such smart, loving, and hilarious siblings. I am so thankful Mom and Dad decided to have both of you. To my best friend, my adventure buddy, and my better half, Ian, thank you from the bottom of my heart. I truly do not believe I would be here if you had not entered into my life. You push me to become a better person every day. The unconditional love and support from you and Butch kept me going when I thought I had nothing left to give. You are my rock and a true inspiration.

Finally, I would like to dedicate this to my late grandfather, Glenn "Bubba" York, Jr. He is the true definition of a hero.

Table of Contents

List of Figures

Chapter I

Introduction

1.1 Significance of the neuromuscular junction

From the time of birth, humans depend on physiological movement in order to survive. This coordinated movement of the human body requires reliable and strong communication between the brain and skeletal muscles. The amount of cellular communication, and the speed at which it occurs, in order to initiate anatomical movement is astonishing. For example, in order to wiggle your toes, an electrochemical signal generated in the brain travels via neurons, the basic unit of the nervous system, to the spinal cord, which harbors specialized neurons called motor neurons that link the brain to every muscle in the body. Once the signal is received by the motor neuron associated with the toe skeletal muscles, the signal then travels down the leg to the toe muscle cell via the motor neuron's long axonal projection, which can reach one meter in length depending on the height of the person. The motor neuron must then relay the signal to the muscle cell (also referred to as muscle fiber), which ultimately responds in the form of muscle contraction. This entire process occurs in a fraction of a second. The coordinated anatomical movement of human's everyday lives depends on this rapid and precise neuromuscular communication—the precipice of which centers around the synapse between a motor neuron and a single muscle fiber, termed the neuromuscular junction (NMJ).

The NMJ was one of the first synapses characterized and remains one of the most well studied synapses to date. In 1928, Santiago Ramon y Cajal—considered by many to be the founder of modern neuroscience—used light microscopy to describe neuromuscular synaptogenesis and regeneration (Cajal, 1928). Shortly thereafter, Sir Henry Dale and colleagues utilized the NMJ to provide the first demonstration that chemical messengers called neurotransmitters are used in synaptic transmission, for which he won the 1936 Nobel Prize (Dale et al., 1936). Following that discovery, Bernard Katz and colleagues used the NMJ to show that the neurotransmitter acetylcholine (ACh) is released from the presynaptic terminal in discrete vesicular 'quanta' (Katz, 1966). For this pivotal work, which proved to be consistent across all synapses, Katz was awarded the Nobel Prize in 1970. In addition to these influential discoveries, the first neurotransmitter receptor to be purified and molecularly cloned was the acetylcholine receptor (AChR) from the electric tissue of *Torpedo marmorata* (Miledi et al., 1971). Thus, the NMJ and various neuromuscular synapses have proven to be a conduit for many seminal discoveries in the field of neuroscience, primarily due to its large size and experimental accessibility.

The primary goal of this dissertation is to gain a comprehensive understanding of the developmental organization of AChRs—the sole neurotransmitter receptor at the vertebrate NMJ—and the processes underlying such an organization. This chapter will discuss the various facets of NMJ structure, development and regulation. Specifically, it considers the steps leading to the formation and structure of the NMJ (Section 1.2), the process leading to muscle contraction (Section 1.3), the signaling molecules and pathways underlying NMJ function (Section 1.4), the role of the postsynaptic cytoskeleton (Section 1.5), and diseases affecting the NMJ (Section 1.6). Chapter 2 presents original research

addressing the indispensable role of the postsynaptic cytoskeleton in the formation of the postsynaptic terminal. Chapter 3 presents novel research uncovering the molecular organization of the postsynaptic terminal of the NMJ using super-resolution microscopy techniques. Finally, Chapter 4 reviews the conclusions made from the work presented here and discusses outstanding questions surrounding the development of the NMJ. Overall, the findings of this dissertation address several fundamental questions surrounding synapse biology and neuromuscular communication.

1.2 NMJ synaptogenesis & development

In order to form a reliable neuromuscular synapse, motor neuron axons must traverse long distances to reach the target muscle cell. In the early stages of embryonic development, muscle progenitor cells, called myoblasts, will continue to fuse to the growing muscle fiber. Before innervation by the nerve terminal, AChRs and other postsynaptic proteins aggregate in the central region of the muscle fiber (Lin et al., 2001; Yang et al., 2001). The clustering of AChRs and other postsynaptic proteins, referred to as prepatterning, occurs independently from neuronal input but is dependent on signaling of some key postsynaptic molecules. Specifically, the assembly and activation of a tripartite complex composed of the muscle specific receptor tyrosine kinase (MuSK), its co-receptor low-density lipoprotein receptor-related protein 4 (Lrp4), and the cytosolic adaptor docking protein-7 (Dok-7) induces the local synthesis and trafficking of AChRs to the plasma membrane (Okada et al., 2006; Weatherbee et al., 2006; Kim and Burden, 2008; Muller et al., 2010). Several studies suggest that prepatterning is necessary to help guide the incoming motor neuron and spatially restrict synaptogenesis to the central most part of the muscle fiber (Kim and Burden, 2008; Liu et al., 2008; Chen et al., 2011a). However,

the motor neuron does not always directly innervate prepatterned AChR clusters (**Figure 1.1A**). Synapses can form by either incorporating the pre-existing postsynaptic machinery or assembling new postsynaptic machinery at sites where prepatterned AChR clusters are absent (Flanagan-Steet et al., 2005; Lin et al., 2008). This suggests that the AChR clusters themselves do not pre-determine the site of innervation, rather prepatterning likely acts as a general marker to guide the motor neuron to the central region of the muscle fiber.

Upon innervation, prepatterned AChR clusters that are not directly opposing the motor neuron terminal are rapidly dispersed and recruited to the site of innervation (**Figure 1.1A**). The molecular cross-talk between the motor neuron and muscle fiber orchestrates the development and maturation of the NMJ. Among the molecules involved, agrin, a heparin sulfate proteoglycan secreted from the presynaptic terminal, acts as a master organizer of postsynaptic development and stability (McMahan, 1990). Stimulation of the postsynaptic endplate with nerve-derived agrin triggers the assembly and maturation of the postsynaptic apparatus (Cohen et al., 1997; Jones et al., 1997; Meier et al., 1997). Mice deficient in neural agrin do not form functional NMJs, indicating the importance of neural agrin for proper formation and development of neuromuscular synapses (Gautam et al., 1996). To induce the assembly of the postsynaptic compartment, agrin binds to Lrp4 and activates MuSK signaling, leading to increased AChR synthesis and the accumulation of postsynaptic molecules at the site of agrin stimulation (Kim et al., 2008; Zhang et al., 2008). During these early stages of synaptogenesis, the nascent synapse rapidly grows in size and AChR density.

During postnatal development, the maturing synapse undergoes a dramatic morphological, structural, and molecular transformation. First, a muscle fiber, which is

initially innervated by multiple motor neuron terminals, will become singly innervated through synapse elimination, leaving one NMJ per muscle fiber (Wyatt and Balice-Gordon, 2003). Second, striking morphological alterations occur at the postsynaptic terminal of the muscle fiber, a process referred to as the plaque-to-pretzel transition (**Figure 1.1B**). Early oval-shaped AChR clusters with uniform AChR density begin to develop multiple, large AChR-poor perforations within the AChR cluster, which ultimately transform into elaborate AChR-rich branches resembling the shape of a pretzel (Marques et al., 2000). Throughout this process, the presynaptic terminal precisely mirrors the changes occurring at the postsynaptic terminal (Slater, 1982). The signaling processes that govern the plaque-to-pretzel transition and the cellular origin of these signaling processes (i.e. from the motor neuron or muscle fiber) remain to be fully determined. However, integral studies using aneurally cultured myotubes have provided some insight. Marques *et al*. revealed that AChR clusters undergo the plaque-to-pretzel transition to a remarkable extent when myotubes are aneurally cultured on a substrate containing the basal lamina component laminin (Marques et al., 2000). These data suggest a muscle-intrinsic role in the maturation of the postsynaptic compartment, however, it is likely that cross-talk between both the motor neuron and muscle fiber directs the full morphological maturation of the postsynaptic compartment. While aneural AChR clusters *in vitro* may not contain all molecular and structural components that make up the NMJ *in vivo*, they do provide a great system to easily and reliably study the various aspects of postsynaptic development.

As the molecular components of the postsynaptic terminal undergoes topographical rearrangement, the postsynaptic compartment begins to develop unique structural features. Specifically, the axon terminal of the motor neuron sinks into the muscle fiber, creating a

depression in the membrane of the muscle called the primary gutter. Within the primary gutter, the postsynaptic membrane develops numerous small folds referred to as junctional folds (**Figure 1.2**). The junctional folds can then be further divided into the crest, representing the top of the folds closest to the presynaptic terminal, and the trough, representing the bottom part of the infolded membrane. Although the precise function of the folds remains to be fully determined, they likely play a role in neurotransmission by providing a platform for the spatial segregation of several key postsynaptic molecules involved in neurotransmission. Most notably, AChRs are restricted to the fold crest, whereas, voltage-gated Na^+ channels (VGSC) are restricted at the trough of the folds (**Figure 1.2B**) (Fertuck and Salpeter, 1974; Matthews-Bellinger and Salpeter, 1983; Flucher and Daniels, 1989). Additionally, molecules within the presynaptic terminal also become spatially segregated relative to the junctional folds. Specialized sites mediating the rapid release of ACh, termed active zones, are localized to the area directly opposite that of the opening of the postsynaptic junctional folds (Couteaux and Pecot-Dechavassine, 1970; Dreyer et al., 1973; Patton et al., 2001). This organization of these key pre- and post-synaptic molecules relative to junctional folds likely helps to increase neurotransmission efficiency. Studies mathematically modeling neurotransmission in the presence or absence of junctional folds suggest they may act to reduce the threshold necessary to reach an action potential, thus making neurotransmission more efficient (Martin, 1994).

In addition to the morphological and structural changes, alterations in the molecular composition of the postsynaptic compartment also occurs during early postnatal development. AChRs are composed of five subunits: two alpha subunits, one beta, one delta, and either one gamma or epsilon subunit (Takai et al., 1985). During the early stages

of postnatal development, the embryonic γ AChR subunit is replaced by the adult ε AChR subunit conferring increased calcium conductance of the receptor as well as increased half-life of the receptor (Missias et al., 1996; Villarroel and Sakmann, 1996). The switch from embryonic AChRs to adult AChRs also appears to be important for the structural development of the NMJ. Mice lacking the adult AChR ε subunit retain the embryonic AChR γ subunit throughout development and subsequently fail to fully form junctional folds (Missias et al., 1997), suggesting that the molecular composition of AChRs is not only important for proper AChR function, but is also crucial for the structural development of the NMJ.

1.3 Neurotransmission

Within the fraction of a second it takes to initiate and complete muscle contraction, many processes at the cellular and molecular level must occur. In order to initiate muscle contraction, an electrochemical signal, in the form of an action potential, is sent from neurons residing in the brain to motor neurons located within the spinal column. The action potential, which is represented as a depolarization of the electrochemical gradient across the cell membrane, travels down the long motor neuron axon arriving at the presynaptic terminal of the NMJ. Electron microscopy (EM) studies have shown that numerous vesicles containing the neurotransmitter ACh are concentrated at active zones within the presynaptic terminal (Rowley et al., 2007). The arrival of the action potential triggers the rapid fusion of ACh-containing vesicles to the presynaptic membrane, expelling a large amount of ACh (approx. 10,000 molecules/quantum) into the synaptic space (Kuffler and Yoshikami, 1975). Seminal research by Heuser & Reese using rapid freeze EM captured the steps of the docking and fusion of ACh-containing vesicles during synaptic

transmission (Heuser et al., 1979; Heuser and Reese, 1981). These landmark studies confirmed that active zones are specialized sites for the docking and fusion of neurotransmitter-containing vesicles. EM studies have also determined that active zones are located directly opposite that of the opening of junctional folds (Couteaux and Pecot-Dechavassine, 1970; Dreyer et al., 1973; Patton et al., 2001). Thus, in response to an action potential, ACh is released from the presynaptic active zones into the area of junctional fold openings, where it will bind to and activate AChRs densely clustered along the crest of junctional folds (approx. 10,000 – 20,000 AChRs/μm^2) closest to the presynaptic terminal (**Figure 1.2B**) (Porter and Barnard, 1975b).

AChRs are ligand-gated ion channels that open upon binding of ACh molecules, resulting in the influx of cations and depolarization of the electrochemical gradient across the muscle membrane. If depolarization reaches a certain threshold, an action potential is initiated in the muscle fiber, ultimately result in contraction of the muscle. The unbound ACh in the synaptic cleft is quickly degraded by the ACh-hydrolyzing enzyme acetylcholinesterase (AChE) located throughout the synaptic basal lamina (Colquhoun and Sakmann, 1985). This prevents AChRs from being repeatedly activated from a single release of ACh, and thus, allows for tight regulation of neurotransmission. A disruption in any of the steps between initiation and completion of muscle contraction ultimately negatively impacts muscle function, and is the basis of all neuromuscular disorders.

1.4 Molecular composition & signaling of the NMJ

An in-depth understanding of NMJ development requires not only detailed observation of synaptogenesis and postsynaptic maturation, but also consideration of the molecular signaling underlying these processes. After researchers determined that the motor neuron

organizes AChR clustering at the site of innervation (Anderson and Cohen, 1977; Burden et al., 1979), many groups set off to determine the clustering agent(s) responsible. In the 1980's McMahan and colleagues isolated agrin, aptly named from the Greek word meaning 'to assemble' (Nitkin et al., 1987). Since then, many of the nerve-derived and muscle-derived signaling processes that lead to the formation and maturation of the NMJ have been identified. In this section, we will focus on the molecular components and signaling processes that govern the formation and maturation of the postsynaptic terminal.

Three processes underlie the topographical distribution of AChR clusters during development: clustering of diffuse AChRs, activation of AChR transcription in synaptic nuclei, and the dispersal of non-synaptic AChRs. Each of these processes work in concert with one another to orchestrate and maintain AChR density and organization. At the heart of these processes are two counteracting nerve-derived factors: agrin and acetylcholine. Agrin is a potent inducer of AChR synthesis and clustering, whereas, exposure to ACh causes the dispersal of AChRs (Goldman et al., 1988; Cohen et al., 1997; Jones et al., 1997; Meier et al., 1997). This delicate balance between AChR inducing and dispersing factors is responsible for forming and maintaining a high density of AChRs at the postsynaptic membrane (10,000 – 20,000 AChRs/μm^2) and a drastically reduced AChR density in extrasynaptic regions (<10 AChRs/μm^2) (Porter and Barnard, 1975b, a; Salpeter et al., 1988).

1.4.1 AChR clustering

During synaptogenesis, agrin secreted from the presynaptic terminal activates MuSK through binding to the MuSK co-receptor Lrp4, which then associates with the cytoplasmic Dok-7 protein (Okada et al., 2006; Kim et al., 2008). The activation of MuSK initiates

several signaling pathways, ultimately leading to upregulation of AChR synthesis in synaptic nuclei and increased AChR clustering at the site of agrin stimulation (Sander et al., 2001). Although the initial clustering of AChRs during muscle prepatterning occurs independent of agrin, the subsequent formation and maturation of AChR clusters does depend on nerve-derived agrin exposure (Yang et al., 2001; Samuel et al., 2012). Evidence for the critical role of agrin came from gain- and loss-of-function studies. Notably, ectopic expression of neuronal agrin in mice led to the formation of extrasynaptic agrin patches, where surprisingly complete postsynaptic compartments formed in direct opposition to the agrin patches (Cohen et al., 1997; Jones et al., 1997; Meier et al., 1997; Rimer et al., 1997). Conversely, very few AChR clusters and postsynaptic specializations formed at nerve-muscle contacts in agrin knockout mice (Gautam et al., 1996). These studies confirmed the hypothesis proposed years earlier by McMahan, stating that agrin is an essential nerve-derived organizer of postsynaptic differentiation (McMahan, 1990).

The Lrp4–MuSK–Dok-7 complex is, arguably, an equally important component in the signaling pathway leading to AChR clustering. This complex is required not only for AChR clustering during synaptogenesis, but also for the formation of prepatterned AChR clusters before innervation (Lin et al., 2001; Yang et al., 2001; Okada et al., 2006; Weatherbee et al., 2006). Like agrin-deficient mice, mice lacking any component of the Lrp4–MuSK–Dok-7 complex fail to form prepatterned AChR clusters as well as nerve-induced postsynaptic specializations, and as a result die shortly after birth due to respiratory failure (DeChiara et al., 1996; Okada et al., 2006; Weatherbee et al., 2006).

Downstream of MuSK signaling lies a critical component for the clustering of AChRs: the membrane-associated cytoplasmic protein, rapsyn. Rapsyn directly binds to AChRs to

cluster and stabilize them at the postsynaptic membrane (Gautam et al., 1995). Evidence for the AChR clustering role of rapsyn come from studies showing that AChRs are evenly dispersed when ectopically expressed in non-muscle cells, but when co-expressed with rapsyn form dense AChR clusters (Froehner et al., 1990; Phillips et al., 1991). Additionally, AChR clusters do not form in mice deficient in rapsyn (rapsyn$^{-/-}$), and instead are diffusely distributed, even in the presence of agrin stimulation (Gautam et al., 1995). Thus, rapsyn is indispensable for AChR clustering. Overall, these studies reveal several presynaptic and postsynaptic components that are fundamental in the formation and maintenance of AChR clusters.

1.4.2 AChR dispersal

At the adult NMJ, AChRs are highly concentrated at the postsynaptic membrane and quickly decrease in concentration moving away from the synaptic area. Shortly after innervation by the motor neuron, the amount of extrasynaptic AChRs declines rapidly. Studies found that after denervation the density of extrasynaptic AChRs increased as a result of increased transcription of AChR genes in extrasynaptic nuclei (Merlie et al., 1984; Tsay and Schmidt, 1989). Researchers proposed two explanations for these results: the motor neuron secretes an extrasynaptic AChR-repressive factor, or the electrical activity present during innervation causes a decrease in extrasynaptic transcription of AChR genes. Eventually, evidence was provided showing that electrical activity of the synapse caused a decrease in extrasynaptic AChR transcription, supporting the hypothesis that synaptic activity is responsible for extrasynaptic AChR dispersal (Goldman et al., 1988). Thus, in a fascinating turn of events, the activation of AChRs through synaptic transmission (i.e.

ACh release) negatively regulates distant, extrasynaptic AChRs and the local, synaptic AChRs are, in a sense, resistant to this negative regulation.

1.4.3 Synaptic basal lamina

The NMJ is unique compared to synapses in the central nervous system in that a basal lamina runs through its synaptic cleft (Singhal and Martin, 2011). Compared to the basal lamina ensheathing the non-synaptic area of the muscle fiber, the synaptic basal lamina exhibits a distinct composition and organization of extracellular matrix (ECM) proteins, each of which play important roles in the formation and maintenance of the NMJ. The synaptic basal lamina, extending through the synaptic cleft and into the junctional folds, contains three main types of ECM proteins: heparan-sulfate proteoglycans (i.e. agrin), laminins, and collagens. As discussed above, agrin deposited by the presynaptic terminal is an essential regulator of postsynaptic formation and maintenance. Laminins and collagens, which are synthesized and deposited by the muscle, are primarily involved in the maturation and maintenance of both the pre- and postsynaptic terminals.

Laminins are glycoproteins that are comprised of three distinct subunits (α/β/γ) and play crucial structural and signaling roles within the ECM (Domogatskaya et al., 2012). Within the synaptic basal lamina, three laminin heterotrimers are present: laminin α2β2γ1, laminin α4β2γ1, and laminin α5β2γ1 (Patton et al., 1997). Synaptic laminins have been found to play important roles in various parts of presynaptic and postsynaptic maturation. First, synaptic laminins are involved in ensuring proper maturation of the presynaptic terminal. Notably, laminin β2 has been shown to regulate proper formation and distribution of active zones and synaptic vesicles through its interaction with voltage-gated calcium channels on the presynaptic terminal (Nishimune et al., 2004; Chen et al., 2011b).

Mice lacking laminin β2 have fewer active zones and the synaptic vesicles are dispersed throughout the terminal, instead of clustered at active zones (Noakes et al., 1995). Additionally, the synaptic cleft is infiltrated by processes from the terminal Schwann cell, the myelinating glial cell of the peripheral nervous system responsible for capping the NMJ (Noakes et al., 1995). This infiltration of Schwann cell processes could be representative of decreased synaptic adhesion as a result of the lack of laminin β2. Second, synaptic laminins also play important roles in the development of the postsynaptic terminal. In addition to the presynaptic defects, laminin β2-deficient mice also exhibited fewer junctional folds and the folds that were present were significantly stunted (Noakes et al., 1995), suggesting that laminin β2 is a critical determinant for properly formed synaptic architecture. The strong pre- and post-synaptic phenotypes from laminin β2-deficient mice can likely be attributed to that fact that laminin β2 is a component of all three laminin heterotrimers within the synaptic basal lamina. Alternatively, mice lacking laminin α5 showed significant delays in the plaque-to-pretzel transition (Nishimune et al., 2008). This phenotype was magnified in mice lacking both laminin α5 and laminin α4 (Nishimune et al., 2008), suggesting that laminin α5 and laminin α4 may play a role in the plaque-to-pretzel transition of AChR clusters. Third, synaptic laminins are also involved in ensuring proper alignment of the presynaptic and postsynaptic terminals. Work from Joshua Sanes lab showed that laminin α4 is necessary for the proper alignment of active zones and junctional folds. Unlike laminin β2-deficient mice, laminin α4-deficent mice have normal numbers of active zones and junctional folds, but these structures are no longer aligned with one another (Patton et al., 2001). Interestingly, laminin α4 localization is restricted to a small region at the crest of junctional folds (**Figure 1.2B**) (Patton et al., 2001), placing

it in the ideal location to mediate the alignment of active zones with junctional folds. Overall, synaptic laminins are necessary for defining and aligning synaptic ultrastructures of both the pre- and postsynaptic terminals during development.

Members of the collagen superfamily are an important and abundant part of the muscle basal lamina, involved in various aspects of muscle development. At the synaptic basal lamina, collagens are primarily involved in the maturation and maintenance of the adult NMJ. Specifically, collagen IV has been found to be crucial for maintenance of the adult NMJ. Collagen IV is not expressed at the synapse until very late in development, approximately three weeks after birth, after the NMJ has taken on the adult form (Fox et al., 2007). As one would expect, mice lacking collagen IV do not exhibit any NMJ defects at three weeks postnatal, since collagen IV is not expressed until this time. However, by two months of age, collagen IV-deficient mice exhibit fragmented presynaptic and postsynaptic terminals, where some parts of the presynaptic terminal are partially retracted leaving AChR-rich branches unopposed (Fox et al., 2007). Like collagen IV, collagen XIII also appears to be important for maintaining synaptic adhesion. Analogous to collagen IV expression, collagen XIII is not present at the synaptic cleft until approximately two weeks of age (Latvanlehto et al., 2010). Additionally, collagen XIII-deficient mice show incomplete adhesion of the pre- and postsynaptic terminals to the synaptic basal lamina at the NMJ (Latvanlehto et al., 2010).

The collagen-like protein collagen Q (ColQ) plays a different role within the synaptic basal lamina than the adhesion and maintenance role of collagen IV and collagen XII. Although ColQ is structurally similar to other collagen proteins, it is not considered a canonical member of the collagen family of proteins (Ricard-Blum, 2011). Instead, ColQ

acts as a structural subunit of the ACh-hydrolyzing enzyme acetylcholinesterase (AChE) (Krejci et al., 1997; Massoulie and Millard, 2009). The binding of ColQ to the catalytic subunits of AChE creates a collagen tail on the AChE/ColQ hetero-oligomer, which is necessary to anchor AChE within the synaptic cleft (Singhal and Martin, 2011). In the absence of ColQ, AChE is unable to localize to the synaptic cleft, causing an inability to degrade ACh in order to terminate neurotransmission (Feng et al., 1999). As a result, ColQ-deficient mice die within the first month after birth (Feng et al., 1999). Thus, the various forms of synaptic collagens and collagen-like proteins each play distinct roles in ensuring proper synaptic adhesion and neurotransmission.

1.5 Postsynaptic cytoskeleton

The postsynaptic cytoskeleton plays crucial roles in the overall formation and development of the NMJ. Actin filaments and microtubules concentrated within the postsynaptic compartment are involved in the structural support and stability, trafficking of postsynaptic molecules, and dynamic topological reorganization. Recently, intermediate filaments have also been implicated in maintaining the overall structural integrity of postsynaptic specializations. This section will cover the critical functions of the postsynaptic cytoskeleton and some outstanding questions remaining in the field.

1.5.1 Actin biology

The actin cytoskeleton is a crucial part of all aspects of cell biology, including structural support of the cell, cell migration, and trafficking to name a few (Pollard and Borisy, 2003). Actin is a highly versatile molecule where individual actin monomers (globular actin, G-actin) can bind to one another creating a filamentous actin (F-actin) polymer. The

polymerization of G-actin into F-actin is a reversible process referred to as depolymerization. Actin filaments are polarized structures, where actin monomers are preferentially added to the (+) end of actin filaments and disassembled from the (-) end (Blanchoin et al., 2014). The ability of actin to easily fluctuate between G-actin and F-actin lies at the core of its diverse functionality. The organization and dynamics of actin networks is tightly controlled by numerous actin binding proteins (dos Remedios et al., 2003). Actin binding proteins modulate actin behavior and structure through various means including: promotion or inhibition of polymerization/depolymerization, stabilization of filaments, bundling of filaments, and branching of filaments (Pollard, 2016). This coordinated regulation of actin by actin binding proteins lies at the heart of actin's diverse functionality throughout the cell. For example, the polymerization of actin provides the mechanical force necessary for a variety of membrane processes, including coalescence of membrane associated proteins, endocytosis, and exocytosis (Lanzetti, 2007). Thus, the actin cytoskeleton, together with an arsenal of actin binding proteins, are powerful regulators of vast cellular functions.

1.5.2 Two pools of actin at the NMJ

At the NMJ, several actin binding proteins work in concert with actin to give rise to the various functions of the postsynaptic actin cytoskeleton. Specifically, two pools of actin filaments—stable and dynamic—are critical for the overall development and maintenance of the NMJ. The pool of stable actin filaments provides a stable scaffold for AChRs and other postsynaptic components (Hall et al., 1981). As AChRs begin to cluster at the nascent NMJ, AChRs associate with the postsynaptic actin cytoskeleton, increasing the overall stability of the receptors and anchoring them within the postsynaptic membrane.

AChRs are linked to the underlying actin cytoskeleton through association with rapsyn and/or the dystrophin-glycoprotein complex (Banks et al., 2003). The transmembrane dystrophin-glycoprotein complex connects AChRs to the synaptic basal lamina and the postsynaptic actin cytoskeleton, and thus, provides a secure anchorage for AChRs within the postsynaptic membrane (Ervasti and Campbell, 1993). Whereas, the cytoplasmic rapsyn only links AChRs to the postsynaptic actin network (Antolik et al., 2007). As discussed earlier, the association of AChRs and rapsyn is crucial for the stabilization and clustering of AChRs. The association of AChR–rapsyn complexes with stable actin filaments further stabilizes AChR clusters (Moransard et al., 2003). Several studies have found that rapsyn is able to bind actin filaments directly as well as indirectly through various actin binding proteins, including α-actinin, the cytoskeletal associated protein β-catenin (which binds actin via α-catenin), and the molecular chaperone heat-shock protein 90β (Hsp90β) (Antolik et al., 2007; Zhang et al., 2007; Dobbins et al., 2008; Luo et al., 2008). Hsp90β, which acts to stabilize rapsyn, has also been suggested to cross-link branched actin filaments (Park et al., 2007). It remains to be seen whether AChR–rapsyn complexes associate directly or indirectly with actin *in vivo*. Nonetheless, whether connecting directly or indirectly through rapsyn or the dystrophin-glycoprotein complex, linking AChRs to a network of stable actin filaments is crucial in order to stabilize and maintain AChR clusters.

In contrast to the scaffolding role of stable actin filaments, a pool of highly dynamic actin is required for the trafficking of postsynaptic molecules and the topographical reorganization of the postsynaptic compartment. In the search to identify what regulates the initial clustering of AChRs, Dai *et. al.* found that dynamic actin is enriched at AChR

clusters (Dai et al., 2000). Subsequent experiments revealed that pharmacological disruption of actin dynamics inhibited the formation of new AChR clusters in response to agrin stimulation, indicating dynamic actin may be necessary for the trafficking and clustering of AChRs (Dai et al., 2000). Since that time, several known regulators of actin dynamics have been found to localize to AChR clusters. Namely, work from previous members of the Zheng Lab found that the actin severing protein cofilin is an important regulator of AChR clustering through the modulation of actin dynamics (Lee et al., 2009). Manipulation of cofilin activity or knockdown of cofilin expression resulted in a significant reduction in AChR clustering (Lee et al., 2009). Additionally, live-cell imaging revealed that cofilin localizes to the site of focal agrin stimulation prior to the arrival of AChRs, suggesting that disassembly of the stable cortical actin network may be an important step in the clustering of AChRs (Lee et al., 2009). Several studies have also found that a concentration of highly dynamic actin, actin binding proteins, vesicular trafficking components, and AChR-containing vesicles is present within AChR cluster perforations, suggesting that AChR perforations may represent sites for the endocytosis and exocytosis of AChRs and various postsynaptic components (Lee et al., 2009; Proszynski et al., 2009).

Dynamic actin has also been found to be involved in the topographical reorganization of AChR clusters. New AChRs trafficked to perforations are rapidly incorporated into existing AChR branches, suggesting dynamic actin within perforations may also be involved in the redistribution of AChRs in order to maintain perforations free of AChRs (Bruneau and Akaaboune, 2006). In agreement with this, Proszynski *et al.* found that podosomes, dynamic actin-rich adhesive organelles involved in remodeling the ECM, are localized to AChR perforations. Live-cell imaging showed that the growth and movement

of podosomes directly correlated with the growth and shape of the associated AChR cluster perforation (Proszynski et al., 2009), suggesting that these synaptic podosomes might be involved in the redistribution of AChRs during the plaque-to-pretzel transition.

Several studies aimed at determining signaling pathways regulating the clustering of AChRs further highlight the importance of dynamic actin in this process. Specifically, studies have found that agrin-induced activation of MuSK leads to activation of the small guanosine triphosphatases (GTPases) Rac, Rho, and Cdc42, all of which promote increased actin dynamics at the site of agrin stimulation (Weston et al., 2000). It has been suggested that the promotion of actin polymerization through the activation of these GTPases generates the force necessary to coalesce small AChR clusters during cluster formation, or rearrange AChRs during the plaque-to-pretzel transition (Weston et al., 2000; Tintignac et al., 2015).

Although dynamic actin is clearly involved in the redistribution of AChRs, the underlying mechanism remains unclear. Specifically, what signaling molecules or events initiate the topographical redistribution of AChR clusters? Does this signaling originate from the motor neuron and/or muscle fiber? Experiments have shown that AChR clusters are able to undergo a similar, yet incomplete, plaque-to-pretzel transition in the absence of neuronal input, suggesting that both the motor neuron and muscle fiber likely contribute to this process. However, the precise mechanism remains to be elucidated.

1.5.3 Microtubules

In addition to the actin cytoskeleton, the trafficking of AChRs also dependent upon a microtubule network at the postsynaptic compartment. Recent work by Schmidt and Basu *et al.* showed that a dense network of both dynamic and stable microtubules associates with

the postsynaptic compartment, appearing as a tangled cage of microtubules beneath the postsynaptic membrane (Schmidt et al., 2012). This dense network of microtubules forms in response to agrin stimulation and is responsible for the focal delivery of AChR-containing vesicles via microtubules. Specifically, exposure to agrin triggered local capture of the growing plus-end of dynamic microtubules at the synapse, but not in extrasynaptic regions (Schmidt et al., 2012). This local microtubule capture is mediated in large part by the microtubule plus-end tracking protein, cytoplasmic linker associated protein 2 (CLASP2) (Schmidt et al., 2012). The captured microtubules then provide local delivery of AChR-containing vesicles to the postsynaptic compartment. The subsequent insertion of the microtubule-delivered AChRs into the postsynaptic membrane, however, is dependent on dynamic actin (Schmidt et al., 2012).

1.5.4 Intermediate filaments

Intermediate filaments (IFs), the third element of the cytoskeleton, are composed of a family of related proteins that are structurally and molecularly similar to one another. IFs are different from actin and microtubules in that they are much more flexible and elastic, and less dynamic than actin or microtubules (Mucke et al., 2004; Kreplak et al., 2008), yet stiffen in response to mechanical stress (Janmey et al., 1991). Desmin, a muscle-specific IF, is the most abundant IF in muscle and plays a critical role in maintaining the structural and mechanical integrity of muscle cells (Paulin and Li, 2004). Several studies have found desmin enriched at the postsynaptic compartment of the NMJ (Burden, 1982; Sealock et al., 1989; Mitsui et al., 2000). However, until recently the function of desmin IFs at the NMJ was unclear. Several recent studies have shown that the synapse-specific IF-associated cytoplasmic linker protein, plectin, links IFs to various postsynaptic molecules,

including AChRs, the dystrophin-glycoprotein complex, and the scaffolding protein ankyrin (Rezniczek et al., 2007; Hijikata et al., 2008; Maiweilidan et al., 2011; Mihailovska et al., 2014). The plectin-associated IFs also associate with the contractile apparatus serving to connect the postsynaptic compartment to the contractile apparatus (**Figure 1.2**), which is thought to be crucial for maintaining the structural integrity of the postsynaptic NMJ following muscle contraction (O'Neill et al., 2002; Mihailovska et al., 2014). Mihailovska *et al.* found that knockout of the IF linker plectin caused IFs to retract from the postsynaptic compartment, resulting in fragmentation of AChR clusters and degeneration of junctional folds (Mihailovska et al., 2014). In agreement with this, the NMJs of desmin deficient mice are notably disorganized and junctional folds are often absent or significantly reduced (Agbulut et al., 2001). Thus, linking the postsynaptic compartment to the contractile apparatus via IFs is crucial to maintaining the overall structural integrity of the NMJ—including junctional fold architecture and AChR cluster stability and immobilization—during muscle contraction. The unique structural properties of IFs make them optimally suited to provide the strong, yet flexible, structural support necessary to maintain postsynaptic architecture during the cellularly disruptive process of muscle contraction.

1.5.5 Complementary roles of the postsynaptic cytoskeleton

Actin, microtubules, and IFs each play distinct roles, all of which are vital for the development and maintenance of the postsynaptic terminal. Although research into the precise mechanisms of each of these cytoskeletal components is still on-going, the general role of each is summarized below.

IFs appear to be responsible for the global structural integrity of the synapse by providing the strong, yet flexible support system necessary for the synapse to withstand the mechanical force exerted during muscle contraction. While stable actin filaments are responsible for providing local structural stability to AChRs and the postsynaptic membrane, dynamic actin filaments appear to be necessary for the topographical reorganization of AChRs and the local insertion of molecules into the postsynaptic membrane. Lastly, microtubules and microtubule-associated proteins are primarily responsible for the transport and delivery of AChR-containing vesicles to the postsynaptic compartment.

1.6 Diseases of the NMJ

A number of diseases and environmental toxins can impact synaptic transmission at the NMJ. These diseases can target the presynaptic, synaptic, or the postsynaptic portion of the synapse, and are all characterized by varying degrees of muscle weakness (Ha and Richman, 2015). Often, these diseases disrupt the architecture and structure of the synapse, which has profound consequences on neurotransmission, and thus, proper muscle function (Hirsch, 2007; Slater, 2008). Therefore, these diseases are a prime example of how the structure of the NMJ is intricately linked to its function. A key goal of this dissertation is to obtain a comprehensive understanding of the architectural elements of the postsynaptic terminal, including AChR organization. Determining the intricacies of synaptic architecture and structure will inevitably afford a better understanding of the functional aspects of the NMJ, providing a foundation for the development of better treatments for such neuromuscular diseases. This section will touch on a few select diseases that impact the NMJ.

1.6.1 Amyotrophic lateral sclerosis

Of all the diseases affecting the neuromuscular system, ALS is arguably the most well-known and well-studied disease. ALS—also known as Lou Gehrig's disease—is a lethal and debilitating neurodegenerative disease in which motor neurons progressively die off causing cumulative muscle weakness (Calvo et al., 2014). The rate of progression and severity of the disease varies from patient to patient; however, the average life expectancy of an ALS patient is approximately 3 years from the initial onset of symptoms (Labra et al., 2016). As the disease progresses, muscle weakness becomes more widespread with some muscles becoming paralyzed. In the end, most patients die from respiratory failure as a result of the severe weakening of the diaphragm and the associated muscles required for breathing. There is currently no cure for ALS, and only two medications have been approved by the Food and Drug Administration to help slow the progression of the disease (Scott, 2017).

Although ALS is well-known (recently popularized by the 'Ice Bucket Challenge' that went viral on social media), it is a relatively rare disease with approximately 5 – 6 cases per 100,000 individuals (Chio et al., 2013). There are two types of ALS—sporadic and familial. Sporadic ALS, in which there is no known family history of the disease, accounts for the vast majority of cases (approx. 95%). The remaining 5% of cases are familial, in which there is a genetically inherited component (Byrne et al., 2011). A handful of specific gene mutations and environmental factors have been associated with an increased risk of developing ALS. However, despite extensive research, the cause of motor neuron degeneration remains unknown. Specifically, it is unclear whether the initial degeneration and dysfunction of motor neurons originates from issues with the upper motor neurons

associated with the motor cortex of the brain, or from issues at the NMJ. In principle, the motor neuron axon degeneration could be caused by the lack of neurotrophic factors secreted by the postsynaptic muscle cell (Campanari et al., 2016). Also, loss of AChRs on the muscle surface could lead to the disruption of the NMJ and axonal terminal withdrawal. Thus, more research into the cause of ALS and the role of the NMJ is crucial to determining the etiology of the disease as well as developing more effective treatments for patients.

1.6.2 Myasthenia gravis

Myasthenia gravis (MG), derived from Greek and Latin words meaning "grave muscle weakness", is the most prevalent disease that affects the postsynaptic terminal of the NMJ, with approximately 20 cases per 100,000 people (Robertson et al., 1998; Phillips, 2003). MG is a chronic autoimmune disease that clinically presents as severe muscle weakness that worsens after periods of activity and improves after rest (Mahadeva et al., 2008). These symptoms typically impact muscles of the eyes and face, including muscles involved in eye movement, talking, chewing, swallowing, and breathing. The most common symptoms of MG patients are drooping eyelids, blurred vision, difficulty breathing, slurred speech, and chronic muscle fatigue in the arms and legs (Berrih-Aknin et al., 2014). Although there is currently no cure for this disease, the prognosis of MG is not as 'grave' as the name may suggest. With the combination of immunosuppressant therapy and other treatments, patients usually have a relatively standard quality of life with normal life expectancy. However, approximately 20% of patients experience a myasthenic crisis in which the muscles required for breathing weaken to the point where breathing is significantly impaired and requires immediate medical attention (Alshekhlee et al., 2009). Thus, current therapies could stand to improve from continued research.

Physiologically, MG patients produce antibodies to various postsynaptic components resulting in blockage or degradation of the molecule, hindering the ability of postsynaptic terminal to effectively respond to neurotransmission. The vast majority of patients (approx. 85%) produce antibodies targeted to AChRs (Meriggioli, 2009). At the cellular level, the presence of anti-AChR antibodies causes a number of changes to the postsynaptic terminal. Namely, the binding of anti-AChR antibodies causes the internalization and degradation of AChRs, resulting in the reduction of the number of effective AChRs at the postsynaptic membrane by approximately one-third (Corey et al., 1987). Additionally, patients typically have fewer junctional folds and widened synaptic cleft (Lindstrom, 2000). Therefore, understanding the mechanisms that govern the development and maturation of AChR clusters as well as the postsynaptic architecture is essential for developing more effective treatments for patients with MG.

1.6.3 Congenital myasthenic syndromes

Congenital myasthenic syndromes (CMS) are a heterogeneous group of genetic disorders that can affect the presynaptic, synaptic, or postsynaptic portion of the NMJ (Engel et al., 2003). Approximately 85% of CMS cases involve mutations in postsynaptic molecules (Ha and Richman, 2015). The most prevalent of these involve mutations in AChR subunits, which can cause defects affecting the rate of channel opening or sensitivity to ACh (Engel et al., 2003). Mutations have also been identified in genes encoding key molecules involved in the clustering of AChRs and maintenance of the synaptic structure, including agrin, MuSK, rapsyn, Dok-7, plectin, and VGSCs (Banwell et al., 1999; Maselli et al., 2003; Tsujino et al., 2003; Chevessier et al., 2004; Beeson et al., 2006; Muller et al., 2007; Huze et al., 2009). Although particular symptoms and time of onset may vary

between the different types of CMS, all CMS disorders can be characterized by significant muscle weakness and fatigability caused by impaired neuromuscular transmission. There is currently no cure for these diseases, instead treatment is tailored based on the patient's type of CMS (Engel, 2007). Thus, an increased understanding of the molecular mechanisms that underlie the various types of CMS is vital to producing more effective treatments and potential cures.

1.6.4 Lambert-Eaton myasthenic syndrome

Lambert-Eaton myasthenic syndrome (LEMS) is a rare autoimmune disorder of the NMJ characterized by impaired neurotransmission (Schoser et al., 2017). Approximately 50 – 60% of cases occur as a paraneoplastic disorder, in which LEMS develops due to an immune response triggered by cancer, most often associated with small cell lung carcinoma (SCLC-LEMS) (O'Neill et al., 1988; Gutmann et al., 1992; Wirtz et al., 2002; Titulaer et al., 2011). The remaining cases occur as an autoimmune disorder in the absence of cancer (Non-tumor, NT-LEMS). In either case, patients typically experience progressive proximal muscle weakness and general fatigue, which is caused by the presence of autoimmune antibodies against the P/Q-type voltage-gated calcium channel (VGCC) (Hulsbrink and Hashemolhosseini, 2014). VGCCs consist of a family of heteromeric multi-subunit complexes expressed in a wide range of cell types (Catterall, 2000). The P/Q-type VGCC, located on the presynaptic terminal, is the main VGCC of the NMJ and is responsible for initiating the release of ACh in response to an incoming action potential (Urbano et al., 2002). In response to depolarization of the presynaptic membrane, the P/Q-type VGCC will open, allowing an influx of calcium ions and triggering the release of ACh into the synaptic cleft (Atlas, 2013). In LEMS patients, the presence of P/Q-type VGCC

autoantibodies results in a significant decrease in functional P/Q-type VGCCs, and thus, a significant decrease in the release of ACh (Lang et al., 1987). This disruption in ACh release is what causes impaired neurotransmission and muscle weakness, as the presynaptic ACh stores and the postsynaptic response to ACh release are both normal (Molenaar et al., 1982).

The prognosis for LEMS patients depends on the type of LEMS diagnosed. Patients with NT-LEMS do not typically have a reduced life expectancy, whereas, SCLC-LEMS patients often die as a result of the cancer (Maddison et al., 2001; Maddison et al., 2017). There is currently no cure for LEMS and treatment is generally focused on managing symptoms (Skeie et al., 2010). Research focused on better understanding P/Q-type VGCCs and NMJ neurotransmission in general is needed for the development of improved treatments or a possible cure for LEMS patients.

1.7 Summary

'Structure equals function' is a common ideology across biology that describes how the structure of something is intimately linked to its function. Indeed, this saying also holds true of the NMJ. For example, as discussed previously, defects in the synaptic architecture and the clustering of AChRs are common phenotypes of many neuromuscular diseases (Hirsch, 2007; Slater, 2008; Ha and Richman, 2015). Therefore, obtaining a comprehensive and accurate understanding of the synaptic architecture and how AChRs and other key molecules are distributed in relation to these structures will provide us with a deeper understanding of NMJ function. While the general organization of AChRs has been characterized throughout synaptogenesis and into adulthood (Marques et al., 2000; Kummer et al., 2004), the precise organization of AChRs and the mechanisms responsible

remain unclear. The overall goal of this dissertation is to better understand the precise organization of AChRs and the processes that orchestrate this organization. This work specifically focuses on the organization of AChRs during the early stages of the plaque-to-pretzel transition as well as in the fully mature synapse (**Figure 1.1B**). The research presented in this dissertation will address three essential questions: 1) What is the nanoscale organization of AChRs during the early stages of the plaque-to-pretzel transition? 2) What process(es) regulates the organization of AChRs? and 3) What is the nanoscale distribution of AChRs along junctional folds in the mature synapse? In Chapter 2, I present original work examining the precise organization of AChRs and the mechanisms regulating AChR clustering during early development using aneurally cultured myoblasts. In Chapter 3, I present novel research assessing the nanoscale distribution of AChRs in the fully mature NMJ. The findings of this dissertation help to address the gaps in our knowledge regarding the nanoscale morphology of AChR clusters at the NMJ.

1.7 Figures

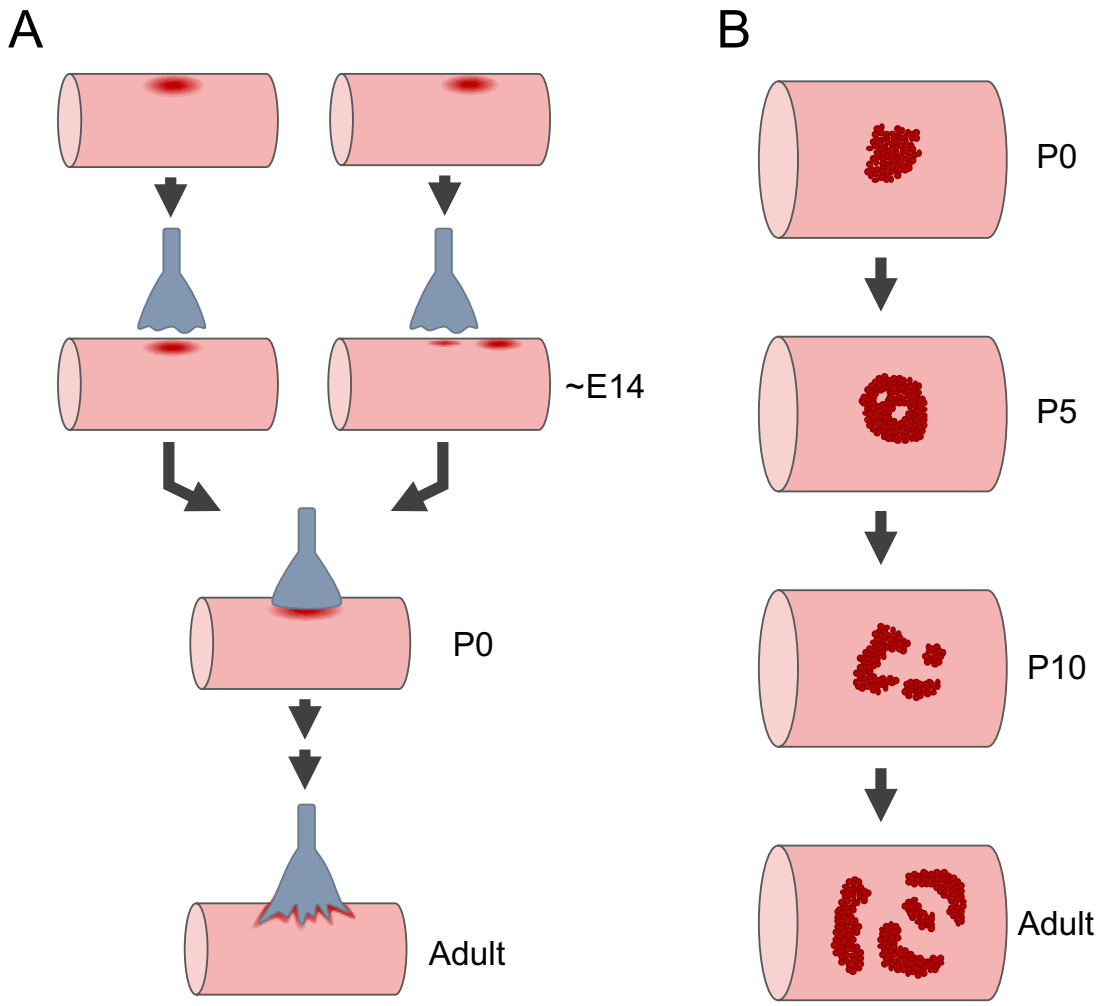

Figure 1.1. Developmental process of the NMJ. **A**, NMJ synaptogenesis throughout development. Before the axon terminal of the motor neuron (blue-grey) innervates the muscle fiber (pink), AChRs will aggregate near the center of the muscle fiber—a process known as pre-patterning. Innervation by the motor neuron can occur either at the site of AChR pre-patterning or where AChRs are absent. AChRs outside of the site of innervation will be trafficked to the nascent synapse. Around the time of birth, the synapse undergoes a dramatic morphological change, referred to as the plaque-to-pretzel transition. During

this time, the synapse will also develop the junctional folds of the postsynaptic terminal. **B**, Plaque-to-pretzel transition of postsynaptic AChR clusters. At the time of birth (P, postnatal day), AChRs (red) are initially clustered into a solid, plaque-shaped cluster at the center of the muscle fiber. Over the next couple of weeks, perforations and branches begin to develop within the AChR cluster. By adulthood, the AChR cluster is transformed into an array of branches that resembles a 'pretzel'-like pattern. Throughout this time, the presynaptic terminal (not shown) precisely mirrors the changes occurring at the postsynaptic terminal.

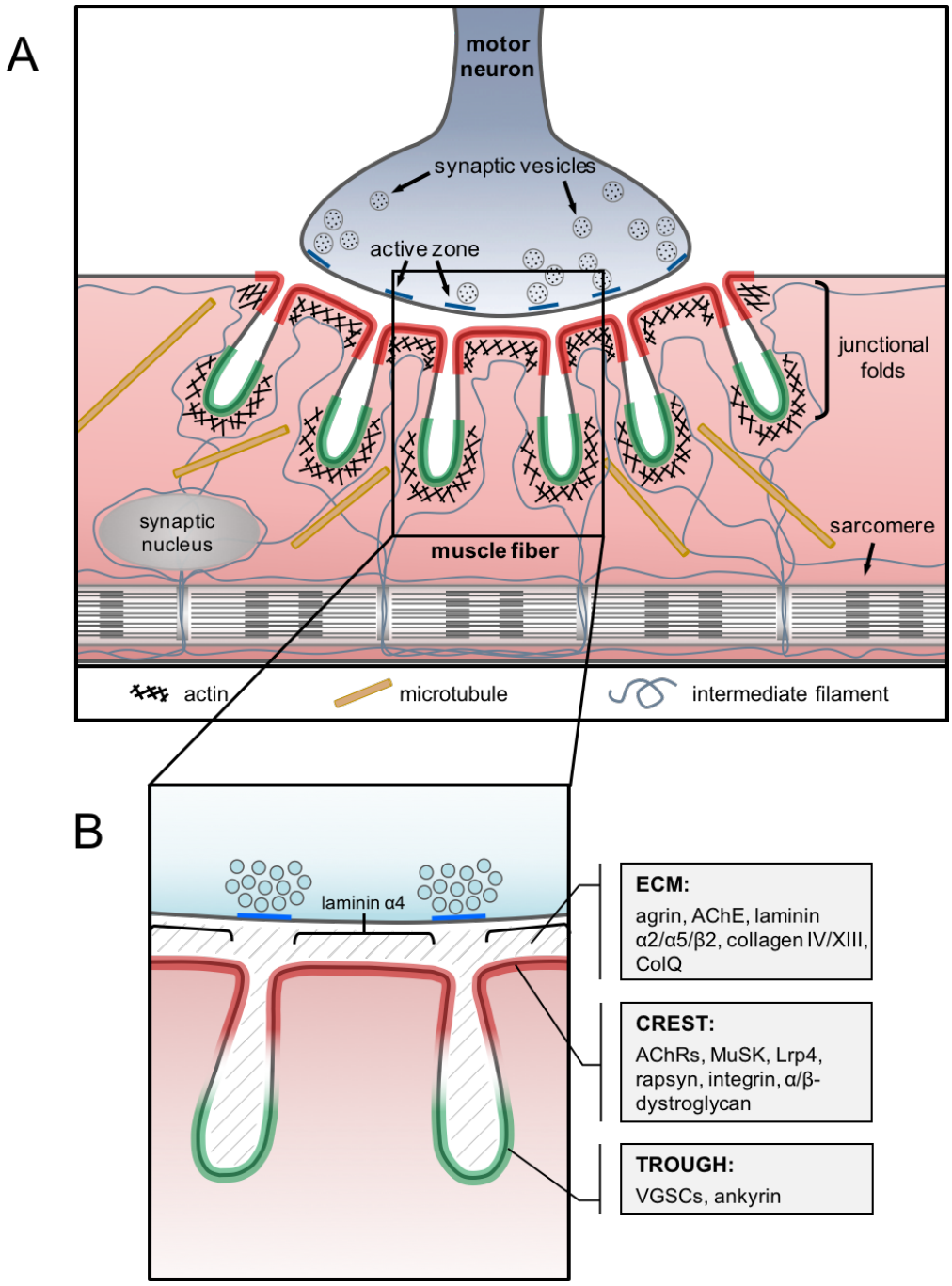

Figure 1.2. Topographical structure and molecular organization of the NMJ. A, Cross section of the adult NMJ depicting the intricate architecture and molecular organization of the postsynaptic terminal. The postsynaptic cytoskeleton—composed of networks of actin, microtubules, and intermediate filaments—plays key roles in ensuring

proper development and maintenance of the postsynaptic structure. The numerous membrane infoldings of the postsynaptic terminal, termed junctional folds, are thought to make neurotransmission more efficient by amplifying the effects of neurotransmitter release. **B**, Many key postsynaptic proteins are spatially segregated to either junctional fold crests (red), closest to the presynaptic terminal, or troughs (green), bottom-most part of the membrane infoldings. The synaptic extracellular matrix (ECM) contains a unique composition of molecular components distributed throughout the synaptic cleft and into the junctional folds. The distribution of laminin α4, however, is restricted within the synaptic cleft to the area above junctional fold crests.

Chapter II

The actin cytoskeleton regulates the clustering of aneural acetylcholine receptors

ABSTRACT

Acetylcholine receptors (AChRs) form densely packed clusters on the postsynaptic membrane of skeletal muscles. During development, these AChR clusters undergo a dramatic structural reorganization, where originally solid oval-shaped AChR plaques morph into an array of multiple AChR-rich branches resembling the shape of a pretzel. Previous studies have shown that the actin cytoskeleton is heavily involved in both the stabilization of AChRs at the postsynaptic membrane as well as the clustering and dynamic reorganization of AChRs. Utilizing aneurally cultured myotubes, we found that AChRs and the postsynaptic cortical actin exhibit a complementary micro-organization to one another, where small, highly dynamic actin puncta are localized within AChR-poor micro-perforations within the aneural AChR cluster. Pharmacological inhibition of dynamic actin puncta resulted in a significant reduction in the accumulation of new AChRs into the aneural cluster membrane. Analysis of molecular components associated with the actin puncta revealed that the actin-associated proteins profilin and cortactin colocalize with actin puncta at aneural AChR clusters. Together, these findings indicate that dynamic actin puncta, along with associated actin binding proteins, are involved in the trafficking and accumulation of AChRs at developing AChR clusters.

This chapter is adapted from:

York AL[1] and Zheng JQ[1, 2, 3] (2017). The actin cytoskeleton regulates the clustering of aneural acetylcholine receptors. *In preparation*.

[1]Department of Cell Biology, [2] Department of Neurology, [3] Center for Neurodegenerative Disease, Emory University School of Medicine, Atlanta, GA 30322

2.1 Introduction

The vertebrate neuromuscular junction (NMJ) undergoes a unique developmental process compared to that of synapses in the central nervous system (Sanes and Lichtman, 1999; Wu et al., 2010; Shi et al., 2012). During early stages of synaptogenesis, before innervation by the motor neuron, acetylcholine receptors (AChRs) will cluster into dense aggregates at the membrane of the developing muscle fiber. This dense clustering of AChRs, referred to as pre-patterning, acts as a landing target for the incoming motor neuron terminal (Lin et al., 2001; Yang et al., 2001; Kim and Burden, 2008). As the nascent synapse begins to mature, the dense AChR clusters will undergo a drastic structural reorganization referred to as the plaque-to-pretzel transition. The originally solid, oval-shaped AChR clusters begin to form multiple large AChR-poor perforations throughout the cluster that merge and elongate, ultimately transforming the cluster into a pretzel-shaped array of multiple AChR-rich branches (Slater, 1982; Balice-Gordon and Lichtman, 1993; Marques et al., 2000). During this process, the motor neuron precisely mirrors the changing shape of the postsynaptic apparatus (Balice-Gordon and Lichtman, 1993), raising the question of whether this process is dictated by the motor neuron and/or the muscle fiber. Compelling evidence revealed that myotubes cultured aneurally on a laminin-coated substrate form AChR clusters that undergo a similar structural reorganization as seen *in vivo* (Kummer et al., 2004), suggesting a muscle-intrinsic role in the maturation of AChR clusters. While aneural AChR clusters *in vitro* may not contain all molecular and structural components that make up the NMJ *in vivo*, they do provide a great system to easily and reliably study the various aspects of NMJ development.

Over the years, much work has been focused on determining the mechanisms responsible for orchestrating NMJ development and has provided many insights into the molecular components involved. Of the molecular components identified thus far, the actin cytoskeleton arguably plays the largest role in the overall development of the NMJ (Dobbins et al., 2006). Two pools of F-actin—stable and dynamic—have been found to play equally important yet opposite roles in the development and maturation of AChR clusters. A stable network of actin filaments is necessary to immobilize AChRs at the postsynaptic membrane through scaffold connections (Hall et al., 1981; Luther et al., 1996), whereas, a highly dynamic pool of actin filaments have been shown to be important for the trafficking and clustering of AChRs (Dai et al., 2000; Lee et al., 2009; Proszynski et al., 2009). In addition to the actin cytoskeleton, several molecules have been identified in the pathway signaling the initial clustering of AChRs, including the heparin sulfate proteoglycan agrin, the muscle-specific kinase (MuSK) receptor, the MuSK co-receptor Lrp4, the cytoplasmic adaptor docking protein-7 (Dok-7), and the AChR scaffolding protein rapsyn just to name a few (Gautam et al., 1995; Bezakova and Ruegg, 2003; Okada et al., 2006; Kim and Burden, 2008; Kim et al., 2008; Zhang et al., 2008). In contrast, the mechanisms that orchestrate the spatiotemporal maturation of AChR clusters remain unclear.

Here, we utilized aneurally cultured myoblasts to determine the actin-involved processes that underlie the formation and maturation of AChR clusters. Using super-resolution microscopy, we identified a novel nanoscale organization of AChRs within developing aneural AChR clusters, where clusters are composed of AChR-poor micro-perforations and AChR micro-puncta. Similarly, the cortical actin cytoskeleton associated

with aneural AChR clusters also exhibits a distinct organization compared to actin in the surround cell area. In the area surrounding AChR clusters, actin is primarily organized into long, continuous actin filaments, whereas, small actin puncta are enriched within AChR clusters. Additionally, the actin puncta enriched at AChR clusters were found to be highly dynamic and involve the actin binding protein, Arp2/3, responsible for initiating branched actin networks. Finally, attenuation of actin dynamics resulted in a significant decrease in AChR accumulation at aneural clusters. These findings suggest that the highly dynamic actin puncta play a role in the trafficking and accumulation of AChRs at developing AChR clusters.

2.2 Results

2.2.1 AChR and actin organization at aneural AChR clusters

Throughout this study, we utilized the aneural myoblast culture system (**Figure 2.1**). Primary myoblasts differentiated on a laminin-coated substrate form AChR clusters that mature to a remarkable extent in the absence of neuronal input (Kummer et al., 2004), providing an easy and reliable system to study the formation and development of AChR clusters. To examine the role of the actin cytoskeleton in AChR clustering, we analyzed the nanoscale spatial relationship between the actin cytoskeleton and aneural AChR clusters using super-resolution microscopy techniques. AChRs and F-actin were co-labeled in differentiated myotubes using fluorescently-tagged BTX and phalloidin, respectively, then imaged using Structured Illumination Microscopy (SIM) and Stochastic Optical Reconstruction Microscopy (STORM). First, analyzing AChR staining we found that AChRs are organized into what we have classified as micro-puncta and micro-

perforations (**Figure 2.2A**, arrow and arrowhead). Upon closer examination, a higher concentration of AChRs appears to outline the micro-perforations, which are typically approximately 1 μm in diameter (**Figure 2.2B**). To confirm that the micro-perforations are not a consequence of the fixation method employed, we performed live-cell STORM imaging of differentiated myotubes. We found that AChR micro-perforations and micro-puncta were also present when imaged in live cells, suggesting they are not a product of fixation (**Figure 2.2C**).

Next, we analyzed the underlying actin cytoskeleton and found that F-actin exhibits a distinctive organizational pattern within and surrounding aneural AChR clusters. In the area surrounding aneural clusters F-actin appears as long continuous actin filaments. However, within aneural AChR clusters this filamentous actin pattern is replaced with a punctate pattern of F-actin, where F-actin primarily forms small punctate structures within aneural clusters (**Figure 2.2A**). Interestingly, the majority of actin puncta are located at the center of AChR micro-perforations, where there appears to be a higher concentration of AChRs surrounding individual actin puncta (**Figure 2.2B**). The presence of numerous actin puncta localized to aneural AChR clusters and, specifically, within AChR micro-perforations suggests a potential role for actin puncta in the formation and/or development of AChR clusters.

2.2.2 Dynamic F-actin puncta are concentrated at aneural AChR clusters

To better understand and characterize the actin puncta at aneural AChR clusters, we performed live cell microscopy to analyze the relationship between actin puncta and AChRs over time. To do this, we utilized a lentiviral expression system to express the F-actin probe, F-tractin-tdTomato (Schell et al., 2001), in differentiated myotubes and imaged

over the course of 10 minutes using Total Internal Reflection Fluorescence (TIRF) microscopy. TIRF microscopy allows for the excitation of fluorophores within a very thin optical section of the specimen, therefore minimizing the background fluorescence from outside the focal plane (Fish, 2009). By tilting the excitation laser to the critical angle, the resulting evanescent waves will excite only the fluorophores immediately adjacent to the coverslip. This allows us to selectively analyze the actin network in close proximity to the aneural cluster membrane and eliminate background fluorescence from actin throughout the cell. After performing live-cell TIRF microscopy, we found that the vast majority of F-actin puncta at aneural AChR clusters are highly dynamic (**Figure 2.3A**). Throughout the imaging period F-actin puncta will appear and disappear in and out of the focal plane, with only a few actin puncta remaining static throughout the imaging period (**Figure 2.3A**, panels 1 – 3). These dynamic actin puncta appear to be specific to the AChR clusters, however, puncta are also present in the area surrounding AChR clusters. We, therefore, sought to quantitatively determine if actin puncta are specifically enriched at AChR clusters. To do this we created an intensity projection of the standard deviation of the time lapse series. This results in a single projected image highlighting the dynamic puncta, where the intensity is directly correlated to the dynamics of the actin puncta (i.e. static puncta will have a much lower deviation/fluorescence than dynamic puncta). The number of dynamic puncta was quantified within the AChR cluster, near the cluster (defined as 3 μm away from the cluster), and outside of the cluster. We found the dynamic actin puncta to be significantly enriched within the AChR cluster compared to near and outside the AChR cluster area (**Figure 2.3B**), implying that the actin puncta are specific to aneural AChR clusters. The concentration of highly dynamic actin puncta at aneural AChR

clusters further suggests that dynamic actin puncta may be involved in the clustering of AChRs.

2.2.3 Actin binding proteins associated with aneural actin puncta

To further characterize the actin puncta at aneural AChR clusters, we sought to identify molecular associates of the actin puncta by immunofluorescence. We targeted the actin binding proteins cortactin and profilin, which help regulate actin polymerization. Cortactin has been shown to be concentrated at aneural AChR clusters and involved in the clustering of AChRs via the actin cytoskeleton (Madhavan et al., 2009). Therefore, we wanted to determine if cortactin mediates the clustering of AChRs through the association with these dynamic actin puncta. Immunostaining for cortactin reveals a punctate staining pattern, which appears to be concentrated at AChR clusters (**Figure 2.4A**). Additionally, the vast majority of cortactin puncta are localized to AChR micro-perforations, where they colocalize with actin puncta (**Figure 2.4A**, lower panel). These data suggest that the role of cortactin in the clustering of AChRs may be through its association with the dynamic actin puncta at AChR clusters.

Profilin is a highly-studied actin binding protein that functions to modulate actin dynamics through its interaction with actin monomers (Witke, 2004). Specifically, profilin encourages the nucleotide exchange of actin monomers from ADP-actin to ATP-actin to promote (+) end actin polymerization. Four isoforms of profilin have been identified (profilin 1 – 4), each of which has a unique expression profile across various tissues (Krishnan and Moens, 2009; Tariq et al., 2016). All four isoforms of profilin are expressed in skeletal muscle, although to varying degrees, where profilin-4 is most abundant and profilin-1 is least abundant (Tariq et al., 2016). In these experiments, we used a non-

isoform specific antibody to profilin in order to generally examine profilin at AChR clusters. Previous studies in the central nervous system have found that profilin is involved in synapse plasticity in dendritic spines (Ackermann and Matus, 2003), however, no such studies have investigated a potential role for profilin at the NMJ. Therefore, we sought to determine if profilin associates with actin puncta at aneural AChR clusters. Similar to cortactin, immunostaining for profilin also revealed a punctate staining pattern enriched at AChR clusters (**Figure 2.4B**). Profilin was also found to colocalize with actin puncta at the center of AChR micro-perforations (**Figure 2.4B**, lower panel). These data suggest that profilin associates with dynamic actin puncta and may be involved in promoting actin polymerization at these sites.

2.2.4 Dynamic F-actin puncta are involved in the accumulation of AChRs into aneural clusters

Many tools have been developed to study actin biology. Among these tools, pharmacological inhibitors that interfere with polymerization, depolymerization, and rearrangement of the actin cytoskeleton are among the most prevalently used. In effort to determine the function of actin puncta at aneural AChR clusters, we utilized the membrane-permeable small molecules cytochalasin D (CytoD), latrunculin A (LatA), jasplakinolide (jasp), and CK-666 to disrupt actin dynamics through various means. CytoD functions by capping the (+) end of actin filaments thereby preventing further polymerization of the filament (Cooper, 1987). LatA also inhibits (+) end actin polymerization, however, it does so by binding to and sequestering actin monomers (Yarmola et al., 2000). Jasp, however, binds to and stabilizes actin filaments, thereby inhibiting (-) end depolymerization of actin monomers (Bubb et al., 1994). CK-666 inhibits branched actin polymerization by binding

to Arp 2/3 (actin-related protein 2/3) and preventing it from binding to preexisting actin filaments, thus inhibiting branched actin polymerization (Hetrick et al., 2013).

We first sought to determine if the dynamic actin puncta at AChR clusters are susceptible to the various actin inhibitory reagents, which can provide insight into the make-up of the actin puncta. To do this, differentiated myotubes expressing F-tractin-tdTomato were labeled with Alexa488-BTX and imaged for 5 minutes before and 5 minutes after exposure to low concentrations of each actin inhibitory reagent. Due to the vital role that actin plays in all cells and especially muscle cells, a low concentration of each actin inhibitory drug was used to selectively target highly dynamic actin without disrupting stable actin networks. The concentration of each drug was experimentally determined by analyzing lamellipodia dynamics in the murine neuroblastoma cell line, Cath.a-differentiated (CAD) cells. The concentrations that caused lamellipodia growth to cease, but not collapse was chosen for all subsequent experiments (data not shown). The number of dynamic puncta and the total number of puncta (static + dynamic puncta) were quantified by creating fluorescence intensity projections of the time lapse series before and after drug treatment. Maximum intensity projections were used to quantify the total number of actin puncta in cells before and after pharmacological treatment, whereas, standard deviation intensity projections were used to specifically quantify the number of dynamic puncta. Generating intensity projections of the standard deviation of the time lapse series allows us to assess the amount of change in fluorescence intensity overtime, thus, actin puncta that remain static throughout the imaging period will show very low intensity in the projected image, whereas highly dynamic puncta will show very high fluorescence intensity. After quantification of the actin puncta, we found that the

proportion of dynamic puncta was significantly reduced when treated with 200 nM cytoD, 200 nM latA, or 100 μM CK-666 (**Figure 2.5A & 2.5B**), suggesting that these reagents selectively disrupt dynamic actin puncta. The proportion of dynamic actin puncta in AChR clusters treated with 100 nM jasp was unaffected (**Figure 2.5B**). However, the average number of static and dynamic actin puncta was significantly reduced in cells treated with 100 nM jasp (**Figure 2.5C**), suggesting that treatment with jasp disrupts both static and dynamic actin puncta populations. These data show that the dynamic actin puncta are susceptible to actin inhibitory reagents that target actin depolymerization and polymerization, including Arp 2/3 dependent polymerization.

To determine if dynamic puncta enriched at AChR clusters are involved in the formation and/or maintenance of AChR clusters, we exposed differentiated myotubes to low concentrations of each actin inhibitory reagent for 60 minutes and quantitatively analyzed the relative amount of removal of pre-existing AChRs and the insertion of new AChRs into the membrane (see **Figure 2.6A**). A stable pool of actin filaments is necessary for anchoring AChRs at the postsynaptic membrane (Hall et al., 1981; Luther et al., 1996). Therefore, from the above experiments (**Figure 2.6**), treatment with a low concentration of actin inhibitory reagents should—with the exception of jasp—selectively target highly dynamic actin and not affect the stable actin population, and subsequently, the removal of AChRs. We found that exposing aneural AChR clusters to 200 nM CytoD, 200 nM LatA, 100 nM jasp, or 100 μM CK-666 caused a significant decrease in the rate of new AChR insertion into the aneural AChR cluster membrane (**Figure 2.6B & 2.6C**). These results suggest that dynamic actin puncta at AChR clusters are involved in the formation of AChR clusters through the incorporation of newly synthesized AChRs into aneural clusters.

2.3 Discussion

Actin plays a significant role throughout the development of the NMJ (Sanes and Lichtman, 1999; Dobbins et al., 2006; Wu et al., 2010). Previous studies have suggested that two pools of F-actin—stable and dynamic F-actin—are important for the development of AChR clusters. Stable actin filaments provide a secure scaffold for immobilizing AChRs at the postsynaptic membrane (Hall et al., 1981; Luther et al., 1996), whereas, a highly dynamic F-actin network is suggested to be involved in the clustering of AChRs (Dai et al., 2000; Lee et al., 2009; Proszynski et al., 2009). However, the process in which dynamic actin affects the clustering and/or reorganization of AChRs remains unclear. We found that numerous small puncta of highly dynamic actin are present within micro-perforations of the aneural AChR cluster. Furthermore, the dynamic nature of the actin puncta was found to be necessary for the accumulation of AChRs and incorporation into the aneural cluster membrane. We, therefore, hypothesize that these highly dynamic actin puncta represent trafficking hubs for the endocytosis and exocytosis of AChRs and other postsynaptic molecules during AChR cluster development.

The trafficking of membrane-associated proteins, including AChRs, involves the dynamic processes of endocytosis, exocytosis, and endosomal recycling, all of which involve the actin cytoskeleton (Marchand et al., 2002; Lanzetti, 2007). Precise spatiotemporal control of actin polymerization and depolymerization is a key aspect of regulating such vesicular trafficking events (Porat-Shliom et al., 2013; Khaitlina, 2014). For example, the mechanical force generated by actin polymerization is involved in several aspects of vesicular trafficking, such as deformation of the membrane during vesicle

biogenesis, and propelling vesicles through the cytoplasm (Galletta and Cooper, 2009). Moreover, the depolymerization of cortical actin is also necessary to allow for vesicle delivery and subsequent fusion with the membrane (Porat-Shliom et al., 2013). In addition, following fusion of vesicles, actin polymerization provides the mechanical force necessary for the lateral movement of membrane-associated proteins and receptors through the membrane (Dai et al., 2000). The spatiotemporal control of actin dynamics during such processes is tightly regulated by several actin binding proteins, including, but not limited to the branched actin nucleation complex, Arp2/3, the cortical actin binding protein, cortactin, and the actin monomer binding protein, profilin (Bezanilla et al., 2015). Branched actin, nucleated by Arp2/3, is necessary for many aspects of endocytosis and exocytosis, including vesicle formation, vesicle fission, cargo expulsion, and membrane integration (Tran et al., 2015). The formation of this branched actin network also requires cortactin, which activates the Arp2/3 complex and couples Arp2/3-dependent polymerization through binding to the vesicle fission regulator, dynamin 2 (Weed and Parsons, 2001; Zhu et al., 2005). Additionally, studies analyzing endocytosis in yeast found that profilin activity is involved in endocytosis through its ability to catalyze nucleotide exchange of actin monomers and promote actin polymerization (Wolven et al., 2000). Thus, a dynamic actin network, spatiotemporally regulated by several actin binding proteins, is necessary for various aspects of vesicular trafficking.

Previous work from the Zheng Lab using cultured *Xenopus* myocytes found results similar to what we report here. Specifically, they showed that dynamic actin, along with the F-actin severing protein cofilin, are present at aneural AChR clusters and associate with sites of vesicular trafficking. Additionally, the inhibition of cofilin activity regulation

caused a decrease in AChR clustering, indicating that properly regulating actin dynamics is crucial for AChR cluster formation (Lee et al., 2009). This study in conjunction with the data presented here support our hypothesis that dynamic actin puncta represent sites of endo- and exocytosis for AChR trafficking. However, the actin puncta and associated AChR micro-perforations characterized in this study appear much smaller than those found in the *Xenopus* myocytes. This could simply be due to inherent differences in AChR clusters in a mammalian system compared to *Xenopus*. Alternatively, the small AChR micro-perforations and actin puncta could represent the genesis of the plaque-to-pretzel transition and overall maturation of the AChR cluster.

Proszynski *et al*. also characterized dynamic actin puncta within AChR perforations at aneural AChR clusters and concluded that the actin puncta are in fact structures called podosomes (Proszynski et al., 2009). Podosomes are dynamic, actin-based structures that act as sites of attachment to, and degradation of, the extracellular matrix (ECM) (Murphy and Courtneidge, 2011; Bernadzki et al., 2014). Proszynski *et al*. hypothesized that the 'synaptic podosomes' characterized are directly responsible for the maturation and reorganization of AChR clusters during the plaque-to-pretzel transition, where they could potentially act to reorganize AChR clusters through the degradation of the ECM, generation of lateral force on AChRs, and/or remodeling of the underlying actin scaffold (Proszynski et al., 2009).

It is certainly possible that the actin puncta characterized here and in *Xenopus* myocytes represent core components of synaptic podosomes. After all, actin puncta were found to colocalize with cortactin (**Figure 2.4A**) and cofilin (Lee et al., 2009), both components of podosomes (Zalli et al., 2016). However, there are some key differences between the actin

puncta characterized in this study and synaptic podosomes. First, actin puncta described here are much smaller in diameter (approx. 1 μm) and consume the entire AChR micro-perforation, unlike synaptic podosomes where a characteristic 'cortex' of adhesive podosomal proteins is situated directly between the actin-based core and the edge of the cluster perforation (Proszynski et al., 2009; Murphy and Courtneidge, 2011). Second, podosomes are highly dynamic structures that often fuse, divide, and move laterally (Gimona et al., 2008; Luxenburg et al., 2012). However, no lateral movement of the actin puncta was detected in this study. Actin puncta were only observed appearing and disappearing from the focal plane directly beneath the postsynaptic membrane. This can occur either through movement of actin puncta in the z-axis (i.e. intact actin structures moving into and out of the focal plane) or through de novo formation and disassembly of actin puncta at the AChR cluster membrane. Lastly, the actin puncta characterized here were only found within AChR micro-perforations, and absent from the larger AChR perforations. Whereas, synaptic podosomes are localized to large AChR perforations, which are a characteristic feature of the plaque-to-pretzel transition and AChR cluster maturation (Proszynski et al., 2009; Proszynski and Sanes, 2013).

Altogether, the data presented suggests actin puncta play a role in the trafficking and accumulation of AChRs, but are likely not representative of synaptic podosomes. One key piece of evidence for this is in the pharmacological disruption of the actin puncta which resulted in a significant decrease in new AChR insertion into the cluster, suggesting a role in the trafficking or accumulation of AChRs, whereas synaptic podosomes are not thought to traffic AChRs to developing clusters (Bernadzki et al., 2014). Therefore, we believe these actin puncta likely represent trafficking hubs for the endocytosis and exocytosis of

AChRs and other postsynaptic proteins. It is possible that the actin puncta are precursors of synaptic podosomes, where the actin puncta first act as trafficking hubs for the initial formation of AChR clusters and subsequently develop into podosomes during the maturation of AChR clusters. However, more experiments are necessary to confirm this. Nonetheless, the data presented here show that a dynamic actin cytoskeleton is crucial for the formation of AChR clusters. In conclusion, this study contributes to a growing body of knowledge showing that the actin cytoskeleton delicately balances between a stable actin network immobilizing AChRs and a highly dynamic actin cytoskeleton trafficking AChRs.

2.4 Materials & Methods

Antibodies & chemical reagents

The following antibodies were used in this study: rabbit anti-profilin antibody (1:250; Cytoskeleton, APUF01), polyclonal rabbit anti-cortactin antibody (1:100; Bethyl Laboratories, A302-608A), Alexa Fluor 647-conjugated goat anti-rabbit IgG (1:400; Invitrogen). Alexa Fluor 488 and Alexa Fluor 647 conjugated α-bungarotoxin (BTX) were purchased from Molecular Probes (B13422 & B35450, respectively). The actin inhibitory drugs cytochalasin D, latrunculin A, and CK-666 were purchased from Sigma. Jasplakinolide was purchased from Invitrogen. Stock solutions of all actin inhibitory drugs were prepared in sterile DMSO (Sigma). AlexaFluor568-phalloidin was purchased from Invitrogen.

Primary myoblast culture & differentiation

Primary myoblasts were isolated and cultured as previously described with the exception of a Percoll gradient (Bondesen et al., 2004). Briefly, adult wild-type C57BL/6

mice were sacrificed by CO2 exposure and the hindlimb muscles were immediately dissected and minced. The minced tissue was then washed with sterile phosphate-buffered saline (PBS) and treated with 0.1% pronase (Calbiochem) in DMEM for 60 mins at 37ºC with gentle agitation to digest the tissue. Following digestion, the tissue was triturated to encourage myoblasts release from the tissue. The triturated tissue was then passed through 100 μm Steriflip filter (EMD Millipore) to separate myoblasts from large tissue pieces then centrifuged for 10 minutes at 1400×g to clear myoblasts from larger cell debris. Isolated primary myoblasts were cultured in growth media (Ham's F-10 media + 20% fetal bovine serum (FBS; Atlanta Biologicals) + 1% penicillin/streptomycin) supplemented with 5 ng/ml basic fibroblast growth factor (bFGF; PeproTech) at 37ºC in a 5% CO2/95% air humidified atmosphere. All myoblasts were cultured and maintained on tissue culture dishes coated with 0.1 mg/ml collagen (Gibco).

For imaging experiments, primary myoblasts were differentiated on No. 1.5 glass coverslips coated first with 0.1 mg/ml poly-D-lysine (Millipore) in sterile 0.1M borate buffer (50 mM boric acid + 12.5 mM sodium tetraborate, pH 8.5) for 24 hours at 37ºC. Coverslips were then coated with 20 μg/ml laminin (Sigma) in PBS for 2 – 3 hours at 37ºC. To induce differentiation, growth media was replaced with differentiation media (DMEM + 5% horse serum (Atlanta Biologicals) + 1% penicillin/streptomycin) and incubated for 3 – 4 days at 37ºC in a 5% CO2/95% air humidified atmosphere, replacing the differentiation media every 24 hours.

Lentiviral production & transduction

The pLVTHM lentiviral vector containing F-tractin-tdTomato and the associated packaging plasmids pMD2.G and psPAX2 was generously provided by fellow lab member

Kenneth Myers, PhD. For lentiviral production, 293T cells (a generous gift from Dr. Criss Hartzell, Emory University) were cultured to approximately 90% confluency in DMEM + 10% FBS + 1% penicillin/streptomycin in a 10 cm dish, then cotransfected with 15 μg pLVTHM-Ftractin-tdTomato, 11.5 μg psPAX2, and 3 μg pMD2.G using Lipofectamine2000 (Thermo Fisher Scientific). Viral supernatant was collected 24 and 48 hours after transfection and concentrated by ultra-centrifugation at 100,000×g for 2.5 hours at 4ºC. Lentiviral concentrates were stored at -80ºC until use. For lentiviral transduction, primary myoblasts were cultured to approximately 50% confluency on collagen-coated dishes and incubated with lentiviral particles for 2 – 3 days. Transduced myoblast cultures were expanded and stored at -80ºC until use.

Immunofluorescence

Differentiated primary myotubes were fixed with 4% (v/v) paraformaldehyde (Polysciences Inc.) + 4% (w/v) sucrose (Sigma) in PBS. Cells were then incubated with BTX (1:500) for 30 minutes before permeabilization to ensure only surface AChRs are labeled. Cells were permeabilized with 0.1% Triton-X100 (Sigma) for 10 minutes then blocked with blocking buffer (4% bovine serum albumin (BSA; Sigma) + 1% goat serum + 0.1% Triton-X100 in PBS) for 1 hour. Cells were then incubated with primary antibodies diluted in blocking buffer overnight at 4ºC. After washing with PBS, the cells were then incubated with secondary antibodies and Alexa568-phalloidin for 1 hour. Cells were mounted onto glass slides with Fluoromount-G (SouthernBiotech) for structured illumination microscopy. Cells imaged using total internal reflection fluorescence microscopy or stochastic optical reconstruction microscopy were mounted in an open chamber with PBS or photoswitching imaging buffer, respectively.

AChR accumulation & removal assay

The amount of AChR removal and new AChR accumulation into clusters was assessed by using the following fluorescence labeling scheme (**Figure 2.6A**). Primary myoblasts expressing F-tractin-tdTomato were seeded onto No. 1.5 glass coverslips coated with poly-D-lysine and laminin and differentiated for 3 – 4 days. Before imaging, AChRs were labeled with a non-saturating concentration of Alexa Fluor 488-BTX (1:1000) for 30 minutes, followed by a saturating concentration of unlabeled BTX (1:20) for 15 minutes to mask all surface AChRs. Myotubes were then exposed to a non-saturating concentration of Alexa Fluor 647-BTX (1 μg/ml) to label any newly inserted AChRs. Following labeling, myotubes were treated with either 200 nM cytochalasin D, 200 nM latrunculin A, 100 nM jasplakinolide, 100 μM CK-666, or untreated control for 60 minutes. Newly inserted AChRs were labeled with Alexa Fluor 647-BTX (1 μg/ml) for 15 minutes prior to the 60 minute time point. Myotubes were imaged by total internal reflection fluorescence (TIRF) microscopy immediately before and after drug treatment (0 minute and 60 minute time points). Myotubes were imaged in phenol red-free differentiation media containing 20 mM HEPES and maintained at 37ºC throughout imaging.

Microscopy

Three-dimensional structured illumination microscopy (SIM) was performed on a Nikon N-SIM Eclipse Ti-E microscope system equipped with Perfect Focus, 100×/1.49 NA oil immersion objective, and an EMCCD camera (DU-897, Andor Technology, Belfast, UK). Stochastic optical reconstruction microscopy (STORM) was performed using a Nikon Ti-E TIRF inverted microscope equipped with Perfect Focus, 488 nm and 647 nm lasers, and an iXon 897 EMCCD camera (Andor). Images were acquired using a

100×/1.45 N.A. Plan Apo λ objective. Approximately 40,000 frames were collected using total internal reflection fluorescence (TIRF) excitation. Images were reconstructed in Nikon Elements.

Live-cell TIRF microscopy of actin puncta dynamics and AChR accumulation/removal was performed on an Eclipse Ti inverted microscope (Nikon) equipped with a QuantEM electron-multiplying charge-coupled device (EMCCD) camera (Photometrics) and 488 nm and 647 nm lasers. Images were acquired using a 100×/1.49 numerical aperture (NA) Apochromat (Apo) TIRF oil immersion objective. Cells were mounted in a custom live-cell chamber and maintained at 37°C with a heated stage adapter (Warner). Identical exposure and laser intensity settings were carefully maintained for each cell.

Image analysis

All images were obtained using Nikon Elements software. The dynamics of actin puncta before and after treatment with actin inhibitory drugs was quantified using Nikon Elements software. Maximum intensity projections and standard deviation (SD) projections of the time lapse series were created using ImageJ software (National Institutes of Health). SD projections were used to quantify the amount of dynamic and static actin puncta. The intensity of dynamic puncta will have a larger deviation, and subsequently higher intensity in the SD projections, than static puncta. The intensity threshold (in the SD projected images) for what is considered dynamic puncta vs static puncta was determined by identifying static puncta from the live-cell time lapse series. The fluorescence intensity of the static puncta in SD projections was then used as the cut off, where puncta with intensity above the cut off were considered dynamic and puncta below

the intensity cut off were considered static. The proportion of dynamic puncta vs static puncta was then calculated in Excel (Microsoft).

Acknowledgments

I would like to thank Dr. Ken Myers for generously providing lentiviral reagents and support.

2.5 Figures

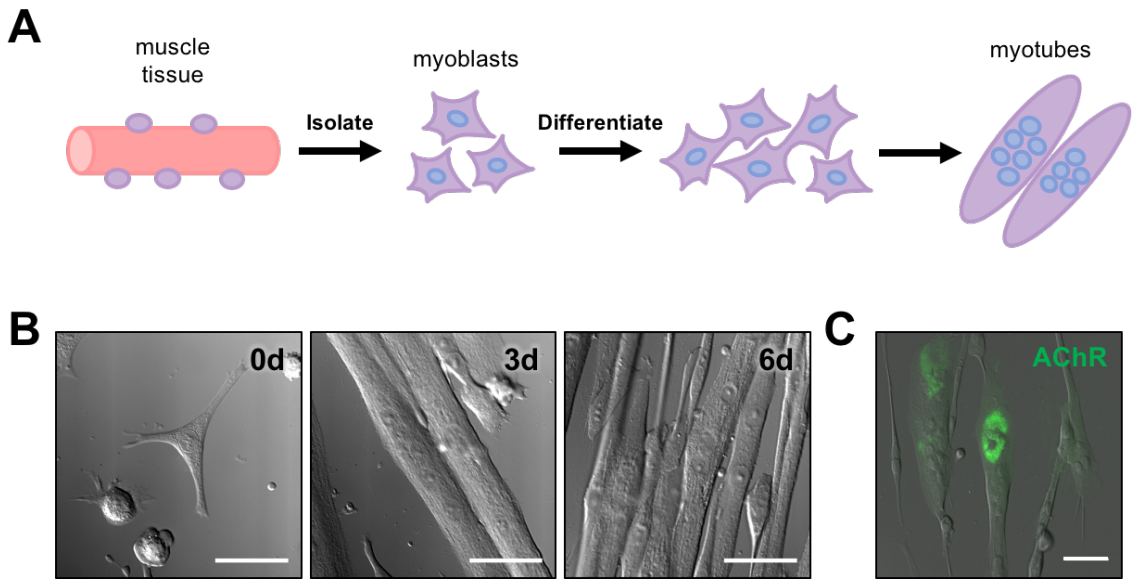

Figure 2.1. Culturing and differentiation of primary myoblasts. (**A**) Schematic representation of primary myoblast isolation and differentiation used for aneural AChR clusters. Skeletal muscle stem cells (myoblasts, purple) are isolated from skeletal muscle tissue (pink) of adult mice and differentiated for 3 – 6 days to form multinucleated myotubes. (**B**) Differential interference contrast (DIC) images of primary myoblast differentiation over 6 days (d). Timestamp refers to the number of days after the start of differentiation. Scale bars: 40 µm. (**C**) Aneural AChR (green) clusters form when myoblasts are differentiated on a laminin-coated substrate. Scale bar: 40 µm.

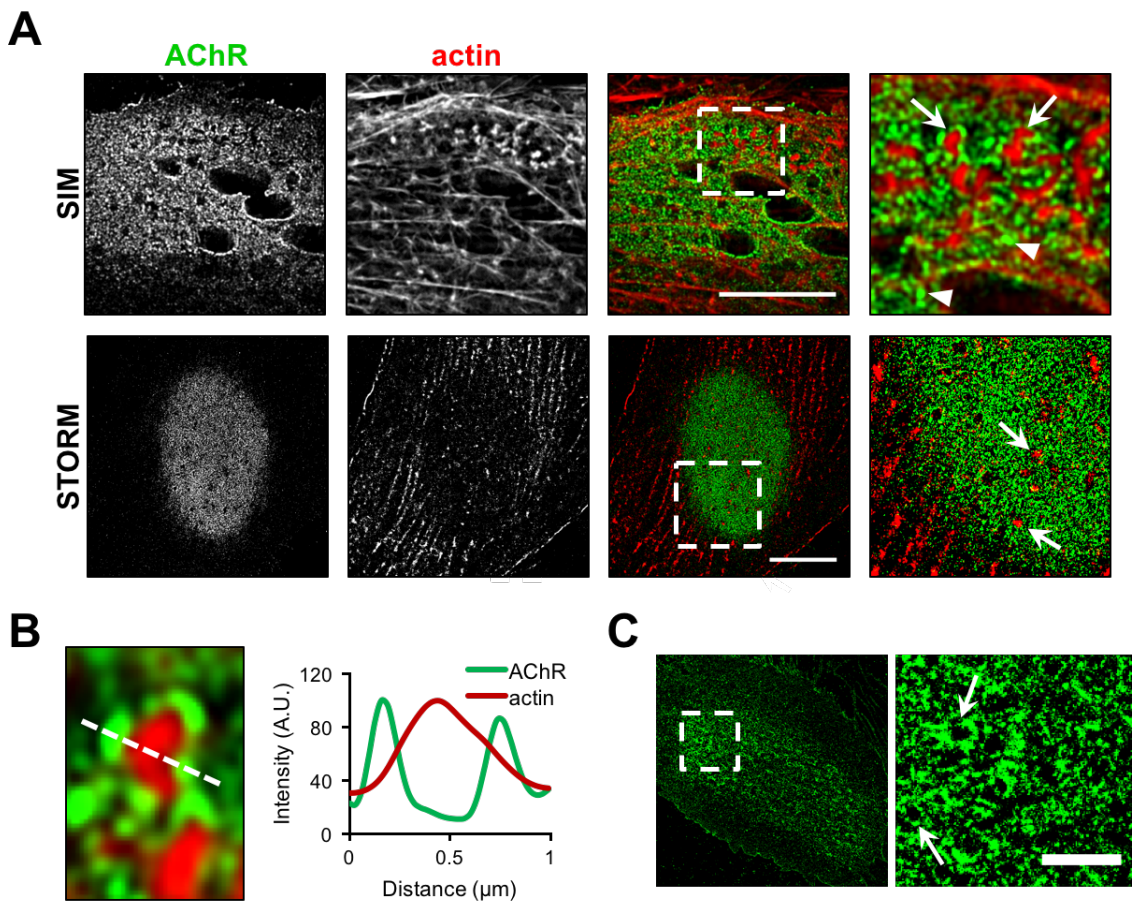

Figure 2.2. AChRs and the associated underlying actin cytoskeleton exhibit a distinct micro-organization. (**A**) Representative SIM and STORM images showing AChR (green) and the underlying F-actin (red) organization. AChRs are organized into micro-puncta (arrowhead) and micro-perforations (arrow). F-actin puncta are enriched within the AChR cluster area. Scale bar: 10 μm. (**B**) A small region of the AChR cluster (left panel) was used to generate a profile line scan, highlighting the localization of actin puncta (red) within AChR micro-perforations (green). (**C**) Live cell STORM imaging of AChR (green) cluster (left panel) shows AChR micro-perforations (arrows) are a cause of fixation conditions. Scale bar: 2 μm.

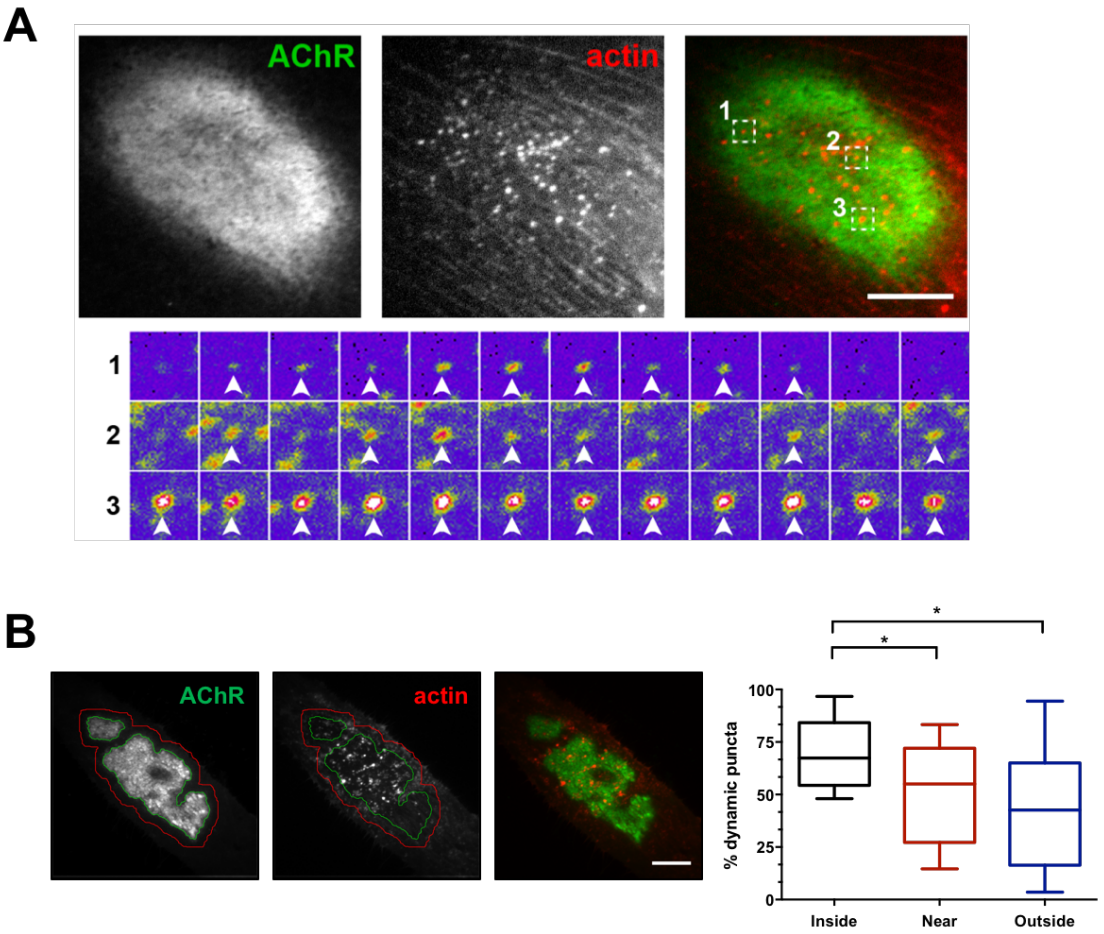

Figure 2.3. Actin puncta at aneural AChR clusters are highly dynamic. (**A**) Representative images from live-cell TIRF imaging of aneurally cultured myotubes expressing F-tractin-tdTomato (red). AChRs (green) were labeled with AlexaFluor 488-BTX. Lower panels show montage highlighting the dynamics of representative F-actin puncta (arrowhead) over time. The majority of actin puncta are highly dynamic, appearing then disappearing over time (panels 1 & 2), however, a few puncta remain static throughout imaging (panel 3). Panel images have been pseudocolored to emphasize changes in fluorescence intensity, where hot colors and cold colors represent high and low intensities, respectively. Each montage image represents 10 second interval. Scale bar: 20 μm. (**B**) Representative standard deviation projected images of TIRF time lapse used to quantify

the relative amount of dynamic actin puncta (graph, right panel). Differentiated myotubes expressing F-tractin-tdTomato (red) were stained with AlexaFluor 488-BTX to label surface AChRs (green). Green outline indicates boundary of AChR cluster that was used to quantify dynamic puncta within AChR cluster (graph, 'inside'). A 3 μm area surrounding AChR cluster border (red line) and the surrounding cell area in frame was used to quantify actin puncta 'near' and 'outside' the AChR cluster area, respectively. *Graph*, box and whisker plot showing the percent of dynamic actin puncta inside, near and outside AChR cluster area. Plots denote 95th (top whisker), 75th (top edge of box), 25th (bottom edge of box), and 10th (bottom whisker) percentiles and the median (bold line in box). Scale bar: 15 μm. *$p < 0.0001$ (Repeated measures one-way ANOVA, n = 10).

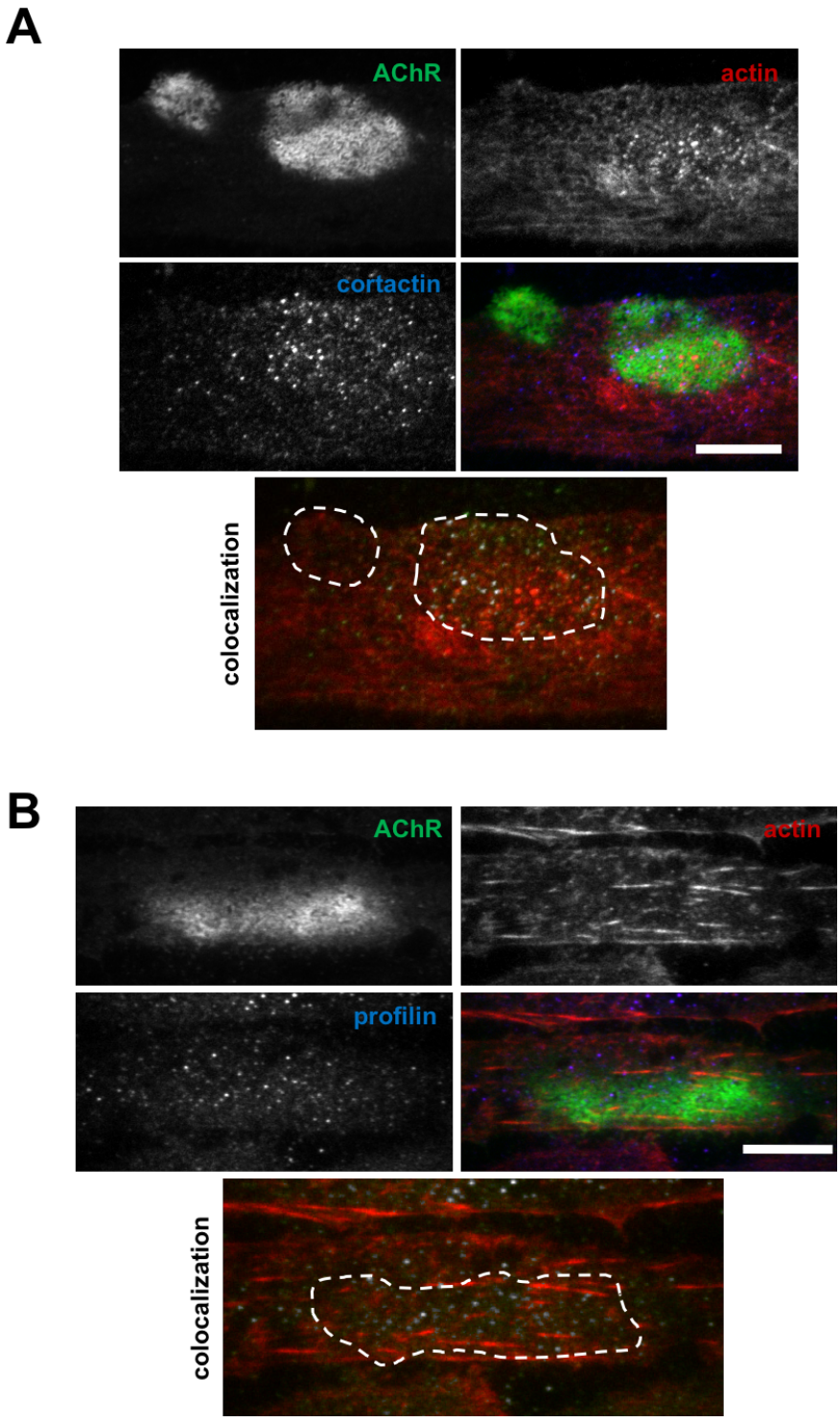

Figure 2.4. Actin binding proteins cortactin and profilin associate with actin puncta at aneural AChR clusters. (**A**) Representative TIRF images showing localization of cortactin (blue) and F-actin (red) at AChR (green) clusters. *Lower panel*, colocalization

between cortactin (green) and F-actin (red) at AChR clusters (outline). Colocalized pixels are pseudocolored grey. Scale bar: 15 μm. (**B**) Localization of profilin (blue) and actin (red) at aneural AChR (green) clusters visualized by TIRF microscopy. *Lower panel*, colocalization map of profilin (green) and actin (red) at AChR clusters (outline). Colocalized pixels are pseudocolored grey. Scale bar: 15 μm.

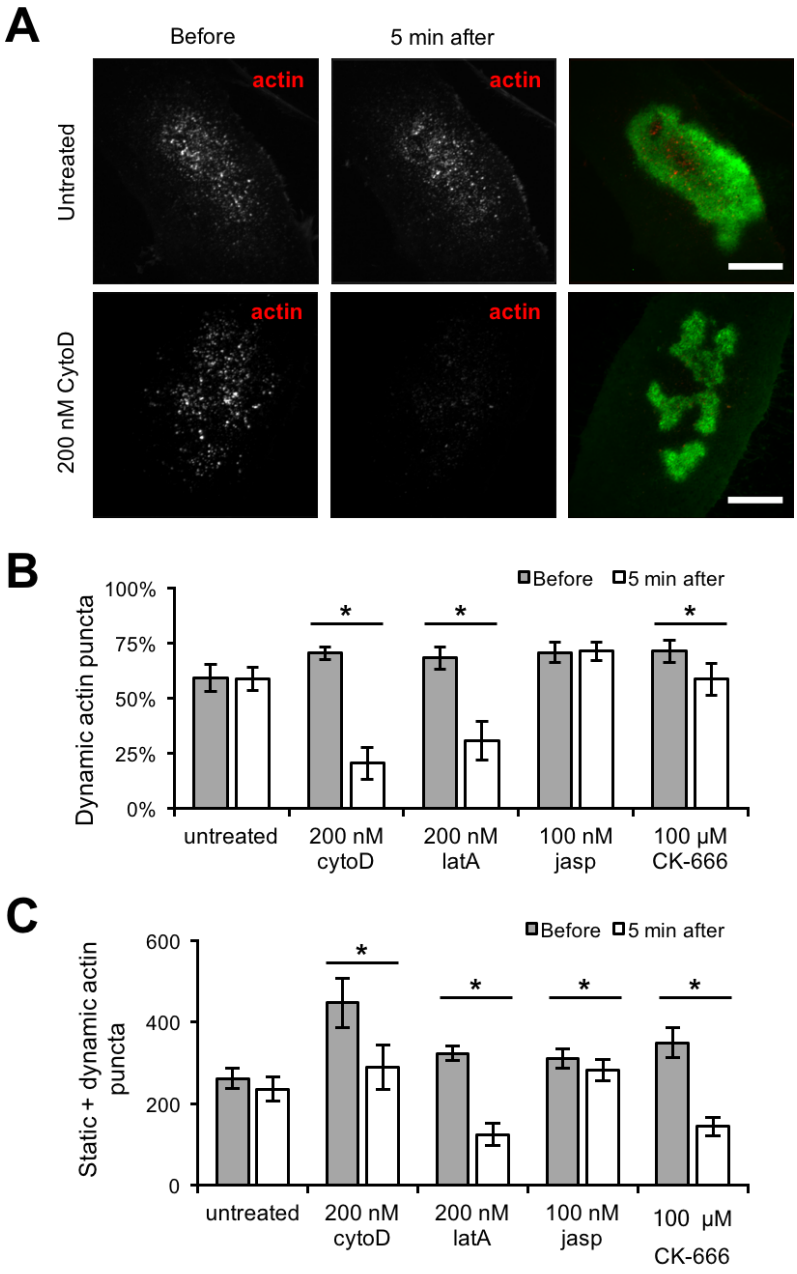

Figure 2.5. Effect of actin drugs on actin puncta dynamics. (**A**) Representative images of differentiated myotubes expressing F-tractin-tdTomato (red). Images are standard deviation projected images of 5 minute time lapse series before and after 200 nM cytochalasin D (cytoD) treatment (lower panels) or untreated (upper panels). AChRs (green) were labeled with AlexaFluor 488-BTX. Dynamic actin puncta were significantly

reduced after treatment with 200 nM cytoD for 5 minutes. Scale bar: 20 μm. (**B**) Quantification of dynamic actin puncta before and after treatment with or without 200 nM cytoD, 200 nM latrunculin A (latA), 100 nM jasplakinolide (jasp), or 100 μM CK-666 for 5 minutes. Error bars represent standard error of the mean (SEM). The number of cells used for this analysis are as follows: untreated (10), cytoD (6), latA (7), jasp (10), CK-666 (9). *$p < 0.02$ (Student's t-test). (**C**) Quantification of the average number of total actin puncta (static + dynamic) before and after treatment with or without each actin drug. Error bars represent SEM. The number of cells used for this analysis are as follows: untreated (10), cytoD (6), latA (7), jasp (10), CK-666 (9). *$p < 0.03$ (Student's t-test).

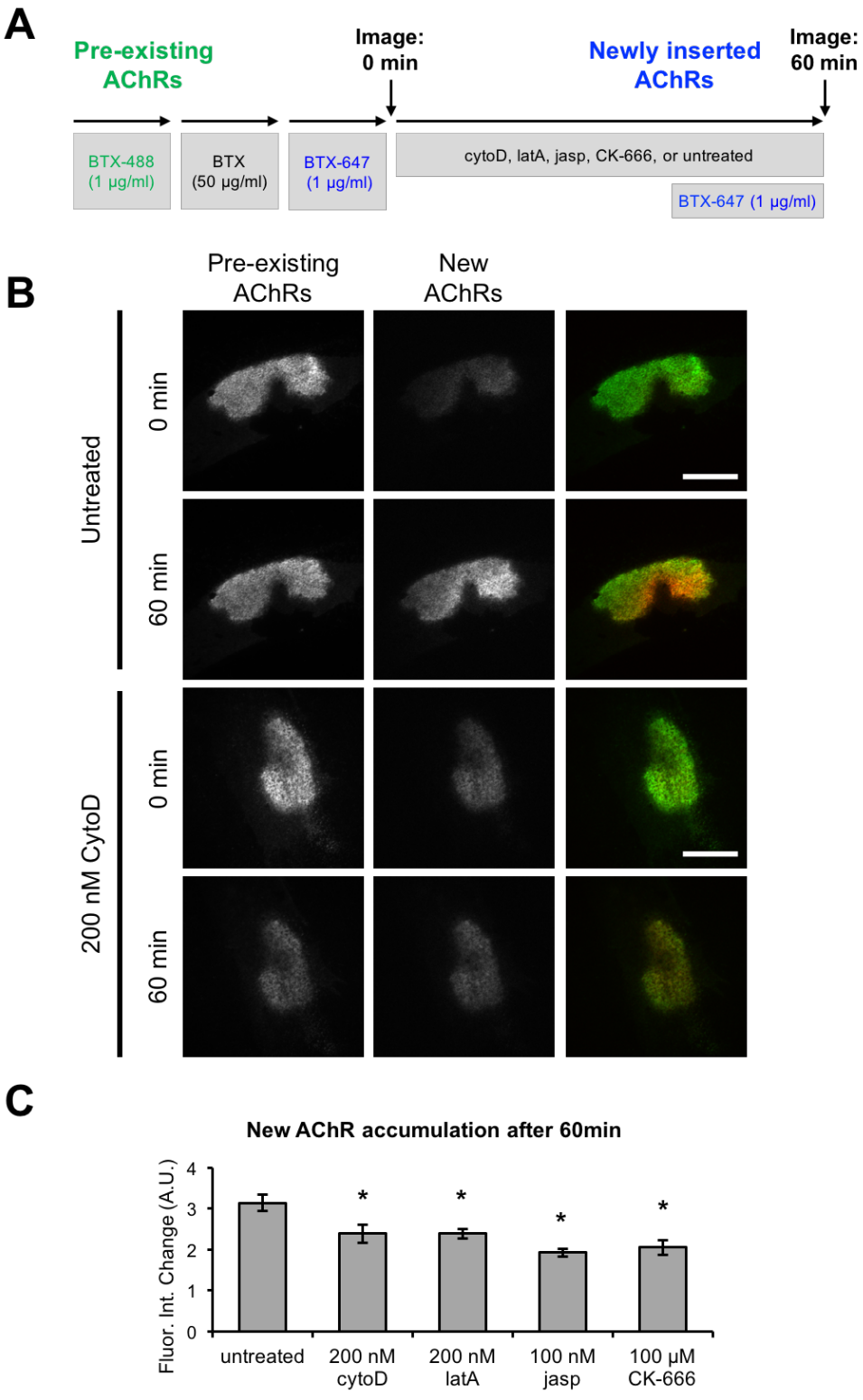

Figure 2.6. Dynamic actin puncta are involved in AChR clustering. (**A**) Schematic of the protocol for the sequential labeling of pre-existing AChRs (green) and newly inserted

AChRs (blue) in live aneurally cultured muscle cells. Pre-existing AChRs were labeled with Alexa Fluor 488-BTX for visualization then saturated with unlabeled BTX (black) to mask all pre-existing AChRs. Cells were then incubated with Alexa Fluor 647-BTX immediately before imaging at the 0 minute time point, providing a baseline for determining the fold increase in newly inserted AChRs. Cells were then treated with or without the actin inhibitory drugs, cytochalasin D (cytoD), latrunculin A (latA), jasplakinolide (jasp), CK-666 for 60 minutes. Immediately prior to imaging at the 60 minute time point, newly inserted AChRs were labeled with Alexa Fluor 647-BTX. The rate of AChR accumulation is determined by analyzing the change in fluorescence intensity of newly inserted AChRs (blue) before and after drug treatment. (**B**) Representative images of pre-existing AChRs (green) and newly inserted AChRs (red) before and after treatment with or without 200 nM cytoD for 60 minutes. The fluorescence intensity of newly inserted AChRs after exposure to cytoD for 60 minutes is reduced compared untreated. Scale bars: 25 μm. (**C**) Quantification of the relative amount of new AChRs inserted into the membrane after exposure to each actin drug for 60 minutes. Error bars represent standard error of the mean (SEM). The number of cells used for this analysis are as follows: untreated (14), cytoD (17), latA (10), jasp (10), CK-666 (10). $*p < 0.02$ (Student's t-test).

Chapter III

Super-resolution microscopy reveals a nanoscale organization of acetylcholine receptors for trans-synaptic alignment at neuromuscular synapses

ABSTRACT

The neuromuscular junction (NMJ) is a chemical synapse formed between motoneurons and skeletal muscle fibers. The vertebrate NMJ uses acetylcholine as the neurotransmitter and features numerous invaginations of the postsynaptic muscle membrane termed junctional folds. Acetylcholine receptors (AChRs) are believed to be concentrated on the crest of junctional folds but their spatial organization remains to be fully understood. In this study, we utilized super-resolution microscopy to examine the nanoscale organization of AChRs at NMJ. Using Structured Illumination Microscopy, we found that AChRs appear as stripes within the pretzel-shaped mouse NMJs, which however, do not correlate with the size of the crests of junctional folds. By comparing the localization of AChRs with several pre- and post-synaptic markers of distinct compartments of NMJs, we found that AChRs are not distributed evenly across the crest of junctional folds as previously thought. Instead, AChR stripes are more closely aligned with the openings of junctional folds as well as with the presynaptic active zone. Using Stochastic Optical Reconstruction Microscopy for increased resolution, we found that each AChR stripe contains an AChR-poor slit at the center that is equivalent to the size of the opening of junctional folds. Together, these findings indicate that AChRs are largely localized to the edges of crests surrounding the opening of folds to align with the presynaptic active zones. Such a nanoscale organization of AChRs potentially enables trans-synaptic alignment for effective synaptic transmission of NMJs.

This chapter is adapted from:

York AL and Zheng JQ (2017). Super-resolution microscopy reveals a nanoscale organization of acetylcholine receptors for trans-synaptic alignment at neuromuscular synapses. eNeuro *4*.

3.1 Introduction

The coordinated anatomical movement of human's everyday lives depends on rapid and precise neuromuscular communication. At the heart of this process lies the neuromuscular junction (NMJ), a specialized synapse between a motor neuron and a single muscle fiber. The NMJ is a large and topographically complex synapse compared to synapses of the central nervous system (Sanes and Lichtman, 1999; Wu et al., 2010; Shi et al., 2012). As with many biological systems, the organization and structural integrity of the NMJ is critical to its function. Defects in synaptic architecture, including misalignment of the pre- and post-synaptic terminals, are a common phenotype of many neuromuscular diseases and genetic defects (Hirsch, 2007; Slater, 2008; Ha and Richman, 2015), as such mapping the precise organization of synaptic components is crucial in order to fully understand NMJ function in healthy individuals.

The vertebrate NMJ is marked by unique structural features. Notably, the axon terminal of a motor neuron sinks into the muscle membrane, creating a characteristic depression referred to as the primary gutter. Within this gutter, are smaller invaginations of the postsynaptic membrane, termed junctional folds. The junctional folds can be further divided into the crest, representing the top of the folds closest to the presynaptic terminal, and the trough, representing the bottom part of the infolded membrane. While the exact function of the junctional folds remains to be fully determined, they likely play a critical role in neurotransmission by providing a platform for the spatial segregation of key postsynaptic molecules. For instance, acetylcholine receptors (AChRs), are present at the crest and partially down the sides of junctional folds, whereas voltage-gated sodium channels (VGSCs) are concentrated at the trough (Fertuck and Salpeter, 1974; Matthews-

Bellinger and Salpeter, 1983; Flucher and Daniels, 1989). Studies involving mathematically modeling of NMJ neurotransmission in the presence or absence of junctional folds have suggested that they may act to reduce the threshold necessary for action potential firing, thus making NMJ neurotransmission more efficient (Martin, 1994).

The alignment of neurotransmitter release sites on the presynaptic terminal with the clusters of neurotransmitter receptors on the postsynaptic membrane represents an important mechanism that ensures efficient and effective neurotransmission in the synapses of the central nervous system (Tang et al., 2016). In vertebrate NMJs, the neurotransmitter acetylcholine (ACh) is released from highly specialized sites on the presynaptic terminal called active zones (Nishimune, 2012). Readily releasable ACh vesicles are docked at the active zones by interacting with the macromolecules in the active zone material (Harlow et al., 2013). Intriguingly, electron microscopy (EM) studies have shown that presynaptic active zones are positioned apposed to the openings of junctional folds (Couteaux and Pecot-Dechavassine, 1970; Dreyer et al., 1973; Patton et al., 2001), whereas AChRs are present across the fold crest and partially down the sides of the infolded membrane (Fertuck and Salpeter, 1974; Matthews-Bellinger and Salpeter, 1983). If this configuration indeed reflects the physiological organization of the NMJ, this would mean that AChRs are, in large part, misaligned from presynaptic active zones — a finding that would theoretically reduce neurotransmission efficiency. While these EM studies provided many seminal insights into the general organization of NMJ components, a detailed analysis of AChR distribution along the junctional folds has previously been precluded by the relatively sparse labeling that occurs with immuno-EM, and the limited resolution of conventional light microscopy.

In this study, we used super-resolution microscopy to examine the nanoscale distribution of AChRs on the postsynaptic membrane. Together with specific markers for distinct compartments of the NMJ, we present evidence that AChRs are not evenly distributed across the crest of the junctional folds, as the previous model predicts. Rather, our data reveal that AChRs are concentrated at the edge of the crest, apposed to the active zone of presynaptic terminals. As a result, the individual AChR-rich stripes seen using conventional fluorescence microscopy are actually composed of AChRs from the edges of two adjacent crests, whereas the AChR-poor space actually represents the central region of the crest, rather than the region between neighboring crests. Collectively, the results from our data builds a new model whereby AChRs on the postsynaptic membrane are concentrated under presynaptic neurotransmitter release sites, allowing for effective synaptic transmission.

3.2 Results

In this study, we sought to utilize super resolution fluorescence microscopy techniques to analyze the spatial distribution of AChRs at the NMJ. The anatomy of muscle tissue can present many hurdles in achieving clean and successful whole-mount immunostaining. While AChRs can be readily labeled by fluorescently tagged α-bungarotoxin (BTX), immuno-labeling of intracellular molecules is complicated by the thick fascia that encapsulates muscle fibers. This thick fascia can limit antibody penetration and generate a significant level of background fluorescence. Here we used the Transversus Abdominis (TVA) muscle, a thin and flat muscle located within the abdominal musculature, and adapted a whole-mount protocol (Murray et al., 2014) with modifications to improve antibody penetration and immuno-labeling of molecules at NMJs (**Figure**

3.1A). Consistently, AChRs are seen concentrating at the motor neuron endplate, appearing as 'pretzels' in the center area of the muscle fibers when imaged 'en face' by laser scanning microscopy (**Figure 3.1B**). An increase in magnification shows that AChRs are not distributed uniformly within the 'pretzel' pattern of NMJ but the particular spatial organization is not well resolved using the conventional light microscopy. With the modified protocol, we were able to label the microtubule network in the intact muscle fibers (**Figure 3.1B**). Consistent with previously published results, microtubules form a cage-like network surrounding the postsynaptic area (Schmidt et al., 2012). Therefore, this TVA muscle preparation and modified staining protocol allow effective antibody penetration for immunolabeling of intracellular proteins in conjunction with surface AChR labeling.

To better resolve the AChR distribution inside the synaptic gutters, we used three-dimensional structured illumination microscopy (SIM), which increases the resolution limit by approximately two-fold compared to conventional light microscopy (Gustafsson, 2000; Gustafsson et al., 2008). Using SIM imaging we found that AChRs are distributed in a 'stripe' pattern, where highly fluorescent AChR stripes are separated by fluorescently poor space (appearing as dark bands) (**Figure 3.2A**). Since AChRs are thought to be concentrated across the crests of junctional folds and absent from the trough of junctional folds, the highly fluorescent AChR stripes could represent the crests of junctional folds separated by the AChR-poor infolded region. To examine this possibility, we performed quantitative analysis on the widths of the AChR stripes and the dark bands by generating intensity profiles (**Figure 3.2B**). Our data show that the average width of the AChR stripes is 149 ± 28 nm (mean ± standard deviation), whereas the AChR-poor bands have a width of 188 ± 66 nm. To determine if these numbers represent the crests or the openings of to

the junctional folds, we performed transmitted electron microscopy (TEM) on TVA muscles and quantified the average widths of the junctional fold crests and openings (**Figure 3.2C**). We found that the openings of the infoldings have a size of 55 ± 9 nm, which is significantly smaller than the width of the dark bands observed with fluorescent staining (**Figure 3.2D**). Even considering the difference in resolution limits, the width of the fluorescently-poor dark bands between stripes is significantly larger and does not correlate with the opening of the membrane infoldings. However, the average distance between AChR stripes (188 ± 66 nm) correlates with the average width of fold crests from EM data (207 ± 61 nm) within the margin of error (**Figure 3.2D**). Therefore, the AChR–rich and –poor stripes are not directly related to the crests and openings to troughs, respectively.

To better understand the relationship between the AChR stripes and junctional folds, we sought to compare the subsynaptic distribution of AChRs to various markers with known localizations. We first compared the subsynaptic localization of AChR and rapsyn. Rapsyn is a highly characterized intracellular protein that immobilizes AChRs at the postsynaptic membrane through scaffolding connections with the underlying actin network (Walker et al., 1984; Antolik et al., 2007). Therefore, we would expect rapsyn to exhibit a very high degree of colocalization with AChRs. Indeed, immunofluorescence of AChRs and rapsyn revealed that they precisely overlap with one another (**Figure 3.3A**, top row). Intensity line profiles of these two signals greatly overlap, supporting the visual impression of colocalization (**Figure 3.3B**), which is further confirmed by the colocalization analysis (**Figure 3.3C**, Manders Coefficient = 82.2% ± 7.7%).

Previous EM studies have shown that active zones on the presynaptic terminal precisely align with the opening of the postsynaptic infoldings (Couteaux and Pecot-Dechavassine, 1970; Dreyer et al., 1973; Patton et al., 2001). Therefore, we used an antibody specific for the active zone protein piccolo to mark the area representing the opening of postsynaptic membrane infoldings. Previous studies have shown that immunofluorescence of active zones at mammalian NMJs appear as discrete puncta (Chen et al., 2012). Consistent with the literature, our immunostaining for piccolo revealed a punctate pattern marking the active zones of the mammalian NMJ. When analyzing the piccolo and AChR staining together, we found that the vast majority of piccolo puncta are localized on top of AChR stripes (**Figure 3.3A**, second row). A representative profile line scan depicts the overlapping nature of piccolo and AChR staining (**Figure 3.3B**). Additionally, colocalization analysis reveals piccolo overlaps with AChRs to a high degree (Manders Coefficient = 67.3% ± 5.4%) (**Figure 3.3C**). These data suggest that AChR stripes may be localized to the area surrounding the infolded membrane region. We also compared the localization of AChRs relative to the trough of junctional folds. Here, we double labeled AChRs and voltage-gated sodium channels (VGSCs), which have been shown to be spatially restricted to the trough of junctional folds (Flucher and Daniels, 1989). VGSC staining was found to largely overlap with AChR stripes (Manders Coefficient = 69.4% ± 8.1%) (**Figure 3.3A & 3.3C**), which is further confirmed by the profile line scan (**Figure 3.3B**). These data, in conjunction with piccolo data, supports the hypothesis that AChRs may be spatially restricted to the area immediately surrounding the opening of infolded membrane.

To further test this hypothesis, we compared the localization of AChRs relative to the junctional fold crests. Integrin α7 is a muscle specific transmembrane receptor that links the cell to the surrounding extracellular matrix (Song et al., 1992; Song et al., 1993). In the mature NMJ, integrin α7 is restricted to the crest of junctional folds (Martin et al., 1996; Schwander et al., 2004). Therefore, we labeled integrin α7 to mark the junctional fold crest and compared this staining to that of AChRs. Similar to AChRs, integrin α7 also exhibits a similar 'stripe' staining pattern (**Figure 3.3A**). However, when overlaid with AChR staining it is apparent that integrin α7 and AChRs occupy distinct domains from one another. Profile line scans depict the alternating pattern of AChR and integrin α7 staining, where integrin α7 is primarily present in the space between AChR stripes (**Figure 3.3B**). Additionally, integrin α7 was found to colocalize with AChRs to a much lower degree (Manders Coefficient = 36.6% ± 14.6%) than that of piccolo and VSVGs (**Figure 3.3C**), suggesting that integrin and AChRs are distributed into distinct nanoscale domains. It should be noted that teased muscle fibers did not have the exactly same orientation for "en face" imaging of NMJs. As a result, a small tilt in the angle of the muscle fiber orientation could affect colocalization analysis due to the three-dimensional nature of the sample. We believe that this is one of the contributing factors to the 'imperfect' colocalization results observed here. Nevertheless, these findings suggest that AChRs and integrin α7 occupy different domains within the junctional folds. Taken together, these data suggest that the localization of AChRs may be restricted to the area immediately surrounding the infolded region and thus absent from the center most part of the fold crest.

Based on previous studies and our results thus far, we hypothesize that AChRs are concentrated at the edge of junctional fold crests and part way down the sides of the infolded membrane. Since the opening of infoldings is below the resolution limit of conventional fluorescence microscopy and SIM, the fluorescent signals from two edges of neighboring crests may combine to give the appearance of a single AChR stripe. To test our hypothesis, we utilized Stochastic Optical Reconstruction Microscopy (STORM), which has a theoretical resolution limit of approximately 10 – 20 nm in the XY-axis and 50 nm in the Z-axis (Rust et al., 2006), providing us with the resolution necessary to visualize the opening of junctional folds. Similar to our SIM data, AChR staining appears as stripes within the overall 'pretzel' pattern of the NMJ (**Figure 3.4A**). Additionally, the size and distance between AChR stripes is consistent with our previous SIM data at approximately 130 nm and 210 nm, respectively. Upon closer analysis of the AChR stripes, we observed a thin, fluorescently poor slit that runs down the center of each stripe (**Figure 3.4B**, arrows). This slit at the center of AChR stripes is clearly highlighted in a profile line scan of a representative stripe showing the decrease in AChR fluorescence at the center of the AChR stripe (**Figure 3.4C**). On average, the width of the slit is 47 ± 5.7 nm (**Figure 3.4D**), which is approximately equivalent to the average width of the openings of infoldings from our EM data (55 ± 8.5 nm). Therefore, the slit running down the center of each AChR stripe likely represents the opening of the infolding of the postsynaptic membrane. This is the first evidence visualizing the opening of membrane infoldings using fluorescence microscopy. Overall, these data support the hypothesis that AChRs are concentrated at the edge of the junctional fold crests, surrounding the opening of membrane infoldings.

3.3 Discussion

AChRs are highly concentrated on the postsynaptic membrane of the NMJ for effective neurotransmission during muscle contraction. The large NMJs in vertebrates are structurally unique, as the postsynaptic muscle membrane forms numerous folds in the sarcolemma that are believed to play an important role in synaptic transmission (Martin, 1994; Shi et al., 2012). Not only do the junctional folds effectively increase the postsynaptic surface area, but they also provide a platform for the spatial segregation of molecules involved in distinct signaling pathways of NMJ neurotransmission. For example, AChRs are concentrated at the fold crest, whereas VGSCs are localized to the troughs of junctional folds (Flucher and Daniels, 1989). The topography of the folds and the spatial segregation of key postsynaptic proteins within them act to facilitate the amplification of synaptic current (Martin, 1994), thus allowing for more efficient neurotransmission. Previous studies using EM and light microscopy have shown that AChRs are distributed along the crest and part way down the junctional folds, but excluded from the trough (Fertuck and Salpeter, 1974; Burden et al., 1979; Matthews-Bellinger and Salpeter, 1983; Flucher and Daniels, 1989; Marques et al., 2000). While such a distribution of AChRs would position them close to the presynaptic membrane, it would not provide the best configuration for synaptic transmission given that the presynaptic active zones are not aligned with the center of the crest, but rather with the opening of membrane infoldings (Couteaux and Pecot-Dechavassine, 1970; Dreyer et al., 1973). Unfortunately, conventional light microscopy lacks the resolution to resolve nanoscale details of AChR distribution. While EM has the nanoscale resolution, immunogold labeling tends to be sparse and biochemical reaction products of horseradish peroxidase may not be spatially

confined. In this study, we present evidence, using two different types of super-resolution fluorescence imaging, that AChRs are concentrated at the edges of the crests of junctional folds. In this case, fluorescence from the two edges of adjacent crests comprises a single AChR stripe observed by conventional light microscopy, whereas the fluorescently poor space (the dark band) between AChR stripes actually represents the top of the fold crest. It should be noted that our data are presented as maximum intensity projections, thus the results are unlikely affected by the summation of signals on the wall of the folds. However, the Z-axis resolution is known to be limited, thus we cannot rule out the possibility that 'en face' imaging might not fully resolve AChR distribution on the wall of junctional folds. Nonetheless, the concentration of AChRs at the edges of the crests essentially creates a trans-synaptic alignment of AChRs with the presynaptic active zones where the neurotransmitter ACh is released (**Figure 3.5**). Concentrating AChRs at the crest edge would likely provide more efficient delivery of ACh to AChRs, and thus more efficient neurotransmission, rather than evenly distributing AChRs across the fold crest. A similar trans-synaptic alignment of active zones and neurotransmitter receptors has also been reported in synapses within the central nervous system (Tang et al., 2016), suggesting this trans-synaptic alignment may represent a conserved mechanism for efficient neurotransmission across various synapses.

Strong synaptic adhesion is important to maintain the integrity of the synapse. One of the key synaptic adhesion molecules at the NMJ is integrin α7, which associates with integrin β1 to form integrin α7β1 (Mayer, 2003; Singhal and Martin, 2011). Integrin α7β1 binding of laminin α4 at NMJs is crucial for the positioning of active zones, such that the loss of laminin α4 results in the misalignment of active zones with junctional folds (Patton

et al., 2001; Sanes, 2003). Our data show that integrin α7 and AChRs appear to occupy largely discrete domains, even though both are localized at the crest of junctional folds. The localization of integrin α7β1 to the center most part of the fold crest could represent a specialized area for synaptic adhesion. It is possible that localizing integrin molecules into distinct nanodomains could enable stronger synaptic adhesion because adhesion molecules would not be interspersed with various other postsynaptic molecules. Additionally, a dense patch of adhesion molecules interacting with the presynaptic terminal through binding to the synaptic basal lamina could also act as a 'barrier', restricting the diffusion of ACh to the area of fold openings where AChRs are concentrated. Clearly, future research is needed to evaluate these possibilities.

The exact function of the junctional folds remains unclear. Many studies have found mutations that result in the loss of junctional folds (Noakes et al., 1995; Barik et al., 2014). However, these mutations usually result in disruptions to various other parts of the postsynaptic compartment, including AChR expression, making the study of junctional fold function very difficult. Nonetheless, studies using mathematical modeling of the NMJ have provided insight into the function of junctional folds. Modeling of neurotransmission with and without junctional folds has suggested that the folds act to amplify synaptic current following ACh release (Martin, 1994). Specifically, the amount of ACh quanta required to initiate muscle contraction is approximately double in the absence of junctional folds (Martin, 1994). Thus, in the presence of junctional folds, fewer AChRs need to be activated in order to initiate muscle contraction. Furthermore, densely clustering AChRs directly opposite that of neurotransmitter release sites could provide another mechanism to further increase the efficacy of NMJ neurotransmission. Currently, there are no

experimental manipulations available that can alter AChR distribution without affecting NMJ structure. However, it is exciting to speculate that tools may be developed in the future allowing detailed analysis of neurotransmission with AChRs concentrated at the edge of the infoldings vs. AChRs distributed across the fold crest.

Defects in junctional folds are a common phenotype of many diseases affecting the NMJ (Hirsch, 2007; Ha and Richman, 2015). For example, patients with myasthenia gravis produce antibodies targeting key postsynaptic molecules, of which AChRs are most often targeted (Hirsch, 2007; Spillane et al., 2010; Ha and Richman, 2015). Binding of the autoimmune antibodies results in the internalization of AChRs, reducing their concentration to about one-third that of normal NMJs (Lindstrom, 2000). AChR–antibody binding also results in damage to the postsynaptic membrane, which typically has reduced folds and a widened synaptic cleft (Hirsch, 2007). Consequently, patients exhibit severe muscle weakness due to a significant disruption in neurotransmission. Therefore, proper muscle function appears to be intricately linked to the structure of the postsynaptic terminal and the localization of AChRs.

In summary, our super-resolution imaging has revealed a distinct nanoscale pattern of AChRs on the postsynaptic membrane of NMJs. A similar nanoscale organization has also been shown in synapses of the central nervous system (Tang et al., 2016), suggesting that nanoscale organization and alignment of presynaptic and postsynaptic components may represent a conserved mechanism to ensure effective synaptic transmission.

3.4 Materials & Methods

Antibodies and chemical reagents

The following antibodies were used in this study: rabbit anti-alpha tubulin (1:200; Abcam, ab15246), mouse anti-rapsyn (1:100; EMD Millipore, MAB2238), rat anti-Integrin α7 (1:200; R&D Systems, MAB3518), mouse anti-sodium channel (1:100; Sigma, S8809), rabbit anti-piccolo (1:500; Synaptic Systems, 142 003). Alexa Fluor 488 conjugated α-bungarotoxin and Alexa Fluor 647 conjugated α-bungarotoxin (1:1000) were purchased from Invitrogen (B13422 & B35450, respectively).

Whole-mount immunofluorescence

Wild-type C57BL/6 mice of mixed sex were sacrificed by exposure to CO2. The pretzel-shaped distribution of AChRs as well as the junctional folds are fully developed by postnatal day 21 (Slater, 1982; Singhal and Martin, 2011). Therefore, mice between 4 – 8 weeks of age were used for all experiments. All procedures were carried out in accordance with National Institutes of Health guidelines for animal use and were approved by the Institutional Animal Care and Use Committee of Emory University. The transversus abdominis (TVA) muscle was dissected as previously described by Murray et. al. (2014). Briefly, the entire abdominal musculature was dissected from the mouse and immediately fixed for 10 minutes in 4% (v/v) paraformaldehyde (Polysciences Inc.) in phosphate-buffered saline (PBS). Following fixation, the superficial layers of muscle were removed revealing the TVA muscle situated in the deepest layer of the abdominal wall. The TVA muscle is a very thin muscle group, making it a great candidate for successful whole-mount immunostaining. After the TVA was carefully cleaned of any fat or fascia, the tissue was

incubated with Alexa Fluor 488 or Alexa Fluor 647 conjugated α-bungarotoxin for 30 minutes to label AChRs. The tissue was then permeabilized with 2% Triton X-100 (Sigma) for 30 minutes, and blocked with 4% bovine serum albumin (BSA) and 1% Triton X-100 in PBS for at least 30 minutes. The tissue was then incubated with primary antibodies diluted in blocking buffer overnight at 4°C. Following extensive washing with PBS, the tissue was incubated with secondary antibodies in blocking buffer for 2 – 4 hours. Following extensive washing with PBS, the tissue was directly mounted onto a glass slide with Fluoromount-G (SouthernBiotech). All NMJs were imaged 'en face'.

For STORM imaging, teased muscles were labeled with Alexa Fluor 647 conjugated α-bungarotoxin and imaged in a photoswitchable imaging buffer containing cysteamine (MEA), glucose, glucose oxidase, and catalase, all obtained from Sigma-Aldrich (Dempsey et al., 2011). The teased muscle fibers were weighed down on a homemade glass bottom dish in order to allow for better imaging of 'en face' NMJs.

Microscopy and image analysis

Laser-scanning confocal images were collected on a Nikon C1 confocal system based on the Nikon Eclipse TE300 inverted microscope (Nikon Instruments, Melville, NY) equipped with a 60×/1.4 numerical aperture (NA) Plan Apo oil immersion objective. Three-dimensional structured illumination microscopy (3D-SIM) was performed on a Nikon N-SIM Eclipse Ti-E microscope system equipped with Perfect Focus, 100×/1.49 NA oil immersion objective, and an EMCCD camera (DU-897, Andor Technology, Belfast, UK). Stochastic optical reconstruction microscopy (STORM) was performed using a Nikon Ti-E TIRF inverted microscope equipped with Perfect Focus, 488 nm and

647 nm lasers, and an iXon 897 EMCCD camera (Andor). Images were acquired using a 100×/1.45 N.A. Plan Apo λ objective. Approximately 40,000 frames were collected using total internal reflection fluorescence (TIRF) excitation. Images were reconstructed in Nikon Elements.

Intensity profile line scans were performed using the original data in Nikon Elements software. The lines were drawn perpendicular to AChR stripes, near the midline of the primary gutter. For piccolo staining specifically, care was taken to place lines in an area where piccolo puncta are present. A 12 pixel line width was used to average intensities at each point along the line in order to reduce signal noise. From the intensity profile line scans, the full width at half maximum of individual AChR stripes was used to quantify the width of AChR stripes. The distance between AChR stripes (i.e. the width of fluorescently poor space between AChR stripes) was quantified using profile line scans as follows: 1) measuring the distance between the centers of two neighboring AChR stripes, and 2) subtracting the average width of AChR stripes from the center-to-center distance. Maximum intensity z-projections were created using ImageJ software (National Institutes of Health, Bethesda, MD). Colocalization analysis was performed on Imaris 8.4 software (Andor) using maximum intensity z-projected images. A mask of the synaptic area was created in order to selectively analyze the degree of colocalization within the synaptic area.

Transmission Electron Microscopy

Mouse TVA muscles were fixed with 2.5% glutaraldehyde in 0.1M cacodylate buffer (pH 7.4). Samples were then washed and post-fixed with 1% osmium tetroxide in the same buffer for 1 hour. After rinsing with de-ionized water, samples were dehydrated through an ethanol series and then placed in 100% ethanol. Following dehydration, muscle samples

were infiltrated with 100% ethanol and Eponate 12 resin (Ted Pella, Inc., Redding, CA) at a 1:1 ratio overnight. After additional infiltration in Eponate 12 resin, muscle samples were placed in labeled Beem capsule and polymerized in a 60°C oven. Ultrathin sections were cut at 70-80 nanometer thick on a Leica UltraCut S ultramicrotome (Leica Microsystems Inc., Buffalo Grove, IL). Grids with ultrathin sections were stained with 5% uranyl acetate and 2% lead citrate. Ultrathin sections were imaged on a JEOL JEM-1400 transmission electron microscope (JEOL Ltd., Tokyo, Japan) equipped with a Gatan US1000 CCD camera (Gatan, Pleasanton, CA).

Experimental design and statistical analysis

All the data were collected from at least three replicas of independently prepared samples. Quantified data were statistically analyzed using one-way ANOVA. The data follow a normal distribution as examined by Anderson-Darling test. P-values are provided in the corresponding figure legends.

Acknowledgements

We thank Dr. Lin Mei (Medical College of Georgia, Augusta University) for providing the initial training of NMJ preparation and labeling, as well as, constructive input toward the project. This research project was supported in part by research grants from National Institutes of Health to JQZ (GM083889, MH104632, and MH108025) and to LM (AG051510, NS082007, NS090083), the Emory University Integrated Cellular Imaging Microscopy Core of the Emory Neuroscience NINDS Core Facilities grant (5P30NS055077), the Robert P. Apkarian Integrated Electron Microscopy Core (UL1TR000454).

3.5 Figures

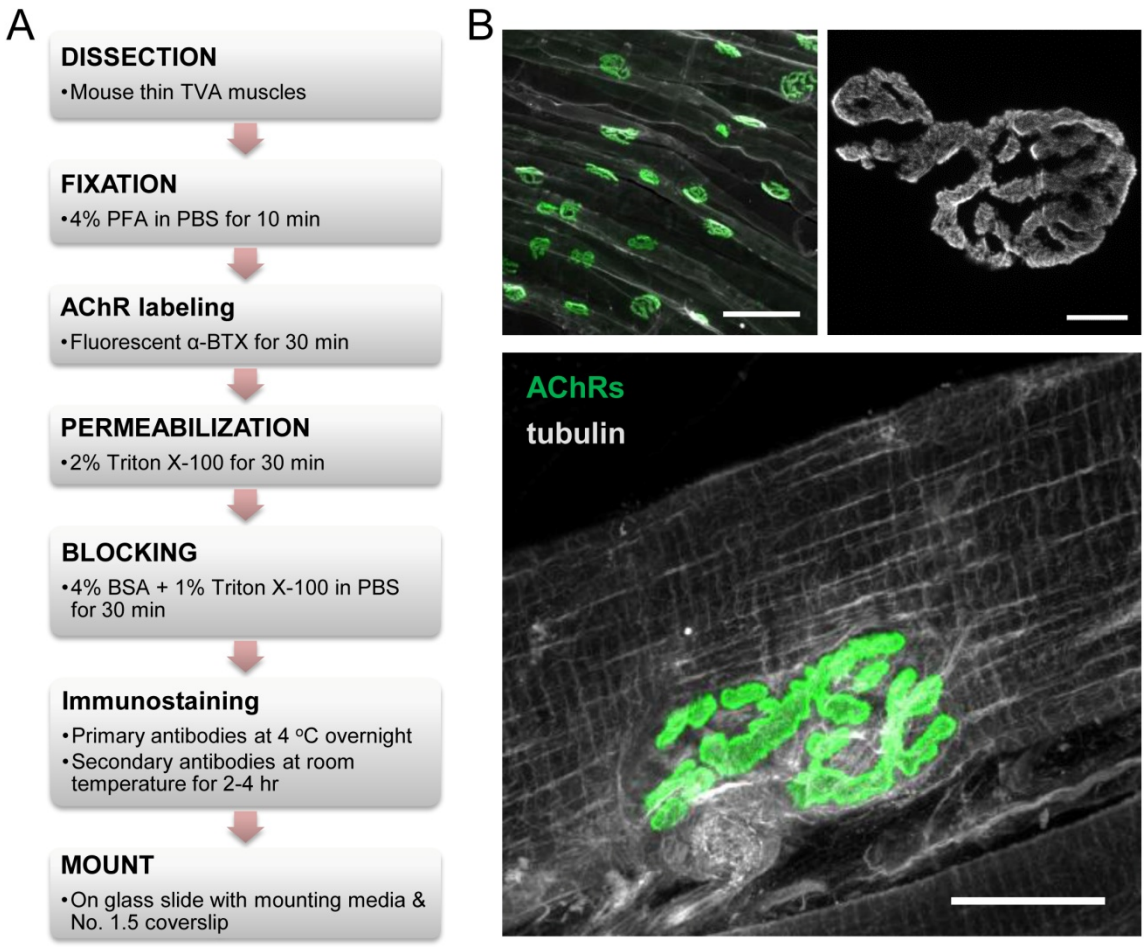

Figure 3.1. Whole-mount immunostaining of the Transversus Abdominis (TVA) muscle for reliable detection of antigens at the NMJ. (**A**) The flow chart depicting the protocol used for clean and reliable immunostaining of muscle fibers. (**B**) Example images of the immunostaining. Top Left: A low magnification image shows NMJ innervation patterns along the TVA muscles. Integrin alpha7 (white), used to highlight the membrane of individual muscle fibers, was co-labeled with AChRs (green) to highlight the innervation pattern along the TVA muscle. Scale bar: 100 µm. Top Right: A high magnification image of an individual NMJ shows the pretzel-shaped AChR distribution at the NMJ of a TVA muscle. Note that AChRs are not uniformly distributed. Scale bar: 5 µm. Bottom: AChRs

(green) were co-labeled with tubulin (white), an intracellular antigen, to show that the whole-mount method enables excellent antibody penetration to label the microtubule network inside the skeletal muscle. Scale bar: 20 μm.

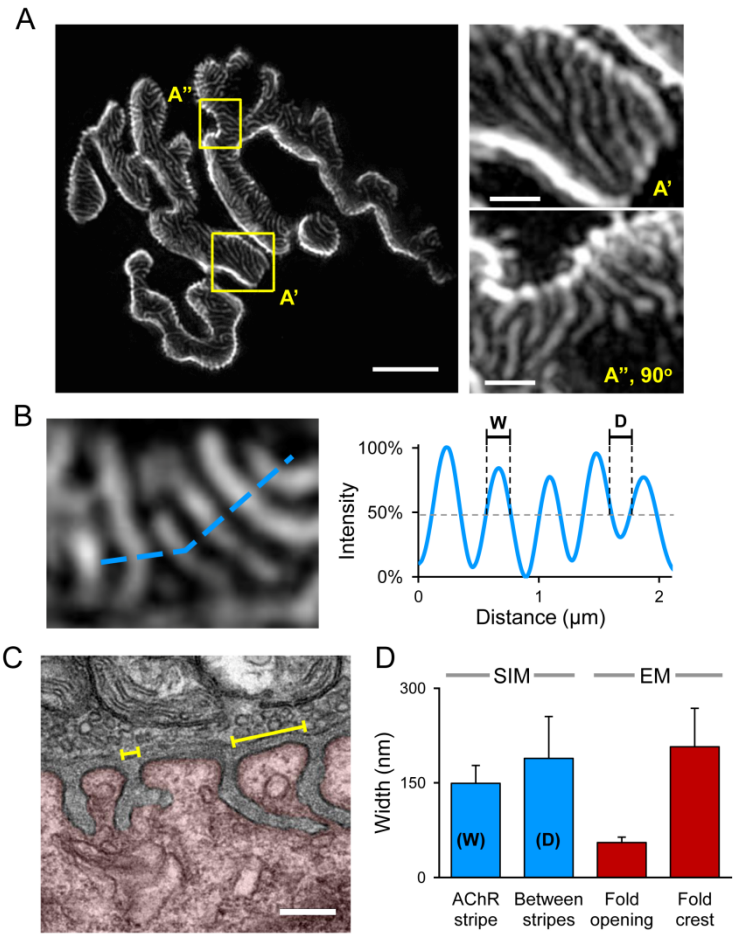

Figure 3.2. AChRs are distributed in stripes that are not correlated with the crest of NMJ junctional folds. (**A**) A representative 3D-SIM image showing the AChR-rich stripes separated by dark bands. Scale bar: 5 μm. The areas enclosed by dashed line rectangles (A' and A") are shown in a high magnification on the right. Scale bar: 1 μm. (**B**) A small region of the AChR stripes (left panel) are used to generate the intensity profile shown on the right. The width of the AChR stripes (W) and the distance between two adjacent stripes (D) are measured and presented in the bar graph in (**D**). (**C**) A representative transmission electron micrograph of an NMJ from the transversus abdominis muscle. The junctional folds are clearly visible at the postsynaptic compartment

(highlighted by red color). Numerous synaptic vesicles and mitochondria are present within the opposing presynaptic terminal. The average width of junctional fold openings and fold crests (red brackets) were manually quantified and presented in the bar graph in (**D**). Scale bar, 0.2 μm. (**D**) The bar graph summarizing the measurement results from the SIM data (blue bars, n=4, >180 stripes) and EM data (red bars; n=7, >40 folds). Error bars represent the standard deviation.

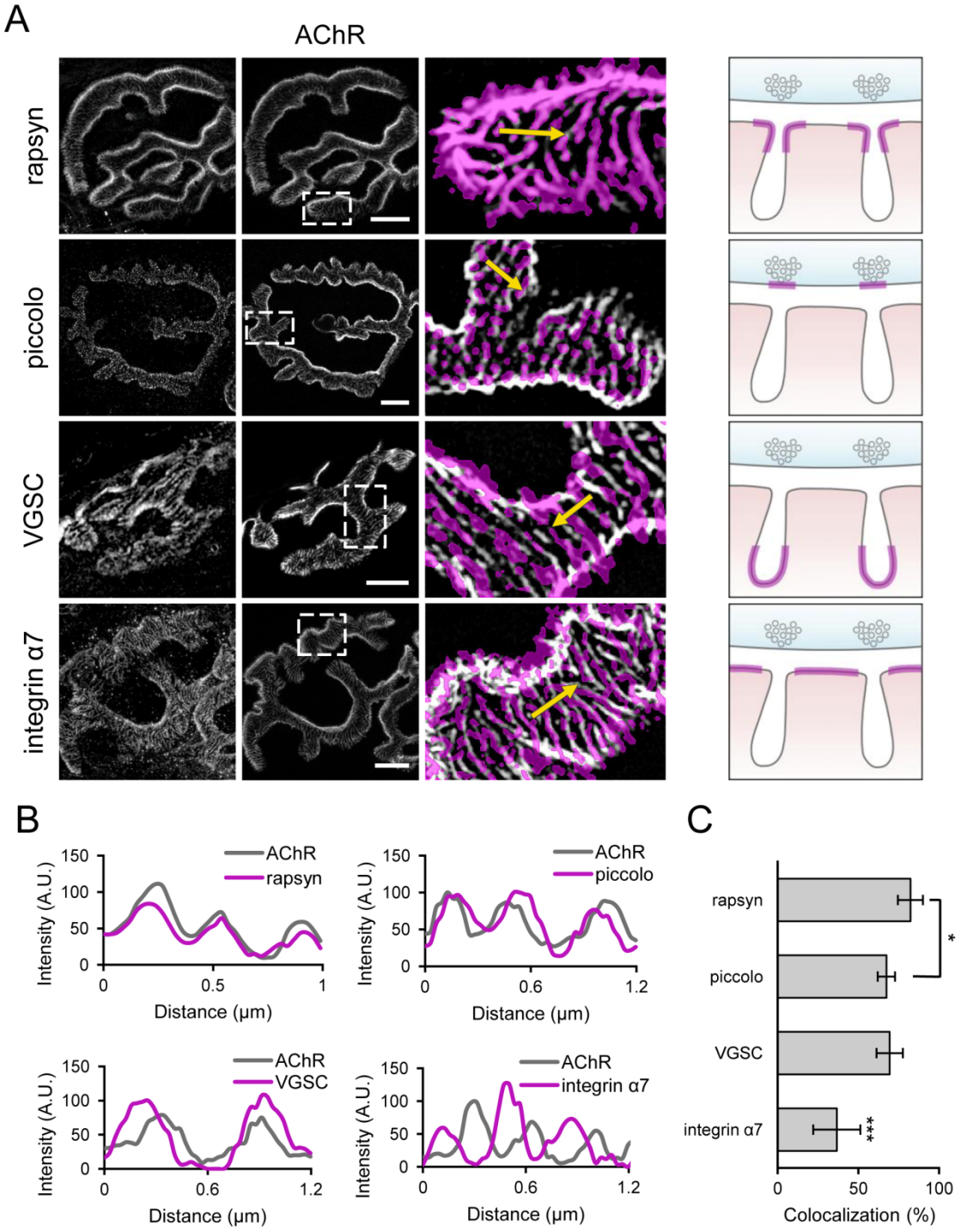

Figure 3.3. Correlation of AChR distribution with specific pre- and post-synaptic markers at NMJs. (**A-B**) Colocalization of AChRs (white) with various synaptic markers

(magenta, threshold). Representative fluorescent images are shown on the right and the schematics on the right depict the known localization of each synaptic marker (magenta line) with respect to the junctional folds. Scale bars: 5 μm. The representative intensity profiles of AChRs (grey) and each of the synaptic markers (magenta) are shown in (**B**). Four markers were examined: Rapsyn, an intracellular AChR scaffolding protein; Piccolo, an active zone component; VGSC, voltage-gated sodium channel; integrin α7, an integrin subunit involved in adhesion in NMJs. (**C**) Quantification of the colocalization of each marker with AChRs. One-way ANOVA analysis: $p = 2.22\times10^{-5}$ (n = 4). Error bars represent the standard deviation. Bonferroni analysis: $*p = 0.012$, $***p < 0.004$.

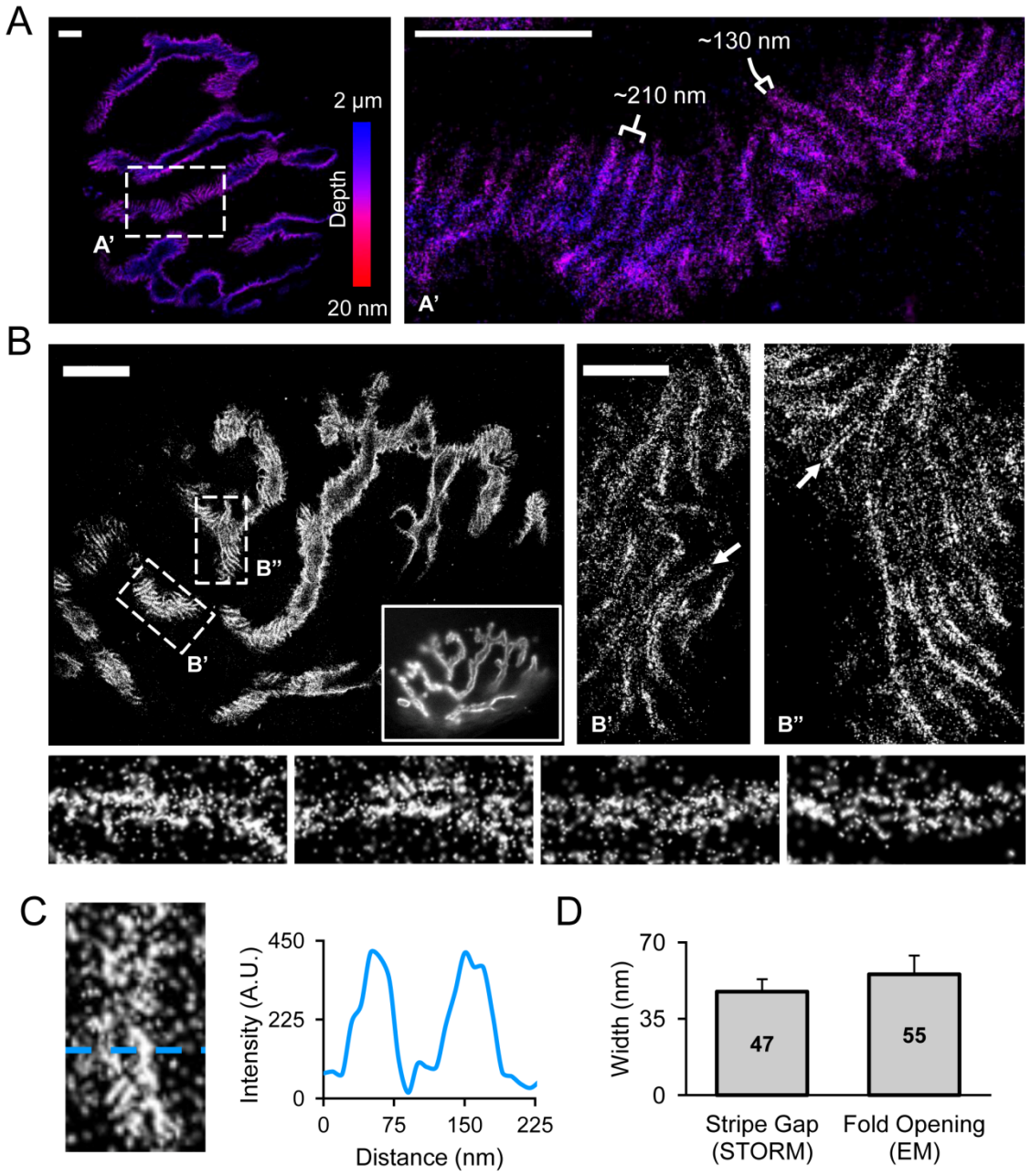

Figure 3.4. Super-resolution imaging reveals AChRs are concentrated around the opening of junctional folds. (**A**) 3D Stochastic Optical Reconstruction Microscopy (3D-STORM) imaging of AChRs highlights the high three-dimensional nature of the postsynaptic membrane. The widths of AChR stripes (approx. 130 nm) and the distance

between stripes (approx. 210 nm) is consistent with quantifications from our previous SIM data. A small region outlined by dashed rectangle (A') is shown in a higher magnification on the right. Color scale bar indicates Z-depth. Scale bars: 2 μm. (**B**) Representative STORM images of AChRs in a NMJ. Scale bar: 5 μm. Inset image shows the same NMJ imaged using widefield microscopy. Close-up regions (B' & B") reveals a thin slit at the center of each AChR stripe (arrow). Scale bar: 1 μm. Bottom, close-up view of individual AChR stripes. (**C**) Representative profile line scan further highlighting the slit at the center of each AChR stripe. (**D**) Quantification of the width of the AChR stripe gap (measured from STORM data, n = 23) and the width of the junctional fold opening (measured from our TEM data, n = 50). Error bars represent the standard deviation. Average width values at center of each bar.

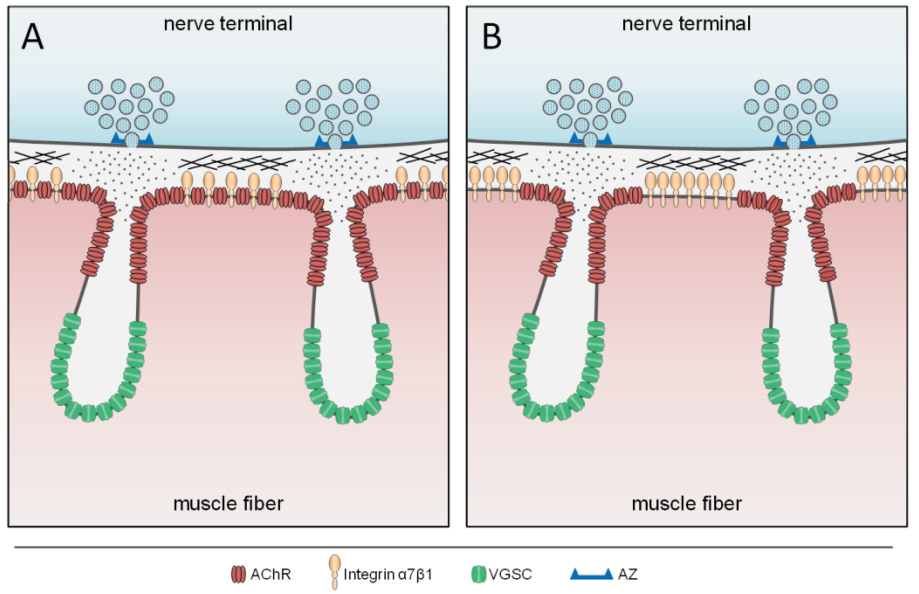

Figure 3.5. Comparison of previous model and our proposed model of AChR distribution. Schematics showing the previous model (**A**) and the proposed revision (**B**) of AChR distribution along junctional fold crests. Classically, it is believed that AChRs (red) are distributed across the entire junctional fold crest and partially down the sides of the infolded membrane and excluded from the trough of junctional folds where voltage-gated sodium channels (VGSC, green) are localized (A). However, we propose that AChRs are instead spatially restricted to the area immediately surrounding the opening of junctional folds and are segregated from the adhesion molecule integrin α7β1 (tan) located at the center-most part of fold crests (B). The spatial segregation of AChRs and integrin α7β1 could be beneficial to maintaining strong synaptic adhesion between the pre- and postsynaptic terminals. Furthermore, this subsynaptic organization would position AChRs directly opposite that of the active zone (AZ, blue bracket), and thus, in the prime position to receive and respond to acetylcholine (dots) release.

Chapter IV

Discussion: from structure to function

Studies examining the NMJ have produced fundamental discoveries for the field of synapse biology (Sanes and Lichtman, 1999). A major focus of research in synapse biology focuses on the regulation of neurotransmitter receptors, including their localization and expression. An in-depth knowledge of neurotransmitter receptor localization and regulation provides a foundation for a comprehensive understanding of synapse function. This is especially true at the large and topographically complex vertebrate NMJ, where the only neurotransmitter receptor is the AChR. Therefore, a comprehensive examination of AChR localization and accumulation is critical to fully appreciate muscle function. The nanoscale localization of neurotransmitter receptors within the postsynaptic membrane has a significant effect on neurotransmission, such that concentrating neurotransmitter receptors opposite that of neurotransmitter release sites acts as a powerful mechanism to maximize the efficiency of neurotransmission (Tang et al., 2016). In fact, studies simulating neurotransmission in glutamatergic synapses of the CNS found that the probability of neurotransmitter receptor activation dramatically decreases the further the receptor is from neurotransmitter release sites (Franks et al., 2003; MacGillavry et al., 2013), thus highlighting the physiological importance of the nanoscale localization of neurotransmitter receptors, including AChRs.

Furthermore, the vast majority (approx. 85%) of patients with the neuromuscular disease myasthenia gravis (MG) produce autoimmune antibodies targeting AChRs, resulting in a dramatic reduction in AChR density at the postsynaptic terminal (Meriggioli, 2009; Ha and Richman, 2015). Additionally, the vast majority of congenital myasthenia syndrome (CMS) cases are a result of mutations in AChRs (Abicht et al., 2012). Therefore, any changes to AChR localization, surface expression, or function will have drastic consequences on neurotransmission and overall muscle function. The work presented in this dissertation examines *where* AChRs are localized in the adult NMJ and *how* AChRs are localized to the postsynaptic terminal during development. The novel observations presented in this dissertation furthers our understanding of NMJ synaptogenesis as well as synapse biology in general.

4.1 Fine-tuning AChR organization at the NMJ

The work in Chapter 2 examined the process regulating AChR trafficking to the postsynaptic membrane. The findings from this study identify a role for highly dynamic actin in the accumulation of AChRs and their insertion into the postsynaptic membrane. Highly dynamic actin filaments were concentrated into small punctate structures that repeatedly appeared and disappeared over time (**Figure 2.3**). Interestingly, these dynamic actin puncta were located within AChR-poor micro-perforations in developing aneural AChR clusters (**Figure 2.2**), and disruption of these dynamic actin puncta resulted in a significant reduction in the accumulation of AChRs at the developing cluster (**Figure 2.5**). These findings strongly suggest that these dynamic actin puncta are likely involved in the clustering of AChRs.

In contrast, the work in Chapter 3 examined the nanoscale localization of AChRs at the adult NMJ using super-resolution microscopy. The findings identified novel nanodomains of postsynaptic receptors at the crest of junctional folds. Specifically, AChRs and the adhesion molecule integrin α7 are separated into distinct nanodomains at junctional fold crests (**Figure 3.3**), where integrin α7 is concentrated at the center of the crest and AChRs are concentrated at the edge of the crest. This places AChRs closest to presynaptic neurotransmitter release sites, which are located directly opposite junctional fold openings (**Figure 3.5**). Until now, AChRs were believed to be distributed across the entire crest of junctional folds (Fertuck and Salpeter, 1974; Matthews-Bellinger and Salpeter, 1983; Marques et al., 2000). However, concentrating AChRs at the crest edge may represent an optimal configuration for efficient and effective neurotransmission.

4.2 What is the role of the actin puncta in NMJ development?

The findings from Chapter 2 raise a question that recurs throughout the study. As discussed above, we know that the AChR cluster-associated dynamic actin puncta are in some way involved in the clustering of AChRs. However, the precise mechanism by which they regulate AChR clustering remains unclear. From the research presented in this dissertation, in combination with previous research examining the role of actin in AChR clustering, two main hypotheses arise: 1) the dynamic actin puncta represent trafficking hubs for the vesicular delivery of postsynaptic components, 2) the dynamic actin puncta represent the core of synaptic podosomes.

Podosomes are highly dynamic, actin-rich adhesive organelles that act as sites of attachment to, and degradation of, the extracellular matrix (ECM) (Murphy and Courtneidge, 2011; Bernadzki et al., 2014). They are classically characterized as a

hallmark of invasive cancer cells, however, Proszynski *et al*. identified actin-based structures at aneural AChR clusters that share the same core characteristics of classic podosomes, and thus, termed them synaptic podosomes (Proszynski et al., 2009). They concluded that the synaptic podosomes are responsible for the reorganization of AChRs during the plaque-to-pretzel transition through degradation of the ECM, lateral movement across clusters, and remodeling of the actin cytoskeleton (Proszynski et al., 2009). The actin puncta described in this dissertation resemble synaptic podosomes in that at the center of a podosome lies a highly dynamic actin punctum (Proszynski et al., 2009), raising the possibility that the actin puncta described in this dissertation are in fact synaptic podosomes. A key distinction, however, is that podosomes contain a characteristic ring of adhesion and scaffolding proteins surrounding the dynamic actin core (Linder and Kopp, 2005). Examination of the synaptic podosomes revealed both the adhesion/scaffolding ring and the non-overlapping actin core fit precisely within AChR cluster perforations (Proszynski et al., 2009). By contrast, the actin puncta described here is directly adjacent to the border which defines the AChR cluster micro-perforation, leaving no space to support an adhesion/scaffolding ring (**Figure 2.2B**). The lack of one of the defining features of podosomes suggests that the actin puncta described here do not represent synaptic podosomes.

A key finding supporting the hypothesis that the actin puncta represent trafficking hubs comes from my experiments analyzing the impact of dynamic actin on AChR clustering. The results from these experiments revealed that the incorporation of new AChRs at aneural clusters is significantly reduced when actin dynamics are reduced (**Figure 2.5**). These results implicate a role for the dynamic actin puncta in the trafficking of AChRs.

Admittedly, the pharmacological inhibitors used to disrupt actin puncta dynamics (cytochalasin D, latrunculin A, jasplakinolide, CK-666) could have impacted the endocytosis and exocytosis of AChRs in a manner unrelated to the actin puncta. However, research conducted by a former member of the Zheng Lab supports my finding that dynamic actin puncta are involved in AChR trafficking (Lee et al., 2009). Using *Xenopus* myocyte cultures, Lee *et al*. found similar punctate concentrations of highly dynamic actin at aneural AChR clusters. Importantly, these foci of dynamic actin were found to associate with vesicular trafficking components, suggesting they are sites of vesicular trafficking. The dynamic actin foci characterized by Lee *et al*. are reminiscent of the dynamic actin puncta described in this dissertation in that both are localized within AChR cluster perforations and both affect AChR accumulation when disrupted.

Additional support for the hypothesis that the actin puncta represent trafficking hubs for AChRs can be found in the molecular components associated with the actin puncta. The actin binding proteins profilin and cortactin, which both regulate actin dynamics through the promotion of actin polymerization (Krishnan and Moens, 2009; Kirkbride et al., 2011), associate with the dynamic actin puncta at AChR clusters (**Figure 2.6**). Notably, cortactin has been shown to be activated by receptor tyrosine kinases to regulate cortical actin assembly and transmembrane receptor organization in a variety of cell types, including neurons (Du et al., 1998; Weed and Parsons, 2001). A key aspect of cortactin function in the cell is its involvement in endocytosis through the association with the branched actin regulator Arp 2/3, as well as, the endocytic vesicle fission regulator, dynamin (Kirkbride et al., 2011). Thus, it is plausible that the local activation of cortactin by the receptor tyrosine kinase, MuSK, promotes the actin turnover and assembly

necessary for the regulation of endo- and exocytosis of AChRs and their subsequent reorganization. Indeed, a previous study examining cortactin function at the NMJ found that cortactin is activated upon stimulation with agrin, and this activity is involved in regulating AChR clustering (Madhavan et al., 2009). Specifically, the inhibition of cortactin activity resulted in reduced AChR clustering. Although this study did not examine vesicular trafficking components in relation to cortactin activity, it does provide substantial evidence supporting the hypothesis that AChR cluster-associated dynamic actin puncta, and the associated actin regulatory proteins, represent trafficking hubs for the delivery and organization of AChRs. Nevertheless, future experiments examining this possibility will be essential in order to fully appreciate the process of NMJ synaptogenesis.

4.3 How do postsynaptic nanodomains relate to NMJ development and function?

The findings from Chapter 3 unveil a novel organization of postsynaptic receptors. These findings challenge the previous model of AChR localization, in which AChRs were thought to be evenly dispersed across the fold crest and partially down the sides of the fold (Fertuck and Salpeter, 1974; Matthews-Bellinger and Salpeter, 1983; Marques et al., 2000). As discussed above, we found that AChRs are actually concentrated at the edge of junctional fold crests and partially down the sides of the folds, placing AChRs directly under neurotransmitter release sites (**Figure 3.5**). AChRs also appear to be organized into a discrete nanodomain at the edge of the fold crest, segregated from integrin α7 molecules, which are concentrated at the center of the fold crest (**Figure 3.3**). These findings, however, raise a few key questions. 1) How does this nanoscale organization of AChRs impact neurotransmission? 2) What regulates this nanoscale organization?

4.3.1 How do postsynaptic nanodomains contribute to NMJ function?

In order to truly determine how clustering AChRs at the crest edge impacts neurotransmission, one would need to be able to precisely alter AChR distribution. Ideally, one would examine neurotransmission with AChRs concentrated at the crest edge compared to AChRs dispersed across the fold crest. Unfortunately, such manipulations are not available. However, a few ideas can be derived from examining the structure and organization of the postsynaptic terminal—after all, structure equals function.

One of the most informative pieces of information in determining the functional impact of concentrating AChRs at the edge of junctional fold crests is the localization of neurotransmitter release sites on the presynaptic terminal. At the mammalian NMJ, neurotransmitter release sites are organized into small discrete puncta along the presynaptic terminal membrane (Chen et al., 2012; Harlow et al., 2013). Electron microscopy (EM) studies have shown that these neurotransmitter release sites are precisely located opposite that of junctional fold openings on the postsynaptic terminal (Couteaux and Pecot-Dechavassine, 1970; Dreyer et al., 1973; Patton et al., 2001). Consequently, during neurotransmission, the neurotransmitter ACh is released into the area of the junctional fold opening, between neighboring fold crests. Thus, if AChRs were in fact evenly distributed across the crest fold, as the previous model predicts, then neurotransmitter release sites would be, in large part, misaligned from AChRs on the crest of junctional folds (**Figure 3.5**). Such an organization, however, would likely hinder the muscle cell's ability to reach the threshold necessary to cause an action potential since the large portion of AChRs at the center of the crest would likely be exposed to very little ACh, resulting in diminished neurotransmission. Alternatively, concentrating AChRs at the edge of the junctional fold

crest, closest to the openings of junctional folds, would place receptors closest to the presynaptic neurotransmitter release sites, ensuring rapid and effective delivery of ACh to postsynaptic AChRs. Indeed, studies simulating neurotransmission in glutamatergic synapses of the CNS found that the localization of neurotransmitter receptors relative to neurotransmitter release sites can impact neurotransmission, even without altered receptor number (Franks et al., 2003; MacGillavry et al., 2013). Neurotransmitter receptors clustered opposite active zones are more likely to be activated in response to neurotransmitter release than receptors uniformly distributed across the postsynaptic terminal (MacGillavry et al., 2013). Therefore, we believe this trans-synaptic alignment of neurotransmitter release sites and AChRs represents the optimal organization to ensure efficient and effective neurotransmission.

One of the most interesting results from our data is the finding that the synaptic adhesion molecule integrin α7 and AChRs are segregated into distinct domains at the crest of junctional folds. This was an initially surprising finding given that the crest of junctional folds is only roughly 200 nm wide, on average (**Figure 3.2**). Nevertheless, these findings raise into question the functional benefit of segregating AChRs and integrin α7 into distinct nanodomains. While further research would be needed to determine the precise function of integrin α7 nanodomains, it is possible they could play a role in aiding synaptic adhesion as well as neurotransmission. First, the segregation of integrin α7 into a distinct nanodomain could enable stronger synaptic adhesion by providing a specialized area for adhesion. This would prevent integrin molecules from intermingling with various postsynaptic components, and potentially diluting adhesion strength. Second, a dense patch of integrin α7 interacting with the presynaptic terminal via the synaptic basal lamina

could also act as a 'barrier', restricting the diffusion of neurotransmitter to the area of fold openings where AChRs are concentrated. Further research is necessary to analyze these possibilities. Nonetheless, the identification of postsynaptic nanoscale domains furthers our understanding of the topographical features of the mature NMJ, which is intricately linked to its function.

4.3.2 What regulates the formation of postsynaptic nanodomains?

The identification of AChR and integrin α7 nanodomains at the crest of junctional folds raises many questions, one of which: what regulates the formation and maintenance of these nanodomains? As discussed above, the actin cytoskeleton plays significant roles in regulating and maintaining AChR localization and clustering (Chapter 2), and as such, actin is likely also responsible for forming and maintaining AChR nanodomains in mature NMJs. Beyond AChRs, the synaptic cortical actin network is also responsible for maintaining many other postsynaptic specializations, including anchoring voltage-gated Na^+ channels (VGSCs) at the trough of junctional folds (Gee et al., 1998). Therefore, it stands to reason that the actin cytoskeleton would likely be involved in forming and maintaining integrin α7 nanodomains at junctional fold crests, however, more research would be needed to confirm this.

4.4 Outlook

Many diseases affecting the NMJ commonly exhibit defects in the synaptic architecture as well as the localization or expression of key postsynaptic molecules, including AChRs (Hirsch, 2007; Slater, 2008; Ha and Richman, 2015). As such, an in-depth understanding of the processes underlying proper development of NMJ architecture is imperative to fully

appreciate, and thus, treat diseases affecting the NMJ. My work exploring the nanoscale organization of AChRs and the mechanisms underlying this organization provides seminal insight into the structure and development of this unique synapse. Going forward, it will be important to connect the structural features of the NMJ with the mechanisms responsible for initiating and orchestrating them. The various advanced microscopy techniques and the newly emerging advances in molecular biology techniques will likely prove helpful in unlocking these unanswered questions.

The development of super-resolution imaging techniques has revolutionized the field of microscopy, and paved the way for many breakthrough discoveries across the biological sciences. The work presented in this dissertation relied heavily upon super-resolution microscopy. Utilizing these new microscopy techniques to reexamine the distribution of AChRs, which many considered to be already determined, provided new insight, ultimately changing the model of receptor distribution along the postsynaptic membrane. In the future, it will be important to utilize the advancements in technology to not only explore new areas of research, but also to reexamine fundamental biological processes and structures in a new light.

4.5 Summary

The structure of the NMJ, including the organization of the molecules within the synapse, is highly correlated to its function. In fact, disruptions in the synaptic architecture and organization of AChRs is a common phenotype of many neuromuscular diseases (Hirsch, 2007; Slater, 2008; Ha and Richman, 2015). As such, it is important that we obtain a clear understanding of the topographical features of the NMJ and how they develop. The questions I address in this dissertation are as follows: 1) What is the nanoscale organization

of AChRs during the early stages of the plaque-to-pretzel transition? 2) What process(es) regulates the organization of AChRs? and 3) What is the nanoscale distribution of AChRs along junctional folds in the mature synapse? Through the work presented in this dissertation, I have identified a novel nanoscale organization of AChRs in the early stages of synaptogenesis and in the fully mature synapse. In the early stages of synapse development before junctional folds form, AChRs are organized into micro-puncta and micro-perforations within the AChR cluster. Whereas, in the fully mature synapse, AChRs are concentrated around the opening of junctional folds to trans-synaptically align with the presynaptic active zone. Through my work, I also determined that dynamic actin puncta located within AChR micro-perforations are involved in the clustering and accumulation of AChRs during the early stages of synaptogenesis. These novel findings provide seminal insight into the organization and development of AChRs, further contributing to our understanding of the NMJ.

References

Abicht A, Dusl M, Gallenmuller C, Guergueltcheva V, Schara U, Della Marina A, Wibbeler E, Almaras S, Mihaylova V, von der Hagen M, Huebner A, Chaouch A, Muller JS, Lochmuller H (2012) Congenital myasthenic syndromes: achievements and limitations of phenotype-guided gene-after-gene sequencing in diagnostic practice: a study of 680 patients. Hum Mutat 33:1474-1484.

Ackermann M, Matus A (2003) Activity-induced targeting of profilin and stabilization of dendritic spine morphology. Nat Neurosci 6:1194-1200.

Agbulut O, Li Z, Perie S, Ludosky MA, Paulin D, Cartaud J, Butler-Browne G (2001) Lack of desmin results in abortive muscle regeneration and modifications in synaptic structure. Cell Motil Cytoskeleton 49:51-66.

Alshekhlee A, Miles JD, Katirji B, Preston DC, Kaminski HJ (2009) Incidence and mortality rates of myasthenia gravis and myasthenic crisis in US hospitals. Neurology 72:1548-1554.

Anderson MJ, Cohen MW (1977) Nerve-induced and spontaneous redistribution of acetylcholine receptors on cultured muscle cells. J Physiol 268:757-773.

Antolik C, Catino DH, O'Neill AM, Resneck WG, Ursitti JA, Bloch RJ (2007) The actin binding domain of ACF7 binds directly to the tetratricopeptide repeat domains of rapsyn. Neuroscience 145:56-65.

Atlas D (2013) The voltage-gated calcium channel functions as the molecular switch of synaptic transmission. Annu Rev Biochem 82:607-635.

Balice-Gordon RJ, Lichtman JW (1993) In vivo observations of pre- and postsynaptic changes during the transition from multiple to single innervation at developing neuromuscular junctions. J Neurosci 13:834-855.

Banks GB, Fuhrer C, Adams ME, Froehner SC (2003) The postsynaptic submembrane machinery at the neuromuscular junction: requirement for rapsyn and the utrophin/dystrophin-associated complex. J Neurocytol 32:709-726.

Banwell BL, Russel J, Fukudome T, Shen XM, Stilling G, Engel AG (1999) Myopathy, myasthenic syndrome, and epidermolysis bullosa simplex due to plectin deficiency. J Neuropathol Exp Neurol 58:832-846.

Barik A, Lu Y, Sathyamurthy A, Bowman A, Shen C, Li L, Xiong WC, Mei L (2014) LRP4 is critical for neuromuscular junction maintenance. J Neurosci 34:13892-13905.

Beeson D, Higuchi O, Palace J, Cossins J, Spearman H, Maxwell S, Newsom-Davis J, Burke G, Fawcett P, Motomura M, Muller JS, Lochmuller H, Slater C, Vincent A, Yamanashi Y (2006) Dok-7 mutations underlie a neuromuscular junction synaptopathy. Science 313:1975-1978.

Bernadzki KM, Rojek KO, Proszynski TJ (2014) Podosomes in muscle cells and their role in the remodeling of neuromuscular postsynaptic machinery. Eur J Cell Biol 93:478-485.

Berrih-Aknin S, Frenkian-Cuvelier M, Eymard B (2014) Diagnostic and clinical classification of autoimmune myasthenia gravis. J Autoimmun 48-49:143-148.

Bezakova G, Ruegg MA (2003) New insights into the roles of agrin. Nat Rev Mol Cell Biol 4:295-308.

Bezanilla M, Gladfelter AS, Kovar DR, Lee WL (2015) Cytoskeletal dynamics: a view from the membrane. J Cell Biol 209:329-337.

Blanchoin L, Boujemaa-Paterski R, Sykes C, Plastino J (2014) Actin dynamics, architecture, and mechanics in cell motility. Physiol Rev 94:235-263.

Bondesen BA, Mills ST, Kegley KM, Pavlath GK (2004) The COX-2 pathway is essential during early stages of skeletal muscle regeneration. Am J Physiol Cell Physiol 287:C475-483.

Bruneau EG, Akaaboune M (2006) The dynamics of recycled acetylcholine receptors at the neuromuscular junction in vivo. Development 133:4485-4493.

Bubb MR, Senderowicz AM, Sausville EA, Duncan KL, Korn ED (1994) Jasplakinolide, a cytotoxic natural product, induces actin polymerization and competitively inhibits the binding of phalloidin to F-actin. J Biol Chem 269:14869-14871.

Burden S (1982) Identification of an intracellular postsynaptic antigen at the frog neuromuscular junction. J Cell Biol 94:521-530.

Burden SJ, Sargent PB, McMahan UJ (1979) Acetylcholine receptors in regenerating muscle accumulate at original synaptic sites in the absence of the nerve. J Cell Biol 82:412-425.

Byrne S, Walsh C, Lynch C, Bede P, Elamin M, Kenna K, McLaughlin R, Hardiman O (2011) Rate of familial amyotrophic lateral sclerosis: a systematic review and meta-analysis. J Neurol Neurosurg Psychiatry 82:623-627.

Cajal SRy (1928) Degeneration and Regeneration of the Nervous System. London: Oxford University Press.

Calvo AC, Manzano R, Mendonca DM, Munoz MJ, Zaragoza P, Osta R (2014) Amyotrophic lateral sclerosis: a focus on disease progression. Biomed Res Int 2014:925101.

Campanari ML, Garcia-Ayllon MS, Ciura S, Saez-Valero J, Kabashi E (2016) Neuromuscular Junction Impairment in Amyotrophic Lateral Sclerosis: Reassessing the Role of Acetylcholinesterase. Front Mol Neurosci 9:160.

Catterall WA (2000) Structure and regulation of voltage-gated Ca2+ channels. Annu Rev Cell Dev Biol 16:521-555.

Chen F, Liu Y, Sugiura Y, Allen PD, Gregg RG, Lin W (2011a) Neuromuscular synaptic patterning requires the function of skeletal muscle dihydropyridine receptors. Nat Neurosci 14:570-577.

Chen J, Billings SE, Nishimune H (2011b) Calcium channels link the muscle-derived synapse organizer laminin beta2 to Bassoon and CAST/Erc2 to organize presynaptic active zones. J Neurosci 31:512-525.

Chen J, Mizushige T, Nishimune H (2012) Active zone density is conserved during synaptic growth but impaired in aged mice. J Comp Neurol 520:434-452.

Chevessier F et al. (2004) MUSK, a new target for mutations causing congenital myasthenic syndrome. Hum Mol Genet 13:3229-3240.

Chio A, Logroscino G, Traynor BJ, Collins J, Simeone JC, Goldstein LA, White LA (2013) Global epidemiology of amyotrophic lateral sclerosis: a systematic review of the published literature. Neuroepidemiology 41:118-130.

Cohen I, Rimer M, Lomo T, McMahan UJ (1997) Agrin-induced postsynaptic-like apparatus in skeletal muscle fibers in vivo. Mol Cell Neurosci 9:237-253.

Colquhoun D, Sakmann B (1985) Fast events in single-channel currents activated by acetylcholine and its analogues at the frog muscle end-plate. J Physiol 369:501-557.

Cooper JA (1987) Effects of cytochalasin and phalloidin on actin. J Cell Biol 105:1473-1478.

Corey AL, Richman DP, Agius MA, Wollmann RL (1987) Refractoriness to a second episode of experimental myasthenia gravis. Correlation with AChR concentration and morphologic appearance of the postsynaptic membrane. J Immunol 138:3269-3275.

Couteaux R, Pecot-Dechavassine M (1970) [Synaptic vesicles and pouches at the level of "active zones" of the neuromuscular junction]. C R Acad Sci Hebd Seances Acad Sci D 271:2346-2349.

Dai Z, Luo X, Xie H, Peng HB (2000) The actin-driven movement and formation of acetylcholine receptor clusters. J Cell Biol 150:1321-1334.

Dale HH, Feldberg W, Vogt M (1936) Release of acetylcholine at voluntary motor nerve endings. J Physiol 86:353-380.

DeChiara TM, Bowen DC, Valenzuela DM, Simmons MV, Poueymirou WT, Thomas S, Kinetz E, Compton DL, Rojas E, Park JS, Smith C, DiStefano PS, Glass DJ, Burden SJ, Yancopoulos GD (1996) The receptor tyrosine kinase MuSK is required for neuromuscular junction formation in vivo. Cell 85:501-512.

Dempsey GT, Vaughan JC, Chen KH, Bates M, Zhuang X (2011) Evaluation of fluorophores for optimal performance in localization-based super-resolution imaging. Nat Methods 8:1027-1036.

Dobbins GC, Zhang B, Xiong WC, Mei L (2006) The role of the cytoskeleton in neuromuscular junction formation. J Mol Neurosci 30:115-118.

Dobbins GC, Luo S, Yang Z, Xiong WC, Mei L (2008) alpha-Actinin interacts with rapsyn in agrin-stimulated AChR clustering. Mol Brain 1:18.

Domogatskaya A, Rodin S, Tryggvason K (2012) Functional diversity of laminins. Annu Rev Cell Dev Biol 28:523-553.

dos Remedios CG, Chhabra D, Kekic M, Dedova IV, Tsubakihara M, Berry DA, Nosworthy NJ (2003) Actin binding proteins: regulation of cytoskeletal microfilaments. Physiol Rev 83:433-473.

Dreyer F, Peper K, Akert K, Sandri C, Moor H (1973) Ultrastructure of the "active zone" in the frog neuromuscular junction. Brain Res 62:373-380.

Du Y, Weed SA, Xiong WC, Marshall TD, Parsons JT (1998) Identification of a novel cortactin SH3 domain-binding protein and its localization to growth cones of cultured neurons. Mol Cell Biol 18:5838-5851.

Engel AG (2007) The therapy of congenital myasthenic syndromes. Neurotherapeutics 4:252-257.

Engel AG, Ohno K, Shen XM, Sine SM (2003) Congenital myasthenic syndromes: multiple molecular targets at the neuromuscular junction. Ann N Y Acad Sci 998:138-160.

Ervasti JM, Campbell KP (1993) Dystrophin-associated glycoproteins: their possible roles in the pathogenesis of Duchenne muscular dystrophy. Mol Cell Biol Hum Dis Ser 3:139-166.

Feng G, Krejci E, Molgo J, Cunningham JM, Massoulie J, Sanes JR (1999) Genetic analysis of collagen Q: roles in acetylcholinesterase and butyrylcholinesterase assembly and in synaptic structure and function. J Cell Biol 144:1349-1360.

Fertuck HC, Salpeter MM (1974) Localization of acetylcholine receptor by 125I-labeled alpha-bungarotoxin binding at mouse motor endplates. Proc Natl Acad Sci U S A 71:1376-1378.

Fish KN (2009) Total internal reflection fluorescence (TIRF) microscopy. Curr Protoc Cytom Chapter 12:Unit12 18.

Flanagan-Steet H, Fox MA, Meyer D, Sanes JR (2005) Neuromuscular synapses can form in vivo by incorporation of initially aneural postsynaptic specializations. Development 132:4471-4481.

Flucher BE, Daniels MP (1989) Distribution of Na+ channels and ankyrin in neuromuscular junctions is complementary to that of acetylcholine receptors and the 43 kd protein. Neuron 3:163-175.

Fox MA, Sanes JR, Borza DB, Eswarakumar VP, Fassler R, Hudson BG, John SW, Ninomiya Y, Pedchenko V, Pfaff SL, Rheault MN, Sado Y, Segal Y, Werle MJ, Umemori H (2007) Distinct target-derived signals organize formation, maturation, and maintenance of motor nerve terminals. Cell 129:179-193.

Franks KM, Stevens CF, Sejnowski TJ (2003) Independent sources of quantal variability at single glutamatergic synapses. J Neurosci 23:3186-3195.

Froehner SC, Luetje CW, Scotland PB, Patrick J (1990) The postsynaptic 43K protein clusters muscle nicotinic acetylcholine receptors in Xenopus oocytes. Neuron 5:403-410.

Galletta BJ, Cooper JA (2009) Actin and endocytosis: mechanisms and phylogeny. Curr Opin Cell Biol 21:20-27.

Gautam M, Noakes PG, Mudd J, Nichol M, Chu GC, Sanes JR, Merlie JP (1995) Failure of postsynaptic specialization to develop at neuromuscular junctions of rapsyn-deficient mice. Nature 377:232-236.

Gautam M, Noakes PG, Moscoso L, Rupp F, Scheller RH, Merlie JP, Sanes JR (1996) Defective neuromuscular synaptogenesis in agrin-deficient mutant mice. Cell 85:525-535.

Gee SH, Madhavan R, Levinson SR, Caldwell JH, Sealock R, Froehner SC (1998) Interaction of muscle and brain sodium channels with multiple members of the syntrophin family of dystrophin-associated proteins. J Neurosci 18:128-137.

Gimona M, Buccione R, Courtneidge SA, Linder S (2008) Assembly and biological role of podosomes and invadopodia. Curr Opin Cell Biol 20:235-241.

Goldman D, Brenner HR, Heinemann S (1988) Acetylcholine receptor alpha-, beta-, gamma-, and delta-subunit mRNA levels are regulated by muscle activity. Neuron 1:329-333.

Gustafsson MG (2000) Surpassing the lateral resolution limit by a factor of two using structured illumination microscopy. J Microsc 198:82-87.

Gustafsson MG, Shao L, Carlton PM, Wang CJ, Golubovskaya IN, Cande WZ, Agard DA, Sedat JW (2008) Three-dimensional resolution doubling in wide-field fluorescence microscopy by structured illumination. Biophys J 94:4957-4970.

Gutmann L, Phillips LH, 2nd, Gutmann L (1992) Trends in the association of Lambert-Eaton myasthenic syndrome with carcinoma. Neurology 42:848-850.

Ha JC, Richman DP (2015) Myasthenia gravis and related disorders: Pathology and molecular pathogenesis. Biochim Biophys Acta 1852:651-657.

Hall ZW, Lubit BW, Schwartz JH (1981) Cytoplasmic actin in postsynaptic structures at the neuromuscular junction. J Cell Biol 90:789-792.

Harlow ML, Szule JA, Xu J, Jung JH, Marshall RM, McMahan UJ (2013) Alignment of synaptic vesicle macromolecules with the macromolecules in active zone material that direct vesicle docking. PLoS One 8:e69410.

Hetrick B, Han MS, Helgeson LA, Nolen BJ (2013) Small molecules CK-666 and CK-869 inhibit actin-related protein 2/3 complex by blocking an activating conformational change. Chem Biol 20:701-712.

Heuser JE, Reese TS (1981) Structural changes after transmitter release at the frog neuromuscular junction. J Cell Biol 88:564-580.

Heuser JE, Reese TS, Dennis MJ, Jan Y, Jan L, Evans L (1979) Synaptic vesicle exocytosis captured by quick freezing and correlated with quantal transmitter release. J Cell Biol 81:275-300.

Hijikata T, Nakamura A, Isokawa K, Imamura M, Yuasa K, Ishikawa R, Kohama K, Takeda S, Yorifuji H (2008) Plectin 1 links intermediate filaments to costameric sarcolemma through beta-synemin, alpha-dystrobrevin and actin. J Cell Sci 121:2062-2074.

Hirsch NP (2007) Neuromuscular junction in health and disease. Br J Anaesth 99:132-138.

Hulsbrink R, Hashemolhosseini S (2014) Lambert-Eaton myasthenic syndrome - diagnosis, pathogenesis and therapy. Clin Neurophysiol 125:2328-2336.

Huze C et al. (2009) Identification of an agrin mutation that causes congenital myasthenia and affects synapse function. Am J Hum Genet 85:155-167.

Janmey PA, Euteneuer U, Traub P, Schliwa M (1991) Viscoelastic properties of vimentin compared with other filamentous biopolymer networks. J Cell Biol 113:155-160.

Jones G, Meier T, Lichtsteiner M, Witzemann V, Sakmann B, Brenner HR (1997) Induction by agrin of ectopic and functional postsynaptic-like membrane in innervated muscle. Proc Natl Acad Sci U S A 94:2654-2659.

Katz B (1966) Nerve, Muscle and Synapse. New York: McGraw-Hill.

Khaitlina SY (2014) Intracellular transport based on actin polymerization. Biochemistry (Mosc) 79:917-927.

Kim N, Burden SJ (2008) MuSK controls where motor axons grow and form synapses. Nat Neurosci 11:19-27.

Kim N, Stiegler AL, Cameron TO, Hallock PT, Gomez AM, Huang JH, Hubbard SR, Dustin ML, Burden SJ (2008) Lrp4 is a receptor for Agrin and forms a complex with MuSK. Cell 135:334-342.

Kirkbride KC, Sung BH, Sinha S, Weaver AM (2011) Cortactin: a multifunctional regulator of cellular invasiveness. Cell Adh Migr 5:187-198.

Krejci E, Thomine S, Boschetti N, Legay C, Sketelj J, Massoulie J (1997) The mammalian gene of acetylcholinesterase-associated collagen. J Biol Chem 272:22840-22847.

Kreplak L, Herrmann H, Aebi U (2008) Tensile properties of single desmin intermediate filaments. Biophys J 94:2790-2799.

Krishnan K, Moens PDJ (2009) Structure and functions of profilins. Biophys Rev 1:71-81.

Kuffler SW, Yoshikami D (1975) The number of transmitter molecules in a quantum: an estimate from iontophoretic application of acetylcholine at the neuromuscular synapse. J Physiol 251:465-482.

Kummer TT, Misgeld T, Lichtman JW, Sanes JR (2004) Nerve-independent formation of a topologically complex postsynaptic apparatus. J Cell Biol 164:1077-1087.

Labra J, Menon P, Byth K, Morrison S, Vucic S (2016) Rate of disease progression: a prognostic biomarker in ALS. J Neurol Neurosurg Psychiatry 87:628-632.

Lang B, Newsom-Davis J, Peers C, Prior C, Wray DW (1987) The effect of myasthenic syndrome antibody on presynaptic calcium channels in the mouse. J Physiol 390:257-270.

Lanzetti L (2007) Actin in membrane trafficking. Curr Opin Cell Biol 19:453-458.

Latvanlehto A, Fox MA, Sormunen R, Tu H, Oikarainen T, Koski A, Naumenko N, Shakirzyanova A, Kallio M, Ilves M, Giniatullin R, Sanes JR, Pihlajaniemi T (2010) Muscle-derived collagen XIII regulates maturation of the skeletal neuromuscular junction. J Neurosci 30:12230-12241.

Lee CW, Han J, Bamburg JR, Han L, Lynn R, Zheng JQ (2009) Regulation of acetylcholine receptor clustering by ADF/cofilin-directed vesicular trafficking. Nat Neurosci 12:848-856.

Lin S, Landmann L, Ruegg MA, Brenner HR (2008) The role of nerve- versus muscle-derived factors in mammalian neuromuscular junction formation. J Neurosci 28:3333-3340.

Lin W, Burgess RW, Dominguez B, Pfaff SL, Sanes JR, Lee KF (2001) Distinct roles of nerve and muscle in postsynaptic differentiation of the neuromuscular synapse. Nature 410:1057-1064.

Linder S, Kopp P (2005) Podosomes at a glance. J Cell Sci 118:2079-2082.

Lindstrom JM (2000) Acetylcholine receptors and myasthenia. Muscle Nerve 23:453-477.

Liu Y, Padgett D, Takahashi M, Li H, Sayeed A, Teichert RW, Olivera BM, McArdle JJ, Green WN, Lin W (2008) Essential roles of the acetylcholine receptor gamma-subunit in neuromuscular synaptic patterning. Development 135:1957-1967.

Luo S, Zhang B, Dong XP, Tao Y, Ting A, Zhou Z, Meixiong J, Luo J, Chiu FC, Xiong WC, Mei L (2008) HSP90 beta regulates rapsyn turnover and subsequent AChR cluster formation and maintenance. Neuron 60:97-110.

Luther PW, Samuelsson SJ, Bloch RJ, Pumplin DW (1996) Cytoskeleton-membrane interactions at the postsynaptic density of Xenopus neuromuscular junctions. J Neurocytol 25:417-427.

Luxenburg C, Winograd-Katz S, Addadi L, Geiger B (2012) Involvement of actin polymerization in podosome dynamics. J Cell Sci 125:1666-1672.

MacGillavry HD, Song Y, Raghavachari S, Blanpied TA (2013) Nanoscale scaffolding domains within the postsynaptic density concentrate synaptic AMPA receptors. Neuron 78:615-622.

Maddison P, Lang B, Mills K, Newsom-Davis J (2001) Long term outcome in Lambert-Eaton myasthenic syndrome without lung cancer. J Neurol Neurosurg Psychiatry 70:212-217.

Maddison P, Gozzard P, Grainge MJ, Lang B (2017) Long-term survival in paraneoplastic Lambert-Eaton myasthenic syndrome. Neurology 88:1334-1339.

Madhavan R, Gong ZL, Ma JJ, Chan AW, Peng HB (2009) The function of cortactin in the clustering of acetylcholine receptors at the vertebrate neuromuscular junction. PLoS One 4:e8478.

Mahadeva B, Phillips LH, 2nd, Juel VC (2008) Autoimmune disorders of neuromuscular transmission. Semin Neurol 28:212-227.

Maiweilidan Y, Klauza I, Kordeli E (2011) Novel interactions of ankyrins-G at the costameres: the muscle-specific Obscurin/Titin-Binding-related Domain (OTBD) binds plectin and filamin C. Exp Cell Res 317:724-736.

Marchand S, Devillers-Thiery A, Pons S, Changeux JP, Cartaud J (2002) Rapsyn escorts the nicotinic acetylcholine receptor along the exocytic pathway via association with lipid rafts. J Neurosci 22:8891-8901.

Marques MJ, Conchello JA, Lichtman JW (2000) From plaque to pretzel: fold formation and acetylcholine receptor loss at the developing neuromuscular junction. J Neurosci 20:3663-3675.

Martin AR (1994) Amplification of neuromuscular transmission by postjunctional folds. Proc Biol Sci 258:321-326.

Martin PT, Kaufman SJ, Kramer RH, Sanes JR (1996) Synaptic integrins in developing, adult, and mutant muscle: selective association of alpha1, alpha7A, and alpha7B integrins with the neuromuscular junction. Dev Biol 174:125-139.

Maselli RA, Dunne V, Pascual-Pascual SI, Bowe C, Agius M, Frank R, Wollmann RL (2003) Rapsyn mutations in myasthenic syndrome due to impaired receptor clustering. Muscle Nerve 28:293-301.

Massoulie J, Millard CB (2009) Cholinesterases and the basal lamina at vertebrate neuromuscular junctions. Curr Opin Pharmacol 9:316-325.

Matthews-Bellinger JA, Salpeter MM (1983) Fine structural distribution of acetylcholine receptors at developing mouse neuromuscular junctions. J Neurosci 3:644-657.

Mayer U (2003) Integrins: redundant or important players in skeletal muscle? J Biol Chem 278:14587-14590.

McMahan UJ (1990) The agrin hypothesis. Cold Spring Harb Symp Quant Biol 55:407-418.

Meier T, Hauser DM, Chiquet M, Landmann L, Ruegg MA, Brenner HR (1997) Neural agrin induces ectopic postsynaptic specializations in innervated muscle fibers. J Neurosci 17:6534-6544.

Meriggioli MN (2009) Myasthenia gravis with anti-acetylcholine receptor antibodies. Front Neurol Neurosci 26:94-108.

Merlie JP, Isenberg KE, Russell SD, Sanes JR (1984) Denervation supersensitivity in skeletal muscle: analysis with a cloned cDNA probe. J Cell Biol 99:332-335.

Mihailovska E, Raith M, Valencia RG, Fischer I, Al Banchaabouchi M, Herbst R, Wiche G (2014) Neuromuscular synapse integrity requires linkage of acetylcholine receptors to postsynaptic intermediate filament networks via rapsyn-plectin 1f complexes. Mol Biol Cell 25:4130-4149.

Miledi R, Molinoff P, Potter LT (1971) Isolation of the cholinergic receptor protein of Torpedo electric tissue. Nature 229:554-557.

Missias AC, Chu GC, Klocke BJ, Sanes JR, Merlie JP (1996) Maturation of the acetylcholine receptor in skeletal muscle: regulation of the AChR gamma-to-epsilon switch. Dev Biol 179:223-238.

Missias AC, Mudd J, Cunningham JM, Steinbach JH, Merlie JP, Sanes JR (1997) Deficient development and maintenance of postsynaptic specializations in mutant mice lacking an 'adult' acetylcholine receptor subunit. Development 124:5075-5086.

Mitsui T, Kawajiri M, Kunishige M, Endo T, Akaike M, Aki K, Matsumoto T (2000) Functional association between nicotinic acetylcholine receptor and sarcomeric proteins via actin and desmin filaments. J Cell Biochem 77:584-595.

Molenaar PC, Newsom-Davis J, Polak RL, Vincent A (1982) Eaton-Lambert syndrome: acetylcholine and choline acetyltransferase in skeletal muscle. Neurology 32:1061-1065.

Moransard M, Borges LS, Willmann R, Marangi PA, Brenner HR, Ferns MJ, Fuhrer C (2003) Agrin regulates rapsyn interaction with surface acetylcholine receptors, and this underlies cytoskeletal anchoring and clustering. J Biol Chem 278:7350-7359.

Mucke N, Kreplak L, Kirmse R, Wedig T, Herrmann H, Aebi U, Langowski J (2004) Assessing the flexibility of intermediate filaments by atomic force microscopy. J Mol Biol 335:1241-1250.

Muller JS, Jepson CD, Laval SH, Bushby K, Straub V, Lochmuller H (2010) Dok-7 promotes slow muscle integrity as well as neuromuscular junction formation in a zebrafish model of congenital myasthenic syndromes. Hum Mol Genet 19:1726-1740.

Muller JS et al. (2007) Phenotypical spectrum of DOK7 mutations in congenital myasthenic syndromes. Brain 130:1497-1506.

Murphy DA, Courtneidge SA (2011) The 'ins' and 'outs' of podosomes and invadopodia: characteristics, formation and function. Nat Rev Mol Cell Biol 12:413-426.

Murray L, Gillingwater TH, Kothary R (2014) Dissection of the transversus abdominis muscle for whole-mount neuromuscular junction analysis. J Vis Exp:e51162.

Nishimune H (2012) Active zones of mammalian neuromuscular junctions: formation, density, and aging. Ann N Y Acad Sci 1274:24-32.

Nishimune H, Sanes JR, Carlson SS (2004) A synaptic laminin-calcium channel interaction organizes active zones in motor nerve terminals. Nature 432:580-587.

Nishimune H, Valdez G, Jarad G, Moulson CL, Muller U, Miner JH, Sanes JR (2008) Laminins promote postsynaptic maturation by an autocrine mechanism at the neuromuscular junction. J Cell Biol 182:1201-1215.

Nitkin RM, Smith MA, Magill C, Fallon JR, Yao YM, Wallace BG, McMahan UJ (1987) Identification of agrin, a synaptic organizing protein from Torpedo electric organ. J Cell Biol 105:2471-2478.

Noakes PG, Gautam M, Mudd J, Sanes JR, Merlie JP (1995) Aberrant differentiation of neuromuscular junctions in mice lacking s-laminin/laminin beta 2. Nature 374:258-262.

O'Neill A, Williams MW, Resneck WG, Milner DJ, Capetanaki Y, Bloch RJ (2002) Sarcolemmal organization in skeletal muscle lacking desmin: evidence for

cytokeratins associated with the membrane skeleton at costameres. Mol Biol Cell 13:2347-2359.

O'Neill JH, Murray NM, Newsom-Davis J (1988) The Lambert-Eaton myasthenic syndrome. A review of 50 cases. Brain 111 (Pt 3):577-596.

Okada K, Inoue A, Okada M, Murata Y, Kakuta S, Jigami T, Kubo S, Shiraishi H, Eguchi K, Motomura M, Akiyama T, Iwakura Y, Higuchi O, Yamanashi Y (2006) The muscle protein Dok-7 is essential for neuromuscular synaptogenesis. Science 312:1802-1805.

Park SJ, Suetsugu S, Sagara H, Takenawa T (2007) HSP90 cross-links branched actin filaments induced by N-WASP and the Arp2/3 complex. Genes Cells 12:611-622.

Patton BL, Miner JH, Chiu AY, Sanes JR (1997) Distribution and function of laminins in the neuromuscular system of developing, adult, and mutant mice. J Cell Biol 139:1507-1521.

Patton BL, Cunningham JM, Thyboll J, Kortesmaa J, Westerblad H, Edstrom L, Tryggvason K, Sanes JR (2001) Properly formed but improperly localized synaptic specializations in the absence of laminin alpha4. Nat Neurosci 4:597-604.

Paulin D, Li Z (2004) Desmin: a major intermediate filament protein essential for the structural integrity and function of muscle. Exp Cell Res 301:1-7.

Phillips LH, 2nd (2003) The epidemiology of myasthenia gravis. Ann N Y Acad Sci 998:407-412.

Phillips WD, Kopta C, Blount P, Gardner PD, Steinbach JH, Merlie JP (1991) ACh receptor-rich membrane domains organized in fibroblasts by recombinant 43-kildalton protein. Science 251:568-570.

Pollard TD (2016) Actin and Actin-Binding Proteins. Cold Spring Harb Perspect Biol 8.

Pollard TD, Borisy GG (2003) Cellular motility driven by assembly and disassembly of actin filaments. Cell 112:453-465.

Porat-Shliom N, Milberg O, Masedunskas A, Weigert R (2013) Multiple roles for the actin cytoskeleton during regulated exocytosis. Cell Mol Life Sci 70:2099-2121.

Porter CW, Barnard EA (1975a) The density of cholinergic receptors at the endplate postsynaptic membrane: ultrastructural studies in two mammalian species. J Membr Biol 20:31-49.

Porter CW, Barnard EA (1975b) Distribution and density of cholinergic receptors at the motor endplates of a denervated mouse muscle. Exp Neurol 48:542-556.

Proszynski TJ, Sanes JR (2013) Amotl2 interacts with LL5beta, localizes to podosomes and regulates postsynaptic differentiation in muscle. J Cell Sci 126:2225-2235.

Proszynski TJ, Gingras J, Valdez G, Krzewski K, Sanes JR (2009) Podosomes are present in a postsynaptic apparatus and participate in its maturation. Proc Natl Acad Sci U S A 106:18373-18378.

Rezniczek GA, Konieczny P, Nikolic B, Reipert S, Schneller D, Abrahamsberg C, Davies KE, Winder SJ, Wiche G (2007) Plectin 1f scaffolding at the sarcolemma of dystrophic (mdx) muscle fibers through multiple interactions with beta-dystroglycan. J Cell Biol 176:965-977.

Ricard-Blum S (2011) The collagen family. Cold Spring Harb Perspect Biol 3:a004978.

Rimer M, Mathiesen I, Lomo T, McMahan UJ (1997) gamma-AChR/epsilon-AChR switch at agrin-induced postsynaptic-like apparatus in skeletal muscle. Mol Cell Neurosci 9:254-263.

Robertson NP, Deans J, Compston DA (1998) Myasthenia gravis: a population based epidemiological study in Cambridgeshire, England. J Neurol Neurosurg Psychiatry 65:492-496.

Rowley KL, Mantilla CB, Ermilov LG, Sieck GC (2007) Synaptic vesicle distribution and release at rat diaphragm neuromuscular junctions. J Neurophysiol 98:478-487.

Rust MJ, Bates M, Zhuang X (2006) Sub-diffraction-limit imaging by stochastic optical reconstruction microscopy (STORM). Nat Methods 3:793-795.

Salpeter MM, Marchaterre M, Harris R (1988) Distribution of extrajunctional acetylcholine receptors on a vertebrate muscle: evaluated by using a scanning electron microscope autoradiographic procedure. J Cell Biol 106:2087-2093.

Samuel MA, Valdez G, Tapia JC, Lichtman JW, Sanes JR (2012) Agrin and synaptic laminin are required to maintain adult neuromuscular junctions. PLoS One 7:e46663.

Sander A, Hesser BA, Witzemann V (2001) MuSK induces in vivo acetylcholine receptor clusters in a ligand-independent manner. J Cell Biol 155:1287-1296.

Sanes JR (2003) The basement membrane/basal lamina of skeletal muscle. J Biol Chem 278:12601-12604.

Sanes JR, Lichtman JW (1999) Development of the vertebrate neuromuscular junction. Annu Rev Neurosci 22:389-442.

Schell MJ, Erneux C, Irvine RF (2001) Inositol 1,4,5-trisphosphate 3-kinase A associates with F-actin and dendritic spines via its N terminus. J Biol Chem 276:37537-37546.

Schmidt N, Basu S, Sladecek S, Gatti S, van Haren J, Treves S, Pielage J, Galjart N, Brenner HR (2012) Agrin regulates CLASP2-mediated capture of microtubules at the neuromuscular junction synaptic membrane. J Cell Biol 198:421-437.

Schoser B, Eymard B, Datt J, Mantegazza R (2017) Lambert-Eaton myasthenic syndrome (LEMS): a rare autoimmune presynaptic disorder often associated with cancer. J Neurol.

Schwander M, Shirasaki R, Pfaff SL, Muller U (2004) Beta1 integrins in muscle, but not in motor neurons, are required for skeletal muscle innervation. J Neurosci 24:8181-8191.

Scott A (2017) Drug therapy: On the treatment trail for ALS. Nature 550:S120-S121.

Sealock R, Murnane AA, Paulin D, Froehner SC (1989) Immunochemical identification of desmin in Torpedo postsynaptic membranes and at the rat neuromuscular junction. Synapse 3:315-324.

Shi L, Fu AK, Ip NY (2012) Molecular mechanisms underlying maturation and maintenance of the vertebrate neuromuscular junction. Trends Neurosci 35:441-453.

Singhal N, Martin PT (2011) Role of extracellular matrix proteins and their receptors in the development of the vertebrate neuromuscular junction. Dev Neurobiol 71:982-1005.

Skeie GO, Apostolski S, Evoli A, Gilhus NE, Illa I, Harms L, Hilton-Jones D, Melms A, Verschuuren J, Horge HW, European Federation of Neurological S (2010) Guidelines for treatment of autoimmune neuromuscular transmission disorders. Eur J Neurol 17:893-902.

Slater CR (1982) Postnatal maturation of nerve-muscle junctions in hindlimb muscles of the mouse. Dev Biol 94:11-22.

Slater CR (2008) Structural factors influencing the efficacy of neuromuscular transmission. Ann N Y Acad Sci 1132:1-12.

Song WK, Wang W, Foster RF, Bielser DA, Kaufman SJ (1992) H36-alpha 7 is a novel integrin alpha chain that is developmentally regulated during skeletal myogenesis. J Cell Biol 117:643-657.

Song WK, Wang W, Sato H, Bielser DA, Kaufman SJ (1993) Expression of alpha 7 integrin cytoplasmic domains during skeletal muscle development: alternate forms, conformational change, and homologies with serine/threonine kinases and tyrosine phosphatases. J Cell Sci 106 (Pt 4):1139-1152.

Spillane J, Beeson DJ, Kullmann DM (2010) Myasthenia and related disorders of the neuromuscular junction. J Neurol Neurosurg Psychiatry 81:850-857.

Takai T, Noda M, Mishina M, Shimizu S, Furutani Y, Kayano T, Ikeda T, Kubo T, Takahashi H, Takahashi T, et al. (1985) Cloning, sequencing and expression of cDNA for a novel subunit of acetylcholine receptor from calf muscle. Nature 315:761-764.

Tang AH, Chen H, Li TP, Metzbower SR, MacGillavry HD, Blanpied TA (2016) A trans-synaptic nanocolumn aligns neurotransmitter release to receptors. Nature 536:210-214.

Tariq N, Basharat Z, Butt S, Baig DN (2016) Distribution analysis of profilin isoforms at transcript resolution with mRNA-seq and secondary structure in various organs of Rattus norvegicus. Gene 589:49-55.

Tintignac LA, Brenner HR, Ruegg MA (2015) Mechanisms Regulating Neuromuscular Junction Development and Function and Causes of Muscle Wasting. Physiol Rev 95:809-852.

Titulaer MJ, Maddison P, Sont JK, Wirtz PW, Hilton-Jones D, Klooster R, Willcox N, Potman M, Sillevis Smitt PA, Kuks JB, Roep BO, Vincent A, van der Maarel SM, van Dijk JG, Lang B, Verschuuren JJ (2011) Clinical Dutch-English Lambert-Eaton Myasthenic syndrome (LEMS) tumor association prediction score accurately predicts small-cell lung cancer in the LEMS. J Clin Oncol 29:902-908.

Tran DT, Masedunskas A, Weigert R, Ten Hagen KG (2015) Arp2/3-mediated F-actin formation controls regulated exocytosis in vivo. Nat Commun 6:10098.

Tsay HJ, Schmidt J (1989) Skeletal muscle denervation activates acetylcholine receptor genes. J Cell Biol 108:1523-1526.

Tsujino A, Maertens C, Ohno K, Shen XM, Fukuda T, Harper CM, Cannon SC, Engel AG (2003) Myasthenic syndrome caused by mutation of the SCN4A sodium channel. Proc Natl Acad Sci U S A 100:7377-7382.

Urbano FJ, Rosato-Siri MD, Uchitel OD (2002) Calcium channels involved in neurotransmitter release at adult, neonatal and P/Q-type deficient neuromuscular junctions (Review). Mol Membr Biol 19:293-300.

Villarroel A, Sakmann B (1996) Calcium permeability increase of endplate channels in rat muscle during postnatal development. J Physiol 496 (Pt 2):331-338.

Walker JH, Boustead CM, Witzemann V (1984) The 43-K protein, v1, associated with acetylcholine receptor containing membrane fragments is an actin-binding protein. EMBO J 3:2287-2290.

Weatherbee SD, Anderson KV, Niswander LA (2006) LDL-receptor-related protein 4 is crucial for formation of the neuromuscular junction. Development 133:4993-5000.

Weed SA, Parsons JT (2001) Cortactin: coupling membrane dynamics to cortical actin assembly. Oncogene 20:6418-6434.

Weston C, Yee B, Hod E, Prives J (2000) Agrin-induced acetylcholine receptor clustering is mediated by the small guanosine triphosphatases Rac and Cdc42. J Cell Biol 150:205-212.

Wirtz PW, Smallegange TM, Wintzen AR, Verschuuren JJ (2002) Differences in clinical features between the Lambert-Eaton myasthenic syndrome with and without cancer: an analysis of 227 published cases. Clin Neurol Neurosurg 104:359-363.

Witke W (2004) The role of profilin complexes in cell motility and other cellular processes. Trends Cell Biol 14:461-469.

Wolven AK, Belmont LD, Mahoney NM, Almo SC, Drubin DG (2000) In vivo importance of actin nucleotide exchange catalyzed by profilin. J Cell Biol 150:895-904.

Wu H, Xiong WC, Mei L (2010) To build a synapse: signaling pathways in neuromuscular junction assembly. Development 137:1017-1033.

Wyatt RM, Balice-Gordon RJ (2003) Activity-dependent elimination of neuromuscular synapses. J Neurocytol 32:777-794.

Yang X, Arber S, William C, Li L, Tanabe Y, Jessell TM, Birchmeier C, Burden SJ (2001) Patterning of muscle acetylcholine receptor gene expression in the absence of motor innervation. Neuron 30:399-410.

Yarmola EG, Somasundaram T, Boring TA, Spector I, Bubb MR (2000) Actin-latrunculin A structure and function. Differential modulation of actin-binding protein function by latrunculin A. J Biol Chem 275:28120-28127.

Zalli D, Neff L, Nagano K, Shin NY, Witke W, Gori F, Baron R (2016) The Actin-Binding Protein Cofilin and Its Interaction With Cortactin Are Required for Podosome Patterning in Osteoclasts and Bone Resorption In Vivo and In Vitro. J Bone Miner Res 31:1701-1712.

Zhang B, Luo S, Wang Q, Suzuki T, Xiong WC, Mei L (2008) LRP4 serves as a coreceptor of agrin. Neuron 60:285-297.

Zhang B, Luo S, Dong XP, Zhang X, Liu C, Luo Z, Xiong WC, Mei L (2007) Beta-catenin regulates acetylcholine receptor clustering in muscle cells through interaction with rapsyn. J Neurosci 27:3968-3973.

Zhu J, Zhou K, Hao JJ, Liu J, Smith N, Zhan X (2005) Regulation of cortactin/dynamin interaction by actin polymerization during the fission of clathrin-coated pits. J Cell Sci 118:807-817.